

Novel Fragmentation Processes of 2-Nitrobenzenesulfonyl Amino Acid Anions

by

Tara Edith Tovstiga

Submitted in partial fulfilment of the requirements  
for the degree of Master of Science

at

Dalhousie University  
Halifax, Nova Scotia  
August 2013

© Copyright by Tara Edith Tovstiga, 2013

## TABLE OF CONTENTS

<b>LIST OF FIGURES .....</b>	<b>v</b>
<b>LIST OF SCHEMES .....</b>	<b>viii</b>
<b>LIST OF TABLES .....</b>	<b>xi</b>
<b>ABSTRACT.....</b>	<b>xii</b>
<b>LIST OF ABBREVIATIONS USED.....</b>	<b>xiii</b>
<b>ACKNOWLEDGEMENTS .....</b>	<b>xv</b>
<b>CHAPTER 1 INTRODUCTION .....</b>	<b>1</b>
<b>1.1 Mass Spectrometry and Fragmentation Processes .....</b>	<b>2</b>
<b>1.2 Negative-ion Mass Spectrometry and Fragmentation Processes.....</b>	<b>4</b>
1.2.1 Carboxylic Acids .....	5
1.2.1.1 Decarboxylation of Deprotonated Carboxylic Acids.....	5
1.2.1.2 McLafferty Rearrangements of Ions .....	7
1.2.1.3 $\alpha$ -Hydroxy- and $\alpha$ -Aminocarboxylic Acids .....	8
1.2.1.4 <i>N</i> -(2,4-Dinitrophenyl)amino Acids.....	10
1.2.2 Alcohols and Phenols.....	11
1.2.2.1 Ionization .....	11
1.2.2.2 Smiles Rearrangement .....	13
1.2.3 Sulfonic Acids.....	17
1.2.4 Sulfonamides.....	18
<b>1.3 Amine Protecting Groups.....</b>	<b>22</b>
1.3.1 Use of Ns in Mitsunobu Reactions .....	23

1.4 Thesis Goals .....	25
<b>CHAPTER 2 MATERIALS AND METHODS.....</b>	<b>26</b>
2.1 General Information .....	26
2.2 Mass Spectrometry .....	26
2.3 Benzenesulfonyl Derivatives .....	27
2.3.1 Preparation of Benzenesulfonyl Derivatives .....	27
2.3.2 Preparation of <i>N</i> -2-Nitrobenzenesulfonyl[ <sup>18</sup> O]glycine (5, Ns[ <sup>18</sup> O]Gly) .....	35
2.3.3 Methylation of Ns derivatives.....	36
2.3.3.1 <i>O</i> -Methylation.....	36
2.3.3.2 <i>N</i> -Methylation .....	37
<b>CHAPTER 3 RESULTS AND DISCUSSION.....</b>	<b>39</b>
3.1 Use of the Ns Protecting Group .....	39
3.2 Preparation of Ns Amino Acids .....	41
3.3 Ionization of Ns Amino Acids .....	45
3.4 CID of Deprotonated NsGly: Sequential Neutral Losses .....	48
3.4.1 <i>Ortho</i> Cyclization Pathway.....	52
3.4.2 <i>Ortho</i> Cyclization Pathway 2.....	56
3.4.3 Sulfonamide Rearrangement Pathway .....	58
3.5 Effect of Structural Variations on Fragmentation Processes .....	61
3.5.1 Position of the Nitro Substituent.....	61
3.5.1.1 Dual Bond Cleavage Pathway .....	63
3.5.2 Variations of the <i>Ortho</i> Substituent .....	65
3.5.3 Electron Density of the Aryl Ring .....	70

3.5.4	Substituent at C $\alpha$ of the Amino Acid Subunit.....	71
3.5.5	Ionization Site.....	74
3.5.6	Fragmentation Pathways of Homologous Ns Amino Acids.....	83
3.5.7	Potential Competing Fragmentation Pathways.....	94
<b>CHAPTER 4</b>	<b>CONCLUSIONS.....</b>	<b>98</b>
<b>REFERENCES.....</b>		<b>101</b>

## LIST OF FIGURES

Figure 1.1. Product ion scans performed by space-based and time-based instruments. T = time, Q = quadrupole, q = collision cell. ....	3
Figure 1.2. Structures of 3-phenylbutanoic acid, succinic acid and benzoic acid. ....	6
Figure 1.3. Structures of acetylsalicylic acid, diclofenac, ibuprofen and penicillin G. ....	6
Figure 1.5. Structures of common protecting groups: Boc, Fmoc, Cbz and Ns. ....	23
Figure 3.1. List of Ns amino acids prepared. The symbol denotes an isotopic label ( <sup>13</sup> C, <sup>15</sup> N or <sup>18</sup> O). The yield of the isolated derivative is given in parentheses. ....	43
Figure 3.2. The ESI(-) mass spectrum of NsGly. ....	47
Figure 3.3. The ESI(-) mass spectrum of Ns[ <sup>18</sup> O]Gly. ....	47
Figure 3.4. Product ion mass spectra obtained by CID of A: deprotonated NsGly (CID 17%); B: <i>m/z</i> 212 ion formed in source (CID 18%); C: <i>m/z</i> 184 ion formed in source (CID 22%); D: <i>m/z</i> 157 ion formed in source (CID 26%). Unless indicated otherwise, the mass spectra presented in the figures were collected on the ion trap mass spectrometer. ....	49
Figure 3.5. Product ion mass spectra obtained by CID of A: deprotonated Ns[ <sup>34</sup> S]Gly (CID 18%); B: deprotonated NsGly (CID 18%). ....	50
Figure 3.6. Product ion mass spectra obtained by CID of A: deprotonated Ns[2,2- <sup>2</sup> H <sub>2</sub> ]Gly (CID 17%); B: <i>m/z</i> 214 ion formed in source (CID 18%); C: <i>m/z</i> 186 ion formed in source (CID 22%). ....	51
Figure 3.7. Product ion mass spectra obtained by CID of A: deprotonated Ns[1- <sup>13</sup> C]Gly (CID 18%); B: <i>m/z</i> 213 ion formed in source (CID 18%); C: <i>m/z</i> 184 ion formed in source (CID 22%). ....	51
Figure 3.8. Product ion mass spectra obtained by CID of A: deprotonated Ns[2- <sup>13</sup> C, <sup>15</sup> N]Gly (CID 17%); B: <i>m/z</i> 214 ion formed in source (CID 18%); C: <i>m/z</i> 186 ion formed in source (CID 22%). ....	52
Figure 3.9. Product ion mass spectra of ions obtained by CID of A: deprotonated Ns[ <sup>18</sup> O]Gly (CID 17%); B: <i>m/z</i> 215 ion formed in source (CID 19%); C: <i>m/z</i> 186 ion formed in source (CID 20%). ....	54
Figure 3.10. Product ion mass spectra obtained by CID of A: deprotonated mNsGly (CID 23%); B: deprotonated pNsGly (CID 22%). CID mass spectra of the <i>m/z</i> 186 (CID 24%) and <i>m/z</i> 186 (CID 18%) ions generated in source are shown as insets. ....	62

Figure 3.11. Triple quadrupole CID mass spectra of A: deprotonated NsGly (20 V cone; 10 eV); B: the $m/z$ 212 ion formed in source (30 V cone; 15 eV); C: the $m/z$ 186 ion formed in source (30 V cone; 15 eV).....	64
Figure 3.12. Product ion mass spectra obtained by CID of A: deprotonated 2FBsGly (CID 18%); B: $m/z$ 212 ion generated in source (CID 18%); C: $m/z$ 184 ion generated in source (CID 22%). .....	66
Figure 3.13. Product ion mass spectra obtained by CID of A: deprotonated 2BrBsGly (CID 18%); B: $m/z$ 212 ion formed in source (CID 20%).....	66
Figure 3.14. Product ion mass spectra obtained by CID of A: deprotonated 2,5-DCIBsGly (CID 20%); B: $m/z$ 246 ion formed in source (CID 20%); C: $m/z$ 218 ion formed in source (CID 20%).....	67
Figure 3.15. Mass spectra of deprotonated 2,5-DCIBsGly. A: ESI(-)MS of 2,5-DCIBsGly; B: CID spectrum of $[M - H]^-$ (CID 20%); C: CID spectrum of $[M + 2 - H]^-$ (CID 20%); D: CID spectrum of $[M + 4 - H]^-$ (CID 20%).....	67
Figure 3.16. Product ion mass spectrum obtained by CID of deprotonated 2CF <sub>3</sub> BsGly (CID 22%). CID mass spectrum of $m/z$ 209 (CID 22%) shown in inset. ....	69
Figure 3.17. Product ion mass spectra obtained by CID of A: deprotonated 2,4-DNsGly (CID 15%); B: $m/z$ 257 ion generated in source (CID 17%); C: $m/z$ 229 ion generated in source (CID 22%); D: $m/z$ 202 ion generated in source (CID 30%); E: $m/z$ 183 ion generated in source (CID 30%).....	71
Figure 3.18. Product ion mass spectra obtained by CID of A: deprotonated NsAla (CID 18%); B: $m/z$ 226 ion formed in source (CID 18%); C: $m/z$ 198 ion formed in source (CID 27%).....	73
Figure 3.19. Product ion mass spectra obtained by CID of A: deprotonated Ns2Aib (CID 18%); B: $m/z$ 240 ion formed in source (CID 18%).....	73
Figure 3.20. Product ion mass spectra obtained by CID of A: deprotonated Ns[2,3- <sup>13</sup> C <sub>2</sub> ]Ala (CID 18%); B: $m/z$ 228 ion formed in source (CID 18%); C: $m/z$ 200 ion formed in source (CID 26%).....	74
Figure 3.21. Product ion mass spectra obtained by CID of A: deprotonated NsGlyNH <sub>2</sub> (CID 17%); B: $m/z$ 194 ion formed in source (CID 30%).....	75
Figure 3.22. Product ion mass spectra obtained by CID of A: deprotonated NsNH <sub>2</sub> EtOH (CID 18%); B: $m/z$ 198 ion formed in source (CID 28%).....	76
Figure 3.23. Product ion mass spectrum obtained by CID of deprotonated NsGlyOEt (CID 22%).....	77

Figure 3.24. Product ion mass spectra obtained by CID of A: deprotonated NsSar (CID 17%); B: <i>m/z</i> 156 ion formed in source (CID 19%).	80
Figure 3.25. Product ion mass spectra obtained by CID of A: deprotonated NsSar (CID 17%); B: deprotonated Ns[1- <sup>13</sup> C]Sar (CID 15%); C: deprotonated Ns[2,2- <sup>2</sup> H <sub>2</sub> ]Sar (CID 14%).	80
Figure 3.26. Product ion mass spectra obtained by CID of A: deprotonated mNsSar (CID 20%); B: <i>m/z</i> 229 ion formed in source (CID 18%); C: <i>m/z</i> 186 ion formed in source (CID 24%).	82
Figure 3.27. Product ion mass spectra obtained by CID of A: deprotonated pNsSar (CID 18%); B: <i>m/z</i> 186 ion formed in source (CID 18%).	83
Figure 3.28. Product ion mass spectra obtained by CID of A: deprotonated NsβAla (CID 22%); B: <i>m/z</i> 226 ion formed in source (CID 29%); C: <i>m/z</i> 201 ion formed in source (CID 20%).	84
Figure 3.29. Product ion mass spectra obtained by CID of A: deprotonated Ns3Abu (CID 22%); B: <i>m/z</i> 201 ion formed in source (CID 21%); C: <i>m/z</i> 137 ion formed in source (CID 31%).	88
Figure 3.30. Product ion mass spectra obtained by CID of A: deprotonated Ns3Aib (CID 22%); B: <i>m/z</i> 201 formed in source (CID 21%); C: <i>m/z</i> 137 formed in source (CID 31%).	88
Figure 3.31. Product ion mass spectra obtained by CID of A: deprotonated Ns3APv (CID 22%); B: <i>m/z</i> 201 ion formed in source (CID 20%); C: <i>m/z</i> 203 ion formed in source (CID 21%).	89
Figure 3.32. Product ion mass spectrum obtained by CID of NsNMeβAla (CID 17%).	90
Figure 3.33. Product ion mass spectra obtained by CID of A: deprotonated Ns4Abu (CID 22%); B: deprotonated mNs4Abu (CID 22%); C: deprotonated mNsβAla (CID 22%).	92
Figure 3.34. Product ion mass spectra obtained by CID of A: deprotonated NsAsp (CID 20%); B: <i>m/z</i> 186 ion generated in source (CID 17%).	95
Figure 3.35. Hydrogen bond formation in deprotonated NsAsp.	95

## LIST OF SCHEMES

Scheme 1.1. Ionization and decarboxylation of phenylacetate.....	5
Scheme 1.2. McLafferty rearrangement of a radical cation.....	7
Scheme 1.3. General McLafferty rearrangement of even electron anions.....	8
Scheme 1.4. Fragmentation of lactate, an $\alpha$ -hydroxycarboxylate ion.....	9
Scheme 1.5. Fragmentation of deprotonated glycolic acid to give a hydroxycarbonyl anion, $m/z$ 45.....	9
Scheme 1.6. C2-C3 bond cleavage of 3-phenyllactate.....	10
Scheme 1.7. Base-catalyzed synthesis of 2-methyl-5-nitro-1 <i>H</i> -benzimidazole-3-oxide from <i>N</i> -(2,4-dinitrophenyl)alanine.....	11
Scheme 1.8. CID of deprotonated <i>N</i> -(2,4-dinitrophenyl)alanine to give a cyclized structure with $m/z$ 192. CID of $m/z$ 192 gives several product ions, which were also seen in the CID of the cyclized structure synthesized in solution.....	11
Scheme 1.9. Ionization of <i>p</i> -hydroxybenzoic acid to form either a carboxyphenolate or hydroxybenzoate anion.....	12
Scheme 1.10. Decarboxylation of <i>p</i> -hydroxybenzoic acid from the carboxybenzoate anion.....	13
Scheme 1.11. Smiles rearrangement where $Y^-$ is a nucleophilic function and $X^-$ is a good leaving group.....	13
Scheme 1.12. $S_N2$ reaction of $PhO(CH_2)_4O^-$ leading to the formation of $PhO^-$ and tetrahydrofuran.....	15
Scheme 1.13. <i>Ortho</i> cyclization. $X = OMe, F, Cl, Br, I$ .....	16
Scheme 1.14. Smiles rearrangements in negative ion MS. A: Deprotonated GW4511, a non-nucleoside reverse transcription inhibitor. B: Deprotonated 2-(4,6-dimethoxypyrimidin-2-ylsulfanyl)- <i>N</i> -phenylbenzamide, a derivative of commonly used pesticides.....	17
Scheme 1.15. Elimination of $SO_2$ from deprotonated sulfonic acid.....	18
Scheme 1.16. Three possible mechanisms for the loss of $SO_2$ from sulfonamides.....	19

Scheme 1.17. Fragmentation of hydrochlorothiazide, a sulfonamide diuretic, in ESI(-)MS/MS. <sup>50</sup> .....	20
Scheme 1.18. Fragmentation of a deprotonated sulfonamide antibiotic.....	21
Scheme 1.19. Fragmentation of deprotonated TsGly. ....	22
Scheme 1.20. Conversion of primary amines to the corresponding secondary amine through the Fukuyama-Mitsunobu reaction. P is a protecting group.....	24
Scheme 3.1. Synthesis of (2 <i>S</i> ,6 <i>S</i> )-diaminopimelic acid from protected 5-hydroxynorvaline. ....	39
Scheme 3.2. <i>N</i> -Protection and methylation of alanine (Ala). ....	40
Scheme 3.3. Synthesis of Ns protected amino acids.....	41
Scheme 3.4. Preparation of Ns[ <sup>18</sup> O]Gly from NsGlyOEt.....	44
Scheme 3.5. Methylation of Ns[2,2- <sup>2</sup> H <sub>2</sub> ]Gly to give Ns[2,2- <sup>2</sup> H <sub>2</sub> ]Sar.....	45
Scheme 3.6. Proposed <i>ortho</i> cyclization of deprotonated NsGly to form HONO and a sulfonamide ion at <i>m/z</i> 212. ....	53
Scheme 3.7. Suggested structures for the fragmentation pathway from <i>m/z</i> 212. ....	55
Scheme 3.8. Proposed structures for the fragmentation of <i>m/z</i> 212 to give <i>m/z</i> 141. <sup>18</sup> O labels are shown in red, <sup>2</sup> H labels are shown in blue.....	57
Scheme 3.9. Proposed structures for the fragmentation of <i>m/z</i> 212 to give <i>m/z</i> 140 and 72. <sup>18</sup> O labels are indicated in red, and <sup>2</sup> H labels are indicated in blue. ....	58
Scheme 3.10. Suggested structures for the fragmentation of <i>m/z</i> 259 to form <i>m/z</i> 138 and 76 initiated by sulfonamide rearrangement.....	60
Scheme 3.11. Dual bond cleavage of the <i>m/z</i> 259 ion leading to a sulfinate product ion at <i>m/z</i> 186, through the loss of CO <sub>2</sub> and HNCH <sub>2</sub> . ....	63
Scheme 3.12. Losses of HONO and EtOH from deprotonated NsGlyOEt. ....	78
Scheme 3.13. <i>N</i> -Alkylation and dual bond cleavage of deprotonated NsGlyOEt. ....	78
Scheme 3.14. Fragmentation process of deprotonated NsSar to give ions at <i>m/z</i> 226, 156 and 108.....	81
Scheme 3.15. Decarboxylation of mNsGly (R = H) or mNsSar (R = CH <sub>3</sub> ). ....	83

Scheme 3.16. Proposed structures for the fragmentation of deprotonated Ns $\beta$ Ala to form an ion at $m/z$ 226, followed by fragmentation to form at ion at $m/z$ 184. ....	85
Scheme 3.17. Proposed structure for the fragmentation of in-source $m/z$ 226 to form an ion at $m/z$ 172. ....	86
Scheme 3.18. Fragmentation of deprotonated Ns $\beta$ Ala ( $R^1 = R^2 = R^3 = H$ ), Ns3Abu ( $R^1 = CH_3, R^2 = R^3 = H$ ), Ns3Aib ( $R^1 = R^2 = H, R^3 = CH_3$ ), and Ns3Apv ( $R^1 = H, R^2 = R^3 = CH_3$ ) to form $m/z$ 201, and its subsequent fragmentation to $m/z$ 137 and 107. ....	87
Scheme 3.19. Fragmentation of the $[M - H]^-$ ion of NsNMe $\beta$ Ala (29a) to form 29b through the loss of HONO. ....	90
Scheme 3.20. Fragmentation of the Ns4Abu anion to form the $m/z$ 201 ion and a neutral 5-membered lactone. ....	92
Scheme 3.21. Competing fragmentation processes of deprotonated NsAsp forming complementary ions at $m/z$ 201 and 115. ....	96

## LIST OF TABLES

Table 3.1. Product ions from CID of deprotonated Ns- $\alpha$ -amino acids. ....	46
Table 3.2. Experimental gas phase acidities. ....	69

## ABSTRACT

The identification of specific compounds in biological and environmental samples by mass spectrometry requires the interpretation of ion fragmentation patterns. To overcome the limited understanding of negative-ion fragmentation processes, the collision-induced dissociation (CID) of 2-nitrobenzenesulfonyl (Ns) derivatives of amino acids were investigated. A library of Ns derivatives incorporating isotopic labels and a range of structural variations was prepared and characterized. The ESI(-) mass spectra collected on an ion trap mass spectrometer showed intense peaks corresponding to the deprotonated Ns amino acids. CID experiments established precursor-product ion relationships in four fragmentation pathways of Ns- $\alpha$ - and Ns- $\beta$ -amino acid anions. The fragmentation pathways proposed were consistent with isotopic labeling results, the structural variations of the Ns derivatives, and product ions formed by CID of ions generated in source. A novel loss of an *ortho* substituent (NO<sub>2</sub>, F, Cl or Br) on the aromatic ring was accompanied by cyclization and subsequent successive losses of CO, HCN and SO<sub>2</sub>. A second fragmentation pathway of the ion formed by *ortho* cyclization involved a rearrangement, which resulted in the loss of one oxygen atom originally bonded to sulfur. At higher collision energies provided by a triple quadrupole mass spectrometer, the deprotonated Ns  $\alpha$ -amino acids also fragmented via rearrangement of the sulfonamide group and a dual bond cleavage pathway. Similarly, dual bond cleavage and *ortho* cyclization were observed as prominent pathways for the fragmentation of deprotonated Ns- $\beta$ -amino acids. Overall, the observation of specific fragmentation pathways correlated with anion structure and ionization site. However, the observation of only one of four possible fragmentation processes in the mass spectrum of the Ns derivative of an amino dicarboxylic acid indicated that functional group interactions must also be considered in the interpretation and prediction of fragmentation processes.

## LIST OF ABBREVIATIONS USED

2Aib	2-aminoisobutyric acid
3Abu	3-aminobutyric acid
3Aib	3-aminoisobutyric acid
3Apv	3-aminopivalic acid
4Abu	4-aminobutyric acid
Ala	alanine
Asp	aspartic acid
$\beta$ Ala	$\beta$ -alanine
Boc	<i>tert</i> -butoxycarbonyl
Bs	benzenesulfonyl
Cbz	carboxybenzyl
CI	chemical ionization
CID	collision induced dissociation
d	doublet
DCM	dichloromethane
dd	doublet of doublets
ddd	doublet of doublets of doublets
DNs	dinitrobenzenesulfonyl
DNP	dinitrophenyl
dt	doublet of triplets
EI	electron impact
ESI	electrospray ionization
eV	electron volt
EWG	electron withdrawing group
Fmoc	fluorenylmethoxycarbonyl
Gly	glycine
GlyOEt	glycine ethyl ester
GlyNH <sub>2</sub>	glycinamide
GPA	gas phase acidity
IM-MS	ion mobility mass spectrometry
<i>J</i>	coupling constant
LC	liquid chromatography
m	multiplet
[M – H] <sup>-</sup>	deprotonated molecule
mNs	3-nitrobenzenesulfonyl
mp	melting point
MS	mass spectrometry
MS/MS	tandem mass spectrometry
<i>m/z</i>	mass to charge ratio
NHEtOH	2-aminoethanol
NMR	nuclear magnetic resonance
Ns	2-nitrobenzenesulfonyl
ppb	parts per billion
Ph	phenyl

pKa	negative logarithm of the acid dissociation constant
pNs	4-nitrobenzenesulfonyl
Q	quadrupole
q	quartet or collision cell
QqQ	triple quadrupole
s	singlet or second
Sar	sarcosine
t	triplet
TLC	thin layer chromatography
Ts	tosyl
u	unified atomic mass units

## ACKNOWLEDGEMENTS

I am very fortunate to have had the assistance of many people throughout my time at Dalhousie University. First, I would like to extend my sincere appreciation to my supervisor Dr. Robert White for his guidance, encouragement and patience over the last two years. I would also like to thank my supervisory committee, Dr. Jean Burnell and Dr. David Jakeman for their advice and helpful discussions.

I would like to thank Dr. Mike Lumsden of the NMR<sup>3</sup> for his assistance with NMR experiments and Xiao Feng of the Dalhousie Mass Spectrometry Laboratory for assistance collecting ESI-MS. I would also like to express my gratitude to Dr. J. Stuart Grossert for his helpful suggestions and valuable feedback regarding this project.

I would also like to thank the current and former members of the White group for their company and collaboration. Particularly, I would like to extend special thanks to Dr. Elizabeth Gillis for her work on the theoretical computations for this project. Thank you also to Christie Hollingdale, without whose company and helpful discussions I would not have such an enjoyable time at Dalhousie University.

Finally, I would like to thank my friends and family for their support and encouragement throughout my graduate studies. I would not have completed this journey if not for my parents, who instilled in me a natural curiosity and drive to succeed, and constantly provided me with the love and encouragement I needed to reach my goals. Thank you also to John Camardese, who pushed me to become a better scientist, and kept me going until I achieved my goals.

## CHAPTER 1 INTRODUCTION

Tandem mass spectrometry (MS/MS) is a powerful analytical tool used to identify and monitor compounds. With applications in forensics, environmental analysis and drug testing, MS/MS has improved public safety, pointed out potential environmental contaminants, and contributed to controlling the illegal use of performance enhancing substances in sports.<sup>1-3</sup> As new designer drugs, therapeutics and other substances are developed, broader and more comprehensive analytical methods are needed.<sup>1,3</sup>

The determination of substances by mass spectrometry relies first on the unambiguous identification of unknowns. Identifications are based on characteristic fragmentation patterns collected by mass spectrometry. Often, comparison of the mass fingerprint of the unknown with a library of reference data establishes the identity of the unknown. In other instances, structures of unknown substances must be deduced from accurate mass and fragmentation, a more expensive and labor-intensive task.

A fundamental understanding of fragmentation processes needed to interpret MS/MS spectra, particularly those of even-electron, negative ions, is not very well developed. As a contribution to developing a more comprehensive approach, an investigation of the gas phase reactivity of anions derived from 2-nitrobenzenesulfonyl (Ns) protected amino acids is presented. During the investigation, mass spectrometric and isotopic experiments provided evidence for a novel fragmentation process and the occurrence of several distinct fragmentation pathways originating from a single, multifunctional anion.

## 1.1 Mass Spectrometry and Fragmentation Processes

The fragmentation of odd electron or radical ions, generated by electron ionization (EI), has been extensively studied and libraries containing hundreds of thousands of compounds are available for identification of molecules.<sup>4,5</sup> However, polar and non-volatile compounds are better suited for analysis by electrospray ionization (ESI) or atmospheric pressure chemical ionization, and there is a limited understanding of fragmentation and rearrangement of the even electron ions formed by these processes.<sup>6</sup> With the exception of peptides,<sup>7</sup> there are no comprehensive compound libraries for the identification of even electron ions.

Under the high energy conditions of EI, many fragmentation processes are observed,<sup>8</sup> but the low energy conditions of ESI typically do not lead to fragmentation of even electron ions. While this assists the determination of the mass of protonated and deprotonated molecules, it provides no information on the structure of the ion. Tandem mass spectrometry (MS/MS) incorporating collision-induced dissociation (CID) is therefore necessary to form and analyze product ions. The fragmentation of even electron ions often shows the loss of a neutral molecule and the formation of ion-molecule complexes.<sup>9</sup>

CID processes occur when an ion undergoes energy transfer upon collision with atoms of a noble gas, typically helium or argon. MS/MS can be performed using a spatial configuration in a triple quadrupole spectrometer or in a time-dependent manner using ion trap, orbitrap or Fourier transform ion cyclotron resonance mass spectrometers (Figure 1.1).<sup>8</sup> MS/MS in space requires a quadrupole to select the ion, a collision cell through which the ion must travel, and another quadrupole to scan for the product ions. In ion-trap

mass spectrometers, the selected ion is confined to a region of space for CID and product ions are expelled from the trap for detection. Since all collisions and ion selection take place in the same space, CID can be repeated on successive product ions (i.e., MS<sup>n</sup> experiments, n ≥ 2).

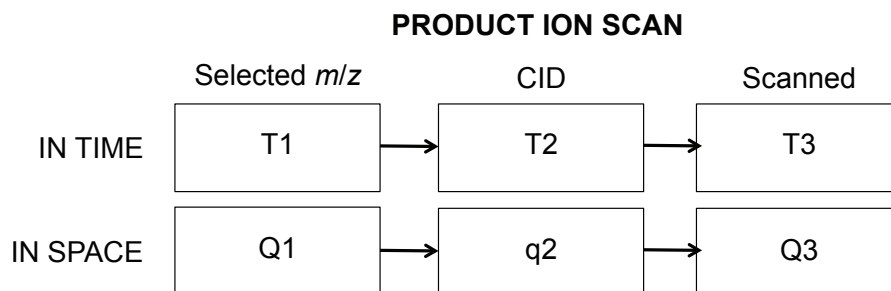


**Figure 1.1.** Product ion scans performed by space-based and time-based instruments. T = time, Q = quadrupole, q = collision cell.

Ions generated in mass spectrometry can be classified in three general ways. Those with a lifetime greater than  $10^{-6}$  s are quite stable and will reach the detector before fragmenting, whereas ions with a short lifetime fragment before leaving the ion source, and only their fragments are detected.<sup>8</sup> Metastable ions, with an intermediate lifetime, are stable enough to be selected by the first analyzer, but have enough internal energy to be fragmented before they reach the second analyzer. Under normal conditions, the probability of ions falling in this category is less than 1%, but this number can be improved using collision-induced dissociation.

The CID process occurs in two main steps.<sup>10</sup> First, collisions between the ions and the neutral targets, usually noble gas atoms, convert translational energy into internal

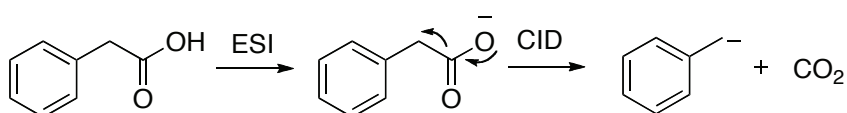
energy and create excited state ions. Generally, the target gas used is helium or argon, which have higher energy excited states, so the ion has a greater chance of becoming excited. In the second step, the excited ion undergoes unimolecular decomposition. Because ion dissociation is slow with respect to ion formation and excitation, the excited ion has time to distribute energy along all internal modes with equal probability. This leads to cleavage at sites with the weakest bonds.<sup>8</sup>

Both ion trap and quadrupole mass spectrometers use low energy collisions (5-40 eV), while magnetic sector mass spectrometers utilize high-energy collisions (greater than 100 eV) to generate fragment ions. Ion traps generally use helium as the collision gas, whereas quadrupole mass spectrometers use argon. Since helium has a low mass, less translational energy is converted to internal energy per collision and usually only the lowest energy fragmentation pathways are observed. By comparison, the higher energy collisions with argon often lead to the observation of multiple fragmentation pathways.<sup>10</sup>

## **1.2 Negative-ion Mass Spectrometry and Fragmentation Processes**

ESI is a technique that involves applying a strong electric field to a solution of analyte.<sup>8</sup> As the solution exits a charged capillary tube, it breaks into highly charged droplets containing a high concentration of analyte. After heating these charged droplets to remove the solvent, the ionized analyte is left in the gas phase and can be analyzed using mass spectrometry. Gas-phase anions are readily formed by molecules containing functional groups that are acidic in aqueous solutions, such as carboxylic acids (pKa 4-5), phenols (pKa 10), sulfonic acids (pKa -2 to -3) and sulfonamides (pKa 8-10).<sup>11,12</sup>

The fragmentation reactions of negative even-electron ions have been classified into four main processes.<sup>9</sup> First, homolytic cleavage reactions can occur, involving the loss of a radical and the formation of a radical anion. Second, an initial ion-neutral complex can be formed, which can lead to a number of different reactions, including displacement of the anion. Decarboxylation falls into this category (Scheme 1.1). Other reactions that can take place include the anion deprotonating a neutral part of the molecule, and rearrangements. The latter includes displacement of an anion by an S<sub>N</sub>2 type reaction occurring between the initially formed anion and a neutral part of the molecule.



**Scheme 1.1.** Ionization and decarboxylation of phenylacetate.

## 1.2.1 Carboxylic Acids

### 1.2.1.1 Decarboxylation of Deprotonated Carboxylic Acids

Decarboxylation of carboxylic acids by CID after negative ion mode soft ionization mass spectrometry conditions has been shown to be a common process.<sup>9,13-17</sup> However, only carboxylate ions with certain structural characteristics will show a neutral loss of 44 u, corresponding to CO<sub>2</sub>.<sup>13</sup> Carboxylate ions that have a phenyl group or conjugated system at the β position, as in phenylacetate, readily undergo decarboxylation (Scheme 1.1).<sup>9,13,14</sup> The anion produced by decarboxylation is resonance stabilized, and

the loss of CO<sub>2</sub> proceeds with a small energy barrier and is a favourable reaction.<sup>13</sup> Carboxylic acids two carbons removed from a conjugated system (e.g., 3-phenylbutanoic acid) and dicarboxylic acids (e.g., succinic acid) also undergo decarboxylation, but stabilization of the charge in the product ion is less apparent. Decarboxylation is observed when the carboxyl group is bonded directly to an sp<sup>2</sup> carbon (e.g., benzoic acid). The structures of these compounds are shown in Figure 1.2.

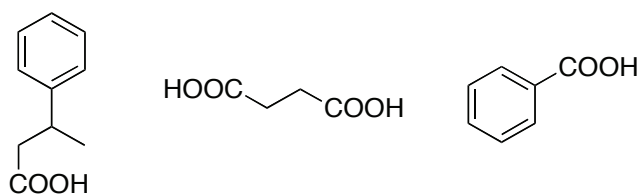


**Figure 1.2.** Structures of 3-phenylbutanoic acid, succinic acid and benzoic acid.

The loss of CO<sub>2</sub> can be used for the characterization of many pharmaceuticals. Acetylsalicylic acid decarboxylates after the loss of H<sub>2</sub>C=C=O in negative ion MS.<sup>6</sup> Other non-steroidal anti-inflammatory drugs such as diclofenac<sup>18,19</sup> and ibuprofen<sup>19,20</sup> also readily undergo decarboxylation. Most penicillins also show the loss of CO<sub>2</sub> as a major fragmentation process.<sup>21</sup> The structures of these compounds are shown in Figure 1.3.

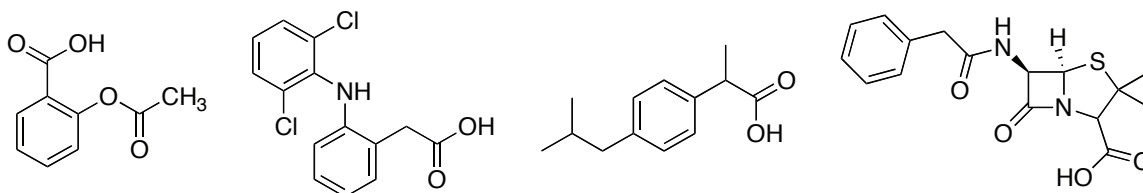
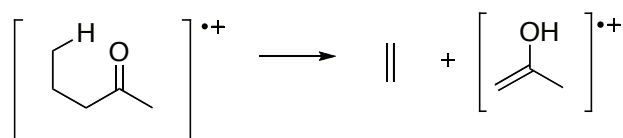


**Figure 1.3.** Structures of acetylsalicylic acid, diclofenac, ibuprofen and penicillin G.

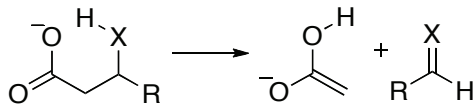
### 1.2.1.2 McLafferty Rearrangements of Ions

The McLafferty rearrangement of radical cations<sup>22</sup> was first described in 1959 and has become one of the most studied processes in mass spectrometry. The radical cation rearrangement requires a carbonyl group with at least one  $\gamma$ -hydrogen atom (Scheme 1.2). Cases involving even electron ions have also been studied.<sup>23–25</sup> Zollinger and Seibl<sup>26</sup> established classification criteria for even electron McLafferty rearrangements. The reaction must involve the transfer of a hydrogen atom  $\gamma$  to the charged site through a 6-membered, cyclic transition state, the hydrogen transfer must be experimentally verified, and the product ion must be linked to the precursor ion through CID.



**Scheme 1.2.** McLafferty rearrangement of a radical cation.

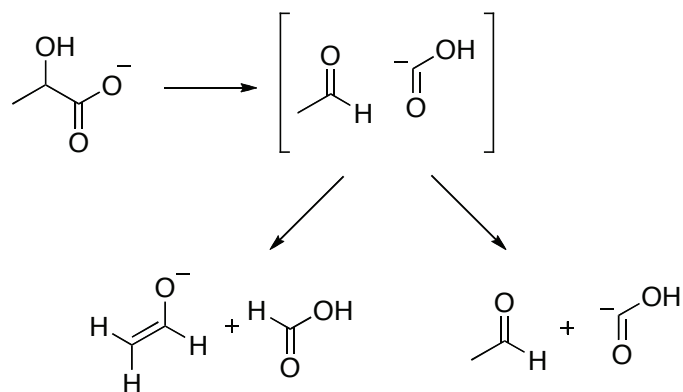
A process that meets these criteria has been seen in the fragmentation of carboxylate ions.<sup>27</sup> A common fragment ion at  $m/z$  59, assigned to  $[\text{C}_2\text{H}_3\text{O}_2]^-$ , was seen in the mass spectra of many carboxylic acids. Further investigation showed that given a suitably acidic proton in the  $\gamma$  position, a McLafferty-type rearrangement took place as the major fragmentation pathway, giving  $m/z$  59 as an abundant product anion. The common process for 3-hydroxybutanoic acid ( $\text{R} = \text{CH}_3$ ,  $\text{X} = \text{OH}$ ), 3-aminopropanoic acid ( $\text{R} = \text{H}$ ,  $\text{X} = \text{NH}_2$ ), and 4-cyanobutanoic acid ( $\text{R} = \text{H}$ ,  $\text{X} = \text{CH}_2\text{CN}$ ) is described in Scheme 1.3. These three simple examples meet the criteria for the McLafferty-type rearrangement of a carboxylate ion.



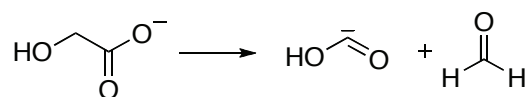
**Scheme 1.3.** General McLafferty rearrangement of even electron anions.

### 1.2.1.3 $\alpha$ -Hydroxy- and $\alpha$ -Aminocarboxylic Acids

In contrast to the McLafferty-type rearrangement of  $\beta$ -hydroxy- or  $\beta$ -aminocarboxyl anions,  $\alpha$ -hydroxy- and  $\alpha$ -aminocarboxyl anions behave differently. Greene *et al.*<sup>28</sup> showed that when there is a hydroxyl group  $\alpha$  to a carboxyl group, either a neutral loss of 46 u will occur, corresponding to  $\text{HCO}_2\text{H}$ , or an ion will be seen at  $m/z$  45, corresponding to the hydroxycarbonyl anion (Scheme 1.4). As illustrated for lactate, the fragmentation reaction involves proton transfer and formation of an ion-neutral complex upon C-C bond cleavage. Dissociation of the ion-neutral complex leads to the  $m/z$  45 anion, whereas proton transfer before dissociation generates formic acid consistent with the observed loss of 46 u and the formation of the complementary enolate ion. The CID of deprotonated glycolic acid also gave a product ion at  $m/z$  45 (Scheme 1.5).

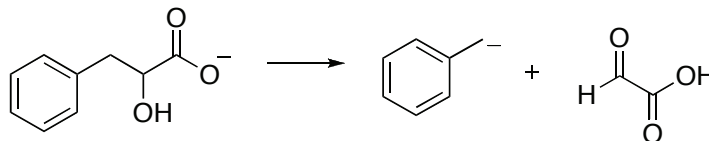


**Scheme 1.4.** Fragmentation of lactate, an  $\alpha$ -hydroxycarboxylate ion.



**Scheme 1.5.** Fragmentation of deprotonated glycolic acid to give a hydroxycarbonyl anion,  $m/z$  45.

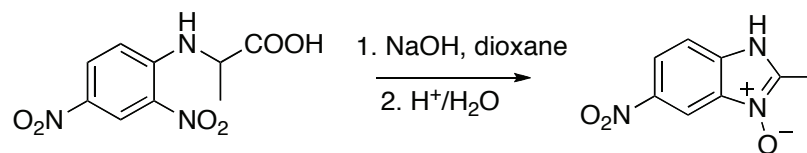
When a  $\beta$ -phenyl substituent was present, as in 3-phenyllactic acid, C1-C2 bond cleavage giving the neutral loss of 46 is still seen, but other fragmentation pathways also occur.<sup>28</sup> C2-C3 bond cleavage giving the benzyl anion and glyoxylic acid was likely due to the stabilizing effect of the phenyl substituent (Scheme 1.6). The loss of H<sub>2</sub>O was likely due to the more acidic benzylic protons in comparison with the methyl protons of the lactate ion. When the phenyl substituent was in the  $\alpha$ -position, the major fragmentation pathway was decarboxylation.<sup>28</sup>



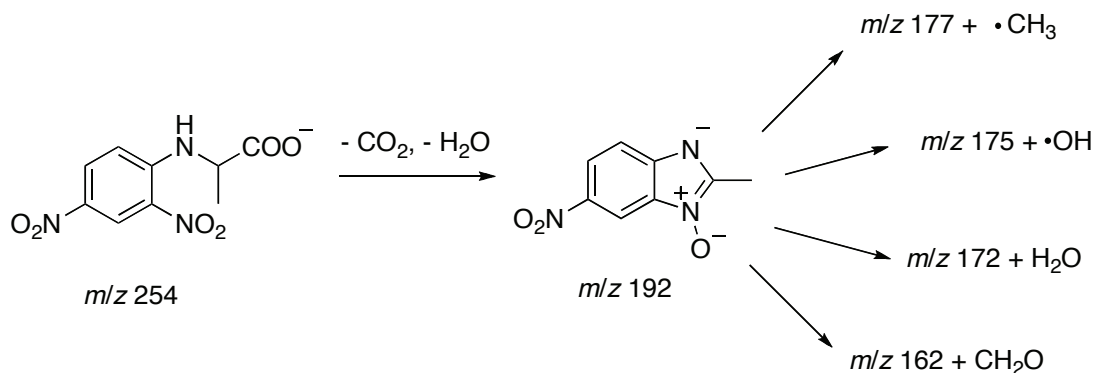
**Scheme 1.6.** C2-C3 bond cleavage of 3-phenyllactate.

#### 1.2.1.4 *N*-(2,4-Dinitrophenyl)amino Acids

Carboxylic acids with other  $\alpha$  substituents are obtained by derivatization of amino acids. *N*-(2,4-Dinitrophenyl)- (DNP) amino acids are of interest because of their use in protein sequencing, for which Sanger received a Nobel Prize in 1958.<sup>29,30</sup> ESI(-)MS/MS was used to investigate these compounds.<sup>31</sup> CID of deprotonated DNP-alanine ( $m/z$  254) gave product ions at  $m/z$  210 and 192, suggesting that the fragmentation occurs in two steps, through successive losses of  $\text{CO}_2$  and  $\text{H}_2\text{O}$ . The CID spectrum of the  $[\text{M} - \text{H}]^-$  ion of 2-methyl-5-nitro-1*H*-benzimidazole-3-oxide ( $m/z$  192), obtained from base-promoted cyclization in solution<sup>31</sup> (Scheme 1.7), gave the same product ions as an  $\text{MS}^3$  experiment on the  $m/z$  192 ion derived from deprotonated DNP-alanine, suggesting that the cyclization reaction in the gas phase (Scheme 1.8) is analogous to the reaction in solution. In this instance, the nitroaryl substituent creates reaction pathways that are not observed in simple aliphatic and aromatic carboxylic acids. Whether this example provides a general pathway for the fragmentation of aromatic nitro derivatives of amino acids requires MS/MS studies of additional compounds, such as Ns amino acids.



**Scheme 1.7.** Base-catalyzed synthesis of 2-methyl-5-nitro-1*H*-benzimidazole-3-oxide from *N*-(2,4-dinitrophenyl)alanine.



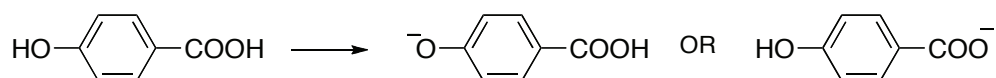
**Scheme 1.8.** CID of deprotonated *N*-(2,4-dinitrophenyl)alanine to give a cyclized structure with *m/z* 192. CID of *m/z* 192 gives several product ions, which were also seen in the CID of the cyclized structure synthesized in solution.

## 1.2.2 Alcohols and Phenols

### 1.2.2.1 Ionization

Schröder and colleagues<sup>32</sup> studied the behavior of *p*-hydroxybenzoic acid in negative mode mass spectrometry. While there has been some debate over whether the hydroxybenzoate or carboxyphenolate anion is formed in the gas phase<sup>33,34</sup> (Scheme 1.9), Schröder showed that in aprotic solvents, the carboxyphenolate anion is preferentially formed, while in protic solvents, the hydroxybenzoate anion is more dominant. Ion

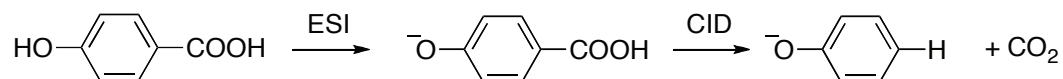
mobility mass spectrometry (IM-MS) can be used to separate conformational isomers based on their shapes, but also can differentiate between ions of the same size due to different strength of interactions between the ions and the neutral gas.<sup>35</sup> Since the hydroxybenzoate ion has stronger ion-dipole interactions with the nitrogen gas used in IM-MS than the carboxyphenolate ion and will have a slower arrival time, IM-MS can be used to assign the arrival times of the two ions in different solvents. To differentiate between the anions, the methyl ester and *p*-methoxybenzoic acid were also tested, as the methyl ester will only form the carboxyphenolate ion, and methoxybenzoic acid will only form the hydroxybenzoate ion.<sup>32</sup> It was determined that in the gas phase, the carboxyphenolate ion is energetically favoured because its charge is largely delocalized, stabilizing the ion, whereas the charge is mostly localized at the carboxyl group in the hydroxybenzoate ion. However, the fraction of hydroxybenzoate ion will increase in protic solvents due to solvation effects.



**Scheme 1.9.** Ionization of *p*-hydroxybenzoic acid to form either a carboxyphenolate or hydroxybenzoate anion.

Both anions undergo decarboxylation; however, the process is more facile with the carboxyphenolate ion (Scheme 1.10). Calculations showed that the intact carboxylic acid in the carboxyphenolate ion undergoes decarboxylation through a 4-membered ring, which is energetically more favourable than decarboxylation of the hydroxybenzoate ion.

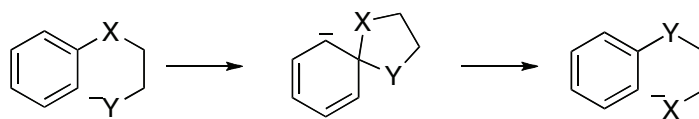
The resulting phenoxide ion formed from the carboxyphenolate is also preferred over the 4-hydroxy phenoxide anion formed through decarboxylation of hydroxybenzoate.



**Scheme 1.10.** Decarboxylation of *p*-hydroxybenzoic acid from the carboxybenzoate anion.

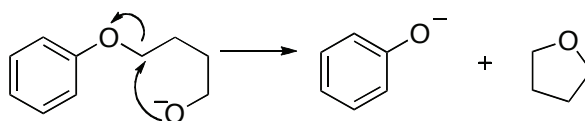
### 1.2.2.2 Smiles Rearrangement

The Smiles rearrangement, which is summarized in Scheme 1.11, has been shown to occur both in solution and the gas phase.<sup>36-41</sup> The rearrangement is characterized by an intramolecular nucleophilic attack on an aromatic ring, resulting in the displacement of a leaving group from the same carbon.<sup>36</sup> This reaction requires a good leaving group (X) and a strong nucleophile (Y). Activation in the aromatic ring by an electron withdrawing group (EWG) such as NO<sub>2</sub>, SO<sub>3</sub>H or a halogen is required in the solution phase; however, the gas-phase Smiles rearrangement has been shown to occur without EWG substitution on the aromatic ring.<sup>38,40,41</sup>



**Scheme 1.11.** Smiles rearrangement where Y<sup>-</sup> is a nucleophilic function and X<sup>-</sup> is a good leaving group.

To demonstrate the participation of the gas-phase Smiles rearrangement, Eichinger and colleagues<sup>40</sup> used isotopic labeling to study the fragmentation of  $\text{PhO}(\text{CH}_2)_n\text{O}^-$  ions. Alcohols were ionized using chemical ionization (CI).  $\text{H}_2\text{O}$  was bombarded with 70 eV electrons, which formed reactive negative ions ( $\text{OH}^-$ ,  $\text{H}^-$  or  $\text{O}^-$ ). Reaction of the negative ions with the neutral analyte led to deprotonation. When  $n = 2-4$ , a phenoxide ion was formed through CID, but whether this occurred with participation of Smiles rearrangement, or only through an  $\text{S}_{\text{N}}2$  reaction (Scheme 1.12) was not certain. The mass spectra of  $\text{PhO}(\text{CH}_2)_n^{18}\text{O}^-$  ( $n = 2$ ) showed that  $\text{Ph}^{16}\text{O}^-$  and  $\text{Ph}^{18}\text{O}^-$  were produced in equal amounts, suggesting that the Smiles rearrangement occurred before fragmentation. When  $n = 4$ , only  $\text{Ph}^{16}\text{O}^-$  was seen, suggesting that fragmentation occurred through a  $\text{S}_{\text{N}}2$  type reaction without participation of the Smiles rearrangement. However, when  $n = 3$ , a 3:2 ratio of  $\text{Ph}^{16}\text{O}^-$  and  $\text{Ph}^{18}\text{O}^-$  was observed, indicating that the Smiles rearrangement and  $\text{S}_{\text{N}}2$  reaction had similar reaction rates at the intermediate carbon chain length. This observation was further supported by the mass spectrum of  $\text{PhS}(\text{CH}_2)_n\text{O}^-$ . When  $n = 2$ , an equal amount of  $\text{PhS}^-$  and  $\text{PhO}^-$  was seen, indicating participation of the Smiles rearrangement. However, when  $\text{PhO}(\text{CH}_2)_n\text{S}^-$  ( $n = 2-4$ ) was fragmented, no Smiles rearrangement occurred,<sup>40</sup> presumably because the sulfur is not a strong enough nucleophile in the gas phase.<sup>42</sup>

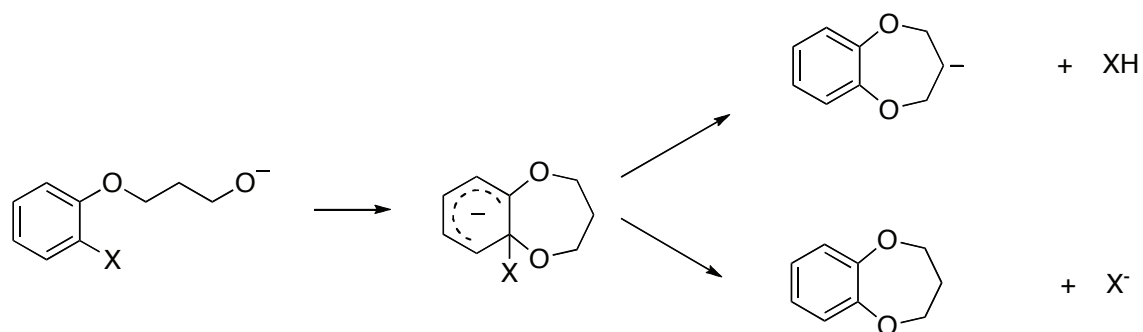


**Scheme 1.12.**  $S_N2$  reaction of  $\text{PhO}(\text{CH}_2)_4\text{O}^-$  leading to the formation of  $\text{PhO}^-$  and tetrahydrofuran.

Wang and colleagues<sup>38</sup> used a combination of experiment and theory to explore the mechanism of the first step of the Smiles rearrangement for the fragmentation of  $\text{PhO}(\text{CH}_2)_n\text{O}^-$ . When  $n = 2$ , the Smiles rearrangement was kinetically favoured, which supports the conclusions made by Eichinger and colleagues.<sup>40</sup> Computational work showed that after the formation of the cyclic Smiles intermediate, ring opening occurred followed by fragmentation to form  $\text{PhO}^-$  and oxirane. When  $n = 3$ , the Smiles rearrangement was the major process, but was in competition with an  $S_N2$  reaction. The energy barriers for the two mechanisms are similar,  $69 \text{ kJ mol}^{-1}$  for the  $S_N2$  reaction vs.  $61 \text{ kJ mol}^{-1}$  for the Smiles rearrangement, explaining why both reactions can occur.

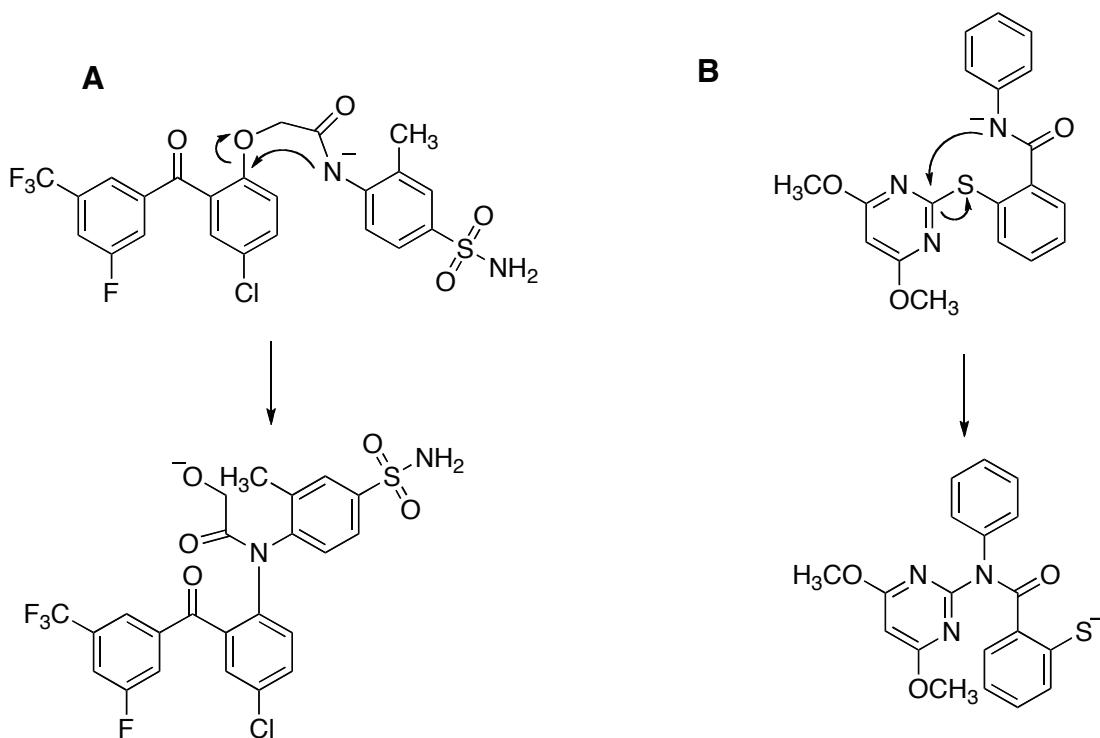
A later study by Eichinger and colleagues<sup>41</sup> investigated the effect of ring substitution on the Smiles rearrangement. Mass spectra were collected for  $\text{XC}_4\text{H}_6\text{O}(\text{CH}_2)_3^{18}\text{O}^-$ , where X was a variety of different substituents at the *ortho*, *meta*, or *para* position. When a substituent at the *ortho* position was a good leaving group (such as OMe, F, Cl, Br, I), cyclization at the *ortho* position was facile (Scheme 1.13), competing with the Smiles rearrangement. If the anion of the substituent (X) was  $\text{MeO}^-$  or  $\text{F}^-$ , both good leaving groups and strong bases, deprotonation (loss of XH) occurred, with almost no  $\text{X}^-$  seen. If the substituent on the aromatic ring was a good leaving group and a very weak base ( $\text{Cl}^-$ ,  $\text{Br}^-$ ,  $\text{I}^-$ ), deprotonation to give a neutral loss of XH was not seen, but a

product ion corresponding to  $X^-$  was present. Compounds with substituents at the *meta* or *para* positions did not show this *ortho* cyclization.



**Scheme 1.13.** *Ortho* cyclization.  $X = \text{OMe}, \text{F}, \text{Cl}, \text{Br}, \text{I}$ .

The Smiles rearrangement has also been observed in more complicated pharmaceutical compounds, for example, a series of benzophenone derivatives under evaluation for use as non-nucleoside reverse transcriptase inhibitors.<sup>39</sup> GW4511 has been shown to undergo a Smiles rearrangement by nucleophilic attack of the acetamide nitrogen on the aromatic ring, leading to elimination of an  $\alpha$ -lactone or  $\text{CO}$  and  $\text{CH}_2\text{O}$  (Scheme 1.14.A). 4,6-Dimethoxypyrimidine derivatives, which are commonly used as pesticides, also undergo a Smiles rearrangement in negative ion MS prior to fragmentation (Scheme 1.14.B).<sup>37</sup>

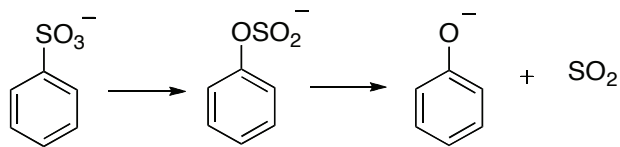


**Scheme 1.14.** Smiles rearrangements in negative ion MS. **A:** Deprotonated GW4511, a non-nucleoside reverse transcription inhibitor. **B:** Deprotonated 2-(4,6-dimethoxypyrimidin-2-ylsulfanyl)-*N*-phenylbenzamide, a derivative of commonly used pesticides.

### 1.2.3 Sulfonic Acids

For most sulfonic acids, the characteristic fragmentation pattern by MS is the loss of  $\text{SO}_2$ .<sup>43–45</sup> Binkley and colleagues<sup>43</sup> studied the fragmentation of aromatic sulfonic acids, and found that these also lost  $\text{SO}_2$  as the major fragmentation to form a phenoxide ion. They proposed that this occurred first through a rearrangement of the sulfonyl group, followed by elimination of  $\text{SO}_2$  (Scheme 1.15). A study by Zhang<sup>45</sup> showed that this

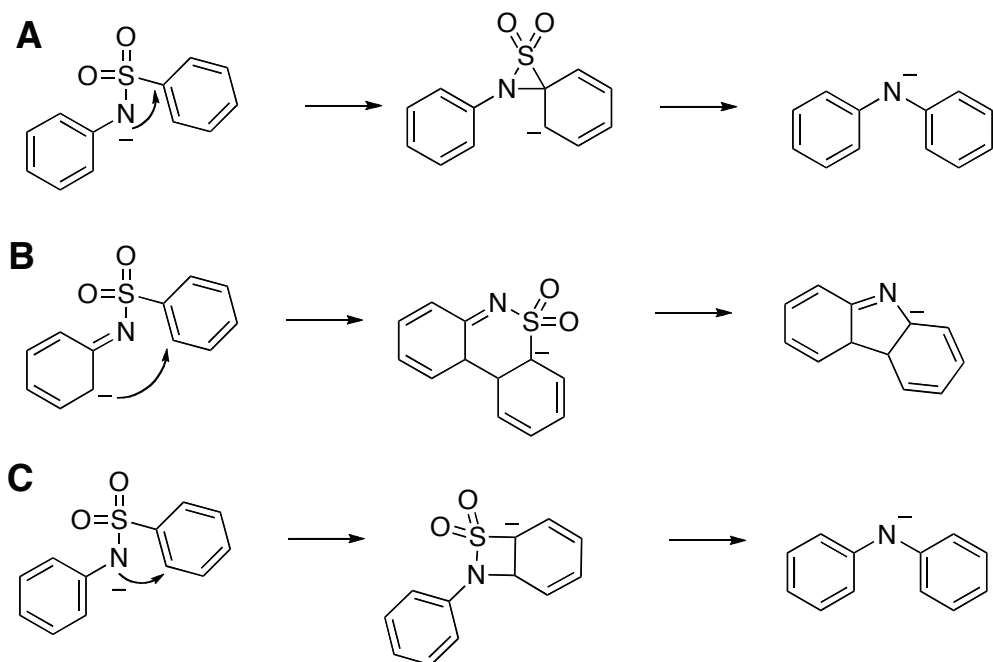
rearrangement could occur through both heterolytic and homolytic cleavage; however, homolytic cleavage has the lower energy barrier.



**Scheme 1.15.** Elimination of SO<sub>2</sub> from deprotonated sulfonic acid.

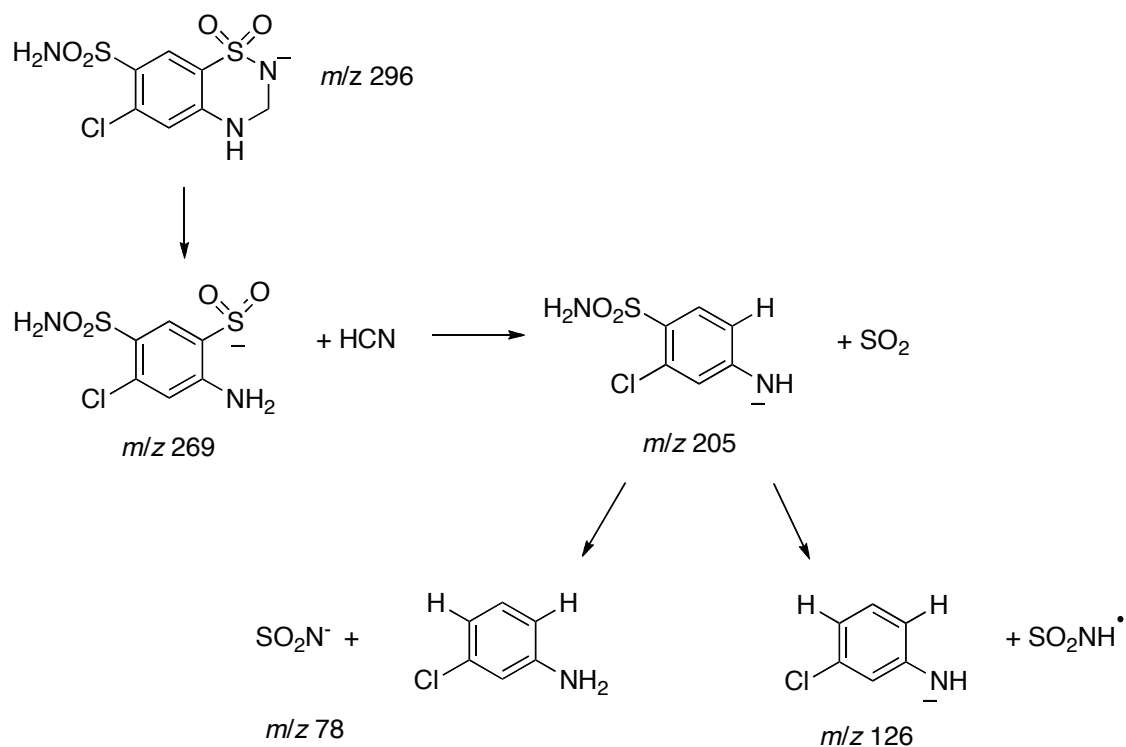
#### 1.2.4 Sulfonamides

Elimination of SO<sub>2</sub> from sulfonamides has also been studied.<sup>46-50</sup> Hu and colleagues<sup>49</sup> examined different mechanisms of SO<sub>2</sub> elimination from aromatic sulfonamides and found that nucleophilic attack of the N at C1 of the phenyl ring is the most favourable reaction. Xiang<sup>46</sup> examined three different possible mechanisms of SO<sub>2</sub> elimination through experimental and computational techniques (Scheme 1.16). Pathway A involves a nucleophilic attack of nitrogen on C1 of the phenyl group, followed by a rearrangement leading to the loss of SO<sub>2</sub>. Pathway B involves the nucleophilic attack of the phenyl group, forming a 6-membered ring prior to SO<sub>2</sub> elimination. Pathway C involved the attack of N of an adjacent carbon atom on the phenyl ring, forming a 4-membered ring. Xiang found that when the substituent on the N atom is aromatic, all three pathways are possible; however, Pathway A has the most favourable energy barrier. When the substituent on N is not aromatic, pathway B is not possible, and Pathway A is still the most favourable.



**Scheme 1.16.** Three possible mechanisms for the loss of SO<sub>2</sub> from sulfonamides.

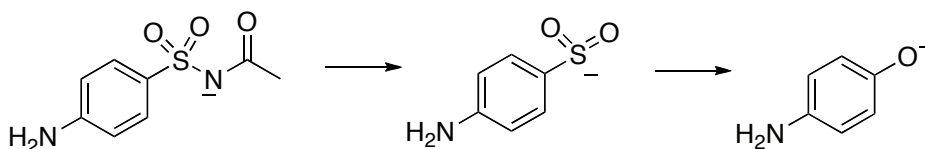
The sulfonamide group is commonly found in drugs and drug candidates. Diuretic drugs increase the excretion of water from the body, and are often misused in sports to either aid in weight loss or mask the consumption of other illegal drugs. Diuretics that have been illegally added to dietary supplements to increase weight loss are also of concern.<sup>51</sup> MS analysis is the standard method for identifying diuretics in various analytes, and fragmentation schemes for sulfonamide diuretics, such as hydrochlorothiazide, have been published (Scheme 1.17). Screening for these fragmentation patterns allows fast and selective identification of many doping agents.



**Scheme 1.17.** Fragmentation of hydrochlorothiazide, a sulfonamide diuretic, in ESI(-)MS/MS.<sup>50</sup>

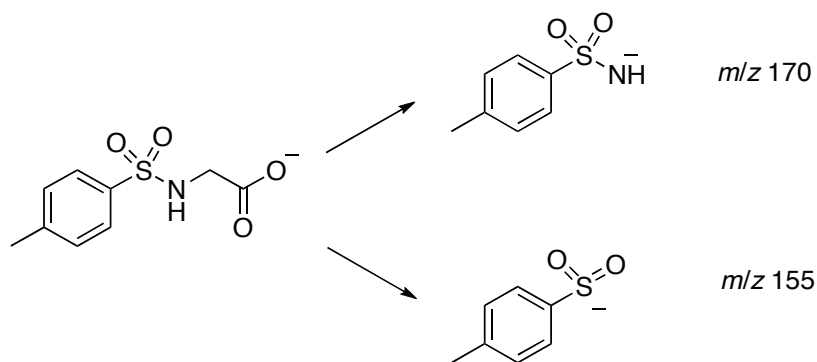
Many other sulfonamides are bacteriostatic antibiotics, effective against most gram positive and many gram negative bacteria.<sup>52</sup> They are often used in animal husbandry, and are given to animals to treat disease and added to feed to improve the growth rate and feed efficiency.<sup>52-54</sup> These compounds are being detected in environmental sources more and more often.<sup>55,56</sup> Antibiotics can enter the environment through sewage, improper disposal, medical waste, discharge from wastewater facilities, and runoff from farmland. Studies have confirmed that the presence of low levels of sulfonamides in the environment are not harmful to human health.<sup>53,57</sup> However, exposure of sub-therapeutic levels of antibiotics can provoke resistance in bacteria.<sup>52-54,58,59</sup> Because of this risk, many MS techniques screening for these compounds in environmental and food samples have

been published.<sup>55,56,60–62</sup> The general structure of a deprotonated sulfonamide antibiotic is shown in Scheme 1.18, with the commonly observed fragmentation processes.<sup>6</sup> It is interesting that the loss of SO<sub>2</sub> from sulfonamide antibiotics is not often seen.



**Scheme 1.18.** Fragmentation of a deprotonated sulfonamide antibiotic.

In unpublished work, J. S. Grossert and R. L. White (Dalhousie University) investigated the gas phase behavior of tosyl (Ts) protected amino acids. Deprotonated tosyl glycine (TsGly) and derivatives of amino acids with aliphatic side chains formed two main product ions, at  $m/z$  170 and  $m/z$  155 (Scheme 1.19). Isotopically labeled derivatives were used to establish the structure of the product ions. The  $m/z$  170 anion further fragmented to form product ions at  $m/z$  79 ( $\cdot\text{SO}_2\text{NH}^-$ ), 80 and 106 ( $\text{MeC}_6\text{H}_4\text{NH}^-$ ) from a rearrangement resulting in loss of SO<sub>2</sub>. The anions at  $m/z$  106 and 79 have also been reported in the fragmentation of *p*-toluenesulfonamide ion.<sup>48</sup> The anion at  $m/z$  155 yielded product ions at  $m/z$  107 ( $\text{MeC}_6\text{H}_4\text{O}^-$ ) through the loss of SO, 91 ( $\text{MeC}_6\text{H}_4^-$ ) through loss of SO<sub>2</sub>, and 64 ( $\text{SO}_2^-$ ). The formation of these product ions has also been observed by Zhang for the fragmentation of *p*-toluenesulfinate ion.<sup>45</sup>



**Scheme 1.19.** Fragmentation of deprotonated TsGly.

### 1.3 Amine Protecting Groups

Amines are polar, basic and nucleophilic and are often difficult to handle and unstable to reaction conditions. Protecting the amine with a suitable protecting group allows selective reactions to take place on other functional groups. It is important that a protecting group will react easily with the functional group needing protection under mild conditions, that it is stable to the reaction conditions after protection, and that it is easily removed without affecting other parts of the molecule. The most common amine protecting groups are carbamates, specifically t-butoxycarbonyl (Boc), 9-fluorenylmethoxy carbonyl (Fmoc) and carboxybenzyl (Cbz, Figure 1.4).<sup>11</sup> Cbz and Boc are easily removed in acidic media, while Fmoc can be removed under mild basic conditions.

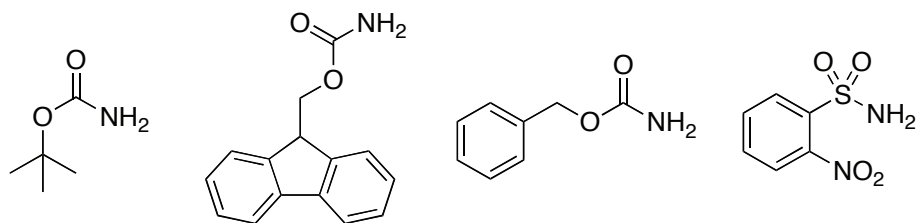


**Figure 1.4.** Structures of common protecting groups: Boc, Fmoc, Cbz and Ns.

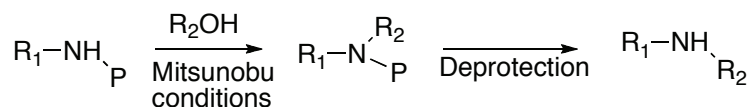
Reaction of amines with 2- or 4-nitrobenzenesulfonyl chloride (NsCl) under basic conditions is used to introduce the Ns or pNs group (Figure 1.4). As described in the recent literature,<sup>63–66</sup> the Ns and pNs groups both protect and activate amines. The groups are stable under acidic and basic conditions, and deprotection with a thiol nucleophile is easy.<sup>63</sup> The 2,4-dinitrobenzenesulfonyl (2,4-DNs) group has also been used as a protecting group and it requires less harsh deprotection conditions. One advantage of the Ns protecting group is that it can be selectively removed when other groups such as Boc or Cbz are present.<sup>63</sup> The Ns group also allows for the selective protection of diamines, and therefore is often used in the solid phase synthesis of polyamines. Ns protected amino acids have also been shown to have some biological activity in the inhibition of aldose reductase activity.<sup>67</sup>

### 1.3.1 Use of Ns in Mitsunobu Reactions

The substitution of primary or secondary alcohols with a nucleophile under certain reaction conditions was first described by Mitsunobu in 1967.<sup>68</sup> The Mitsunobu reaction permits the formation of C-O, C-N, C-S and C-C bonds through the condensation of an acidic component with a primary or secondary alcohol, mediated by the addition of a

phosphine and an azodicarboxylate, such as diethyl azodicarboxylate or diisopropyl azodicarboxylate. This reaction has become a key step in natural product synthesis because of its mild reaction conditions and wide range of applicability, allowing for the synthesis of esters, amines, azides, ethers, cyanides and other functional groups.<sup>69</sup> Although this reaction is widely used, the reaction mechanism is still under some debate.<sup>69,70</sup>

A modification of the Mitsunobu reaction by Fukuyama and coworkers was first described in 1995.<sup>71,72</sup> This modification involved the *N*-alkylation of secondary sulfonamides under Mitsunobu conditions, where the final product is a secondary amine (Scheme 1.20). The *Ns* protecting group is used for its easy protection and removal, and because it activates the nitrogen for alkylation. Improvements on this reaction were later published by Guisado and colleagues,<sup>73</sup> where the reaction was modified to generate primary and secondary amines from primary or secondary alcohols. Using this modification, a lipopeptide lung-targeting gene delivery agent was synthesized. The Fukuyama-Mitsunobu modified reaction has been widely used in the synthesis of polyamine natural products,<sup>65,74–76</sup> peptide nucleic acid monomers,<sup>77</sup> and *N*-alkylation of peptides.<sup>64,66,78</sup>



**Scheme 1.20.** Conversion of primary amines to the corresponding secondary amine through the Fukuyama-Mitsunobu reaction. P is a protecting group.

## 1.4 Thesis Goals

The main goal of this thesis is to characterize the fragmentation pathways of anions formed by deprotonation of Ns derivatives of amino acids. The Ns group is widely used in organic synthesis for the protection and activation of amines, and the sulfonamide group is present in many drugs and drug candidates.

The information gained from this MS/MS investigation provides fundamental knowledge needed for the identification of impurities and metabolites in drug development.<sup>79</sup> Because identifying unknown metabolites can be cost and labour intensive, the characteristic fragmentation patterns established in this thesis are valuable to assist structural elucidation by mass spectrometry. While the interpretation of odd electron mass spectra generated from EI-MS has been widely applied to compound identification, similar interpretations of the mass spectra of even electron ions, particularly negative ions, is limited by lack of data.<sup>6</sup>

In this thesis, the gas phase behaviour of Ns amino acids in ESI(-)MS/MS was elucidated using isotopic labels, structural variations and mass spectrometric experiments. A novel low-energy fragmentation process was characterized and several other fragmentation processes were observed by varying the position of substituents.

## CHAPTER 2 MATERIALS AND METHODS

### 2.1 General Information

Melting points (mp, °C, uncorrected) were determined in open glass capillaries using a Gallenkamp apparatus. <sup>1</sup>H NMR spectra were recorded on a Bruker Tecmag AV-300 or AC-500 spectrometer. Chemical shifts are reported relative to tetramethylsilane (TMS, δ 0.0 in CDCl<sub>3</sub>), or residual solvent (CD<sub>3</sub>OD, δ 3.31; (CD<sub>3</sub>)<sub>2</sub>CO, δ 2.05). Coupling constants (*J*) are reported in Hertz (Hz). [2,2-<sup>2</sup>H<sub>2</sub>]Glycine (98% <sup>2</sup>H) and [1-<sup>13</sup>C]glycine (99% <sup>13</sup>C) were obtained from MSD Isotopes, Montreal QC. D-[2,3-<sup>13</sup>C<sub>2</sub>]-Alanine (99% <sup>13</sup>C) and [2-<sup>13</sup>C, <sup>15</sup>N]glycine (99% <sup>13</sup>C, 98% <sup>15</sup>N) were obtained from Cambridge Isotope Laboratories Inc., Andover MA. 3-Amino-2,2-dimethylpropanoate was synthesized by S. Powers (Honours Report, Department of Chemistry, Dalhousie University, 2007). 2-(Trifluoromethyl)benzenesulfonyl chloride was obtained from Alfa Aesar, Ward Hill MA. All other chemicals were obtained from Sigma-Aldrich, Oakville ON.

### 2.2 Mass Spectrometry

Regular (MS) and tandem (MS/MS) mass spectra were collected on a Thermo-Finnigan LCQ Duo ion trap mass spectrometer by flow injection analysis (20 μL min<sup>-1</sup>) in methanol at a concentration of 1 mg mL<sup>-1</sup>.<sup>27</sup> The ESI needle was set at 3.5 kV and the capillary was maintained at 200 °C. Nitrogen was used as the nebulizing gas and collision-induced dissociation (CID) experiments were carried out using helium as the damping and collision gas. Collision energies are given in arbitrary percentage units

provided by the Xcalibur software. Typically the minimum CID energy (15-30%) needed to make one of the product ion peaks the most intense peak in the MS/MS spectrum is reported.

Spectra were also acquired on a Waters-Micromass Quattro-LC triple quadrupole mass spectrometer using nitrogen as the nebulizing gas and a source temperature of 120 °C. The electrospray needle was set at 3200 V and source cone voltages between 10 and 30 V were used. CID was performed using collisions with argon at energies between 5 and 25 eV. Compounds were dissolved in methanol at 0.1 mg mL<sup>-1</sup>. The flow rate was 20 µL min<sup>-1</sup> and 20 µL of solution were injected.

## **2.3 Benzenesulfonyl Derivatives**

### **2.3.1 Preparation of Benzenesulfonyl Derivatives**

A solution of a substituted benzenesulfonyl chloride (1 or 2 mmol) in dioxane (1.5 mL) was added dropwise to a solution of an amino acid (1 or 2 mmol) dissolved in 10% aqueous K<sub>2</sub>CO<sub>3</sub> (6.0 mL) and dioxane (8.0 mL). The mixture was stirred at room temperature. After 4 h, the mixture was extracted with diethyl ether (3 x 15 mL) and the aqueous layer was acidified with 3 M HCl. Precipitates formed after cooling on ice for 1 h were collected by filtration. In the absence of a precipitate, the product was extracted into ethyl acetate (3 x 5 mL). The combined organic phases were dried with anhydrous MgSO<sub>4</sub> and concentrated by rotary evaporation. Precipitates and residues from rotary evaporation were recrystallized from the solvents indicated.

***N*-2-Nitrobenzenesulfonylglycine (1, NsGly)**

Glycine (153 mg, 2.0 mmol) and NsCl (443 mg, 2.0 mmol) yielded a colourless crystalline solid (227 mg, 44%). mp 157-159 (H<sub>2</sub>O) (lit<sup>67</sup> 158-159); <sup>1</sup>H NMR (300 MHz, CD<sub>3</sub>OD) δ 8.14-8.06 (1H, m), 7.93-7.85 (1H, m), 7.83-7.76 (2H, m), 3.91 (2H, s); ESI(-)MS (relative intensity): *m/z* 259 (100), 212 (5), 184 (2); MS/MS (CID 17%) of *m/z* 259: *m/z* 212 (100), 184 (2), 138 (2).

***N*-2-Nitrobenzenesulfonyl[1-<sup>13</sup>C]glycine (2, Ns[1-<sup>13</sup>C]Gly)**

[1-<sup>13</sup>C]Glycine (151 mg, 1.9 mmol) and NsCl (443 mg, 2.0 mmol) yielded a colourless crystalline solid (266 mg, 43%). mp 158-159 (H<sub>2</sub>O); <sup>1</sup>H NMR (300 MHz, CD<sub>3</sub>OD) δ 8.12-8.06 (1H, m), 7.91-7.84 (1H, m), 7.83-7.75 (2H, m), 3.91 (2H, d, <sup>2</sup>*J*<sub>CH</sub> = 5.4); ESI(-)MS (relative intensity): *m/z* 260 (100), 213 (6); MS/MS (CID 18%) of *m/z* 260: *m/z* 213 (100), 184 (2), 138 (3).

***N*-2-Nitrobenzenesulfonyl[2-<sup>13</sup>C, <sup>15</sup>N]glycine (3, Ns[2-<sup>13</sup>C, <sup>15</sup>N]Gly)**

[2-<sup>13</sup>C, <sup>15</sup>N]Glycine (156 mg, 2.0 mmol) and NsCl (446 mg, 2.0 mmol) yielded a colourless crystalline solid (258 mg, 49%). mp 158-159 (H<sub>2</sub>O); <sup>1</sup>H NMR (300 MHz, CD<sub>3</sub>OD) δ 8.12-8.06 (1H, m), 7.91-7.76 (3H, m), 3.91 (2H, d, <sup>1</sup>*J*<sub>CH</sub> = 141); ESI(-)MS (relative intensity): *m/z* 261 (100), 214 (4), 186 (3); MS/MS (CID 17%) of *m/z* 261: 214 (100), 186 (2), 138 (3).

***N*-2-Nitrobenzenesulfonyl[2,2-<sup>2</sup>H<sub>2</sub>]glycine (4, Ns[2,2-<sup>2</sup>H<sub>2</sub>]Gly)**

[2,2-<sup>2</sup>H<sub>2</sub>]Glycine (155 mg, 2.0 mmol) and NsCl (443 mg, 2.0 mmol) yielded a colourless crystalline solid (256 mg, 49%). mp 156-157 (H<sub>2</sub>O); <sup>1</sup>H NMR (300 MHz, CD<sub>3</sub>OD) δ 8.10-8.06 (1H, m), 7.89-7.76 (3H, m); ESI(-)MS (relative intensity): *m/z* 261 (100), 214 (4), 186 (3); MS/MS (CID 17%) of *m/z* 261: *m/z* 214 (100), 186 (2), 138 (3).

***N*-2,4-Dinitrobenzenesulfonylglycine (6, 2,4-DNsGly)**

Glycine (72 mg, 1.0 mmol) and 2,4-dinitrobenzenesulfonyl chloride (267 mg, 1.0 mmol), yielded a yellow crystalline solid (116 mg, 38%). mp 159-160 (H<sub>2</sub>O); <sup>1</sup>H NMR (300 MHz, CD<sub>3</sub>OD) δ 8.75-8.73 (1H, m), 8.61-8.57 (1H, m), 8.35-8.32 (1H, m), 3.97 (2H, s); ESI(-)MS (relative intensity): *m/z* 304 (100), 257 (20), 229 (2), 183 (5); MS/MS (CID 15%) of *m/z* 304: *m/z* 257 (100), 229 (4), 183 (10).

***N*-2-Nitrobenzenesulfonyl-L-alanine (7, NsAla)**

L-Alanine (180 mg, 2.0 mmol) and NsCl (445 mg, 2.0 mmol) yielded a colourless crystalline solid (240 mg, 43%). mp 165-166 (H<sub>2</sub>O); <sup>1</sup>H NMR (300 MHz, CD<sub>3</sub>OD) δ 8.11-8.09 (1H, m), 7.89-7.78 (3H, m), 4.14 (1H, q, *J* = 7.2), 1.43 (3H, d, *J* = 7.2); ESI(-)MS (relative intensity): *m/z* 273 (100), 226 (3), 198 (2); MS/MS (CID 18%) of *m/z* 273: 226 (100), 198 (8), 138 (4).

***N*-2-Nitrobenzenesulfonyl-D-[2,3-<sup>13</sup>C<sub>2</sub>]alanine (8, Ns[2,3-<sup>13</sup>C<sub>2</sub>]Ala)**

D-[2,3-<sup>13</sup>C<sub>2</sub>]Alanine (93 mg, 1.0 mmol) and NsCl (222 mg, 1.0 mmol) yielded a colourless crystalline solid (149 mg, 54%). mp 160-162 (H<sub>2</sub>O); <sup>1</sup>H NMR (300 MHz, CD<sub>3</sub>OD) δ 8.13-8.07 (1H, m), 7.89-7.76 (3H, m), 4.17 (1H, d of two overlapping q, <sup>1</sup>*J*<sub>CH</sub> = 142, <sup>3</sup>*J*<sub>HH</sub> = 7.1, <sup>2</sup>*J*<sub>CH</sub> = 5.6), 1.43 (3H, ddd, <sup>1</sup>*J*<sub>CH</sub> = 130, <sup>3</sup>*J*<sub>HH</sub> = 7.2, <sup>2</sup>*J*<sub>CH</sub> = 4.4); ESI(-)MS (relative intensity): *m/z* 275 (100), 228 (3), 200 (2), 186 (2); MS/MS (CID 18%) of *m/z* 275: 228 (100), 200 (8), 138 (4).

***N*-2-Nitrobenzenesulfonyl-2-aminoisobutyric acid (9, Ns2Aib)**

2-Aminoisobutyric acid (210 mg, 2.0 mmol) and NsCl (443 mg, 2.0 mmol) yielded a colourless crystalline solid (176 mg, 61%). mp 179-180 (H<sub>2</sub>O); <sup>1</sup>H NMR (300 MHz, CD<sub>3</sub>OD) δ 8.13-8.10 (1H, m), 7.88-7.76 (3H, m), 1.47 (6H, s); ESI(-)MS (relative

intensity):  $m/z$  287 (100), 240 (4), 201 (10), 186 (2); MS/MS (CID 18%) of  $m/z$  287: 240 (100), 212 (4), 138 (4).

#### ***N*-3-Nitrobenzenesulfonylglycine (10, mNsGly)**

Glycine (76 mg, 1.0 mmol) and mNsCl (222 mg, 1.0 mmol) yielded a colourless crystalline solid (160 mg, 62%). mp 149-151 (H<sub>2</sub>O) (lit<sup>80</sup> 149-150); <sup>1</sup>H NMR (300 MHz, CD<sub>3</sub>OD)  $\delta$  8.67 (1H, t,  $J$  = 1.9), 8.45 (1H, ddd,  $J$  = 8.2, 2.2, 1.1), 8.24 (1H, ddd,  $J$  = 8.9, 2.8, 1.1), 7.81 (1H, t,  $J$  = 8.1), 3.82 (2H, s); ESI(-)MS (relative intensity):  $m/z$  259 (100), 186 (2); MS/MS of  $m/z$  259 (CID 23%): 215 (22), 186 (100).

#### ***N*-4-Nitrobenzenesulfonylglycine (11, pNsGly)**

Glycine (150 mg, 2.0 mmol) and pNsCl (444 mg, 2.0 mmol) yielded a colourless crystalline solid (258 mg, 50%). mp 169-170 (H<sub>2</sub>O) (lit<sup>67</sup> 169-171); <sup>1</sup>H NMR (300 MHz, CD<sub>3</sub>OD)  $\delta$  8.40-8.35 (2H, m, AA' of AA'XX'), 8.11-8.07 (2H, m, XX' of AA'XX'), 3.82 (2H, s); ESI(-)MS (relative intensity):  $m/z$  259 (100), 186 (6), 138 (2); MS/MS of  $m/z$  259 (CID 22%): 186 (100), 138 (8).

#### ***N*-2-Bromobenzenesulfonylglycine (12, 2BrBsGly)**

Glycine (75 mg, 1.0 mmol) and 2-bromobenzenesulfonyl chloride (255 mg, 1.0 mmol) yielded a colourless crystalline solid (180 mg, 63%). mp 166-167 (H<sub>2</sub>O/MeOH); <sup>1</sup>H NMR (300 MHz, CD<sub>3</sub>OD)  $\delta$  8.07 (1H, dd,  $J$  = 7.4, 2.2), 7.79 (1H, dd,  $J$  = 7.3, 1.8), 7.53-7.43 (2H, m), 3.77 (2H, s); ESI(-)MS (relative intensity):  $m/z$  294 (100), 292 (92); MS/MS (CID 18%) of  $m/z$  292:  $m/z$  212 (100), 184 (6), 141 (2).

#### ***N*-2-Fluorobenzenesulfonylglycine (13, 2FBsGly)**

Glycine (76 mg, 1.0 mmol) and 2-fluorobenzenesulfonyl chloride (132  $\mu$ L, 1.0 mmol) yielded a colourless crystalline solid (83 mg, 36%). mp 170-171 (H<sub>2</sub>O); <sup>1</sup>H NMR (500

MHz, CD<sub>3</sub>OD)  $\delta$  7.85 (1H, dt,  $J = 7.6, 1.6$ ), 7.64-7.61 (1H, m), 7.33-7.26 (2H, m), 3.83 (2H, s); ESI(-)MS (relative intensity):  $m/z$  232 (100), 212 (2); MS/MS (CID 18%) of  $m/z$  232:  $m/z$  212 (100), 184 (10), 157 (2), 141 (6), 72 (2).

***N*-2,5-Dichlorobenzenesulfonylglycine (14, 2,5-DCIBsGly)**

Glycine (150 mg, 2.0 mmol) and 2,5-dichlorobenzenesulfonyl chloride (245 mg, 1.0 mmol) yielded a colourless crystalline solid (55 mg, 20%). mp 157-159 (H<sub>2</sub>O/MeOH); <sup>1</sup>H NMR (500 MHz, CD<sub>3</sub>OD)  $\delta$  8.00 (1H, s), 7.58 (2H, s), 3.83 (2H, s); ESI(-)MS (relative intensity): 286 (16), 284 (70), 282 (100); MS/MS (20%) of  $m/z$  284: 248 (100), 246 (85), 220 (20), 218 (15), 177 (4), 175 (4); MS/MS (CID 20%) of  $m/z$  282: 246 (100), 218 (18), 175 (5).

***N*-2-Trifluoromethylbenzenesulfonylglycine (15, 2CF<sub>3</sub>BsGly)**

Glycine (75 mg, 1.0 mmol) and 2-trifluoromethylbenzenesulfonyl chloride (154  $\mu$ L, 1.0 mmol) yielded a colourless crystalline solid (65 mg, 23%). mp 145-146 (H<sub>2</sub>O); <sup>1</sup>H NMR (300 MHz, CD<sub>3</sub>OD)  $\delta$  8.21-8.18 (1H, m), 7.93-7.89 (1H, m), 7.80-7.75 (2H, m), 3.82 (2H, s); ESI(-)MS (relative intensity):  $m/z$  282 (100); MS/MS (CID 22%) of  $m/z$  282: 224 (4), 209 (100), 161 (4).

***N*-2-Nitrobenzenesulfonylsarcosine (16, NsSar)**

Sarcosine (176 mg, 2.0 mmol) and NsCl (441 mg, 2.0 mmol) yielded a colourless crystalline solid (176 mg, 32%). mp 136-138 (H<sub>2</sub>O/MeOH); <sup>1</sup>H NMR (300 MHz, CD<sub>3</sub>OD)  $\delta$  8.09-8.06 (1H, m), 7.83-7.72 (3H, m), 4.11 (2H, s), 3.02 (3H, s); ESI(-)MS (relative intensity):  $m/z$  273 (100), 202 (6), 186 (6), 156 (5), 138 (2); MS/MS (CID 22%) of  $m/z$  273: 226 (100), 210 (10), 201 (96), 184 (15), 156 (95), 138 (12).

### ***N*-3-Nitrobenzenesulfonylsarcosine (20, mNsSar)**

Sarcosine (89 mg, 1.0 mmol) and mNsCl (221 mg, 1.0 mmol) yielded a colourless crystalline solid (35 mg, 13%). mp 142-144 (H<sub>2</sub>O); <sup>1</sup>H NMR (300 MHz, CD<sub>3</sub>OD) δ 8.59 (1H, t, *J* = 1.9), 8.49 (1H, ddd, *J* = 8.3, 2.3, 1.1), 8.22 (1H, ddd, *J* = 7.9, 1.7, 1.1), 7.84 (1H, t, *J* = 7.9), 4.09 (2H, s), 2.95 (3H, s); ESI(-)MS (relative intensity): 273 (100); MS/MS (CID 22%) of *m/z* 273: 229 (94), 186 (100).

### ***N*-4-Nitrobenzenesulfonylsarcosine (21, pNsSar)**

Sarcosine (89 mg, 1.0 mmol) and pNsCl (221 mg, 1.0 mmol) yielded a colourless crystalline solid (166 mg, 61%). mp 180-183 (lit<sup>81</sup> 183-184) (H<sub>2</sub>O/MeOH); <sup>1</sup>H NMR (300 MHz, CD<sub>3</sub>OD) δ 8.43-8.39 (2H, m, AA' of AA'XX'), 8.09-8.04 (2H, m, XX' of AA'XX'), 4.06 (2H, s), 2.95 (3H, s); ESI(-)MS (relative intensity): *m/z* 273 (100), 186 (4); MS/MS (CID 18%) of *m/z* 273: 209 (4), 186 (100), 138 (6).

### ***N*-2-Nitrobenzenesulfonylglycine ethyl ester (22, NsGlyOEt)**

Glycine ethyl ester hydrochloride (279 mg, 2.0 mmol) and NsCl (443 mg, 2.0 mmol) yielded a colourless crystalline solid (420 mg, 73%). mp 81-84 (lit<sup>82</sup> 83.5-84.5) (MeOH); <sup>1</sup>H NMR (500 MHz, CD<sub>3</sub>OD) δ 8.11-8.06 (1H, m), 7.90-7.85 (1H, m), 7.83-7.76 (2H, m), 4.01 (2H, q, *J* = 7.1), 3.95 (2H, s), 1.12 (3H, t, *J* = 7.1); <sup>13</sup>C NMR (125 MHz, CDCl<sub>3</sub>) δ 168.7, 148.0, 134.1, 133.9, 133.1, 130.8, 125.9, 62.1, 45.2, 14.2; ESI(-)MS (relative intensity) *m/z* 287 (100), 156 (4); MS/MS (CID 22%) of *m/z* 287: *m/z* 270 (16), 241 (38), 240 (32), 186 (100), 156 (36), 138 (15), 121 (5), 108 (6), 93 (16).

### ***N*-2-Nitrobenzenesulfonylglycinamide (23, NsGlyNH<sub>2</sub>)**

Glycinamide hydrochloride (226 mg, 2.1 mmol) and NsCl (442 mg, 2.0 mmol) yielded a colourless crystalline solid (216 mg, 42%). mp 164-165 (H<sub>2</sub>O/MeOH); <sup>1</sup>H NMR (300

MHz, (CD<sub>3</sub>)<sub>2</sub>CO) δ 8.15-8.12 (1H, m), 8.02-7.98 (1H, m), 7.94-7.87 (2H, m), 6.97 (1H, s), 6.78 (1H, s), 6.51 (1H, s), 3.83 (2H, s); ESI(-)MS (relative intensity): *m/z* 258 (100), 211 (3), 194 (5); MS/MS (CID 17%) of *m/z* 258: 211 (2), 194 (100).

***N*-2-Nitrobenzenesulfonylaminoethanol (24, NsNHEtOH)**

2-Aminoethanol (60 μL, 1.0 mmol) and NsCl yielded a colourless crystalline solid (90 mg, 37%). mp 80-82 (H<sub>2</sub>O); <sup>1</sup>H NMR (500 MHz, CDCl<sub>3</sub>) δ 8.17-8.13 (1H, m), 7.91-7.87 (1H, m), 7.78-7.74 (2H, m), 5.75 (1H, s), 3.76 (2H, t, *J* = 5.1), 3.27 (2H, t, *J* = 5.1), 1.82 (1H, s); ESI(-)MS (relative intensity): *m/z* 245 (100), 198 (14), 138 (4); MS/MS (CID 18%) of *m/z* 245: 198 (100), 181 (15), 138 (18), 133 (7).

***N*-2-Nitrobenzenesulfonyl-β-alanine (25, NsβAla)**

β-Alanine (178 mg, 2.0 mmol) and NsCl (442 mg, 2.0 mmol) yielded a colourless crystalline solid (153 mg, 28%). mp 130-132 (H<sub>2</sub>O) (lit<sup>83</sup> 129.5-131); <sup>1</sup>H-NMR (300 MHz, (CD<sub>3</sub>)<sub>2</sub>CO) δ 8.19-8.16 (1H, m), 8.00-7.91 (3H, m), 3.37 (2H, t, *J* = 6.7), 2.61 (2H, t, *J* = 6.7); ESI(-)MS (relative intensity): 273 (100), 201 (6); MS/MS of *m/z* 273 (CID 22%): 226 (90), 201 (100), 184 (16), 182 (8), 138 (4).

***N*-2-Nitrobenzenesulfonyl-DL-3-aminobutyric acid (26, Ns3Abu)**

DL-3-Aminobutyric acid (205 mg, 2.0 mmol) and NsCl (443 mg, 2.0 mmol) yielded a colourless crystalline solid (176 mg, 61%). mp 119-120 (H<sub>2</sub>O); <sup>1</sup>H NMR (300 MHz, CD<sub>3</sub>OD) δ 8.15-8.09 (1H, m), 7.88-7.77 (3H, m), 3.87 (1H, apparent sextet, *J* = 6.6), 2.55-2.36 (2H, AB of ABX, *J*<sub>AB</sub> = 15.9), 1.16 (3H, d, *J* = 6.7); ESI(-)MS (relative intensity): *m/z* 287 (100), 201 (6); MS/MS (CID 22%) of *m/z* 287: 240 (43), 201 (100), 198 (12), 138 (3).

***N*-2-Nitrobenzenesulfonyl-DL-3-aminoisobutyric acid (27, Ns3Aib)**

DL-3-Aminoisobutyric acid (204 mg, 2.0 mmol) and NsCl (443 mg, 2.0 mmol) yielded a colourless crystalline solid (111 mg, 20%). mp 105-107 (H<sub>2</sub>O); <sup>1</sup>H NMR (300 MHz, CD<sub>3</sub>OD) δ 8.11-8.06 (1H, m), 7.88-7.78 (3H, m), 3.28-3.08 (2H, AB of ABX, *J*<sub>AB</sub> = 13.3), 2.62 (1H, apparent sextet, *J* = 7.1), 1.15 (3H, d, *J* = 7.2); ESI(-)MS (relative intensity): *m/z* 287 (100), 201 (18); MS/MS (CID 22%) of *m/z* 287: 240 (40), 201 (92), 196 (8), 184 (2), 138 (2).

***N*-2-Nitrobenzenesulfonyl-3-amino-2,2-dimethylpropanoic acid (28, Ns3Apv)**

3-Amino-2,2-dimethylpropanoate (19 mg, 0.16 mmol) and NsCl (39 mg, 0.17 mmol) yielded a colourless crystalline solid (10 mg, 52%). (H<sub>2</sub>O); <sup>1</sup>H NMR (300 MHz, CDCl<sub>3</sub>) δ 8.13-8.10 (1H, m), 7.90-7.87 (1H, m), 7.76-7.73 (2H, m), 5.98 (1H, s), 3.14 (2H, d, *J* = 6.6), 1.29 (6H, s); ESI(-)MS (relative intensity): *m/z* 301 (100), 201 (20), 137 (2); MS/MS (CID 22%): 254 (20), 210 (6), 201 (100), 184 (4).

***N*-3-Nitrobenzenesulfonyl-β-alanine (30, mNsβAla)**

β-Alanine (90 mg, 1.0 mmol) and mNsCl (274 mg, 1.0 mmol) yielded a colourless crystalline solid (76 mg, 28%). mp 115-117 (H<sub>2</sub>O); <sup>1</sup>H NMR (300 MHz, CD<sub>3</sub>OD) δ 8.66 (1H, t, *J* = 1.9), 8.48 (1H, ddd, *J* = 1.0, 2.3, 8.2), 8.24 (1H, ddd, *J* = 1.0, 2.7, 7.8), 7.84 (1H, t, *J* = 7.8), 3.17 (2H, t, *J* = 6.7), 2.48 (2H, t, *J* = 6.7); ESI(-)MS (relative intensity): *m/z* 273 (100); MS/MS (CID 22%) of *m/z* 273: 229 (12), 201 (100).

***N*-2-Nitrobenzenesulfonyl-L-aspartic acid (31, NsAsp)**

L-Aspartic acid (264 mg, 2.0 mmol) and NsCl (441 mg, 2.0 mmol) yielded a purple solid (66 mg, 21%). mp 172-173 (H<sub>2</sub>O) (lit<sup>84</sup> 182-184); <sup>1</sup>H NMR (300 MHz, CD<sub>3</sub>OD) 8.16-8.10 (1H, m), 7.93-7.87 (1H, m), 7.83-7.77 (2H, m), 4.43 (1H, apparent t, X of ABX, *J* =

5.4), 2.86 (2H, AB of ABX,  $J_{AB} = 17$ ); ESI(-)MS (relative intensity):  $m/z$  317 (94), 201 (100), 186 (66), 138 (70); MS/MS of  $m/z$  317 (CID 20%): 186 (80), 138 (4), 130 (12), 115 (10).

#### ***N*-2-Nitrobenzenesulfonyl-4-aminobutyric acid (32, Ns4Abu)**

4-Aminobutyric acid (206 mg, 2.0 mmol) and NsCl (445 mg, 2.0 mmol) yielded a colourless crystalline solid (270 mg, 47%). mp 127-180 (H<sub>2</sub>O/MeOH); <sup>1</sup>H NMR (300 MHz, CD<sub>3</sub>OD)  $\delta$  8.10-8.04 (1H, m), 7.86-7.77 (3H, m), 3.09 (2H, t,  $J = 6.9$ ), 2.33 (2H, t,  $J = 7.3$ ), 1.78 (2H, quintet,  $J = 7.1$ ); ESI(-)MS (relative intensity):  $m/z$  287 (100), 201 (6); MS/MS of  $m/z$  287 (CID 20%): 240 (20), 201 (100).

#### ***N*-3-Nitrobenzenesulfonyl-4-aminobutyric acid (33, mNs4Abu)**

4-Aminobutyric acid (103 mg, 1.0 mmol) and mNsCl (221 mg, 1.0 mmol) yielded a colourless crystalline solid (67 mg, 25%). mp 117-120 (H<sub>2</sub>O); <sup>1</sup>H NMR (500 MHz, CD<sub>3</sub>OD)  $\delta$  8.64 (1H, t,  $J = 1.7$ ), 8.47 (1H, dd,  $J = 8.3, 1.3$ ), 8.22 (1H, d,  $J = 7.8$ ), 7.84 (1H, t,  $J = 8.0$ ), 2.95 (2H, t,  $J = 6.9$ ), 2.32 (2H, t,  $J = 7.1$ ), 1.73 (2H, apparent quintet,  $J = 7.0$ ); ESI(-)MS (relative intensity):  $m/z$  287 (100); MS/MS (CID 22%) of  $m/z$  287: 269 (4), 201 (100).

### **2.3.2 Preparation of *N*-2-Nitrobenzenesulfonyl[<sup>18</sup>O]glycine (5, Ns[<sup>18</sup>O]Gly)**

A solution of *N*-2-nitrobenzenesulfonylglycine ethyl ester (100 mg, 0.3 mmol) in dioxane (500  $\mu$ L), H<sub>2</sub>O (320  $\mu$ L), H<sub>2</sub><sup>18</sup>O (80  $\mu$ L, 98% <sup>18</sup>O) and H<sub>2</sub>SO<sub>4</sub> (23  $\mu$ L) was heated at 60 °C. After 24 h, diethyl ether (5 mL) was added and the mixture was extracted with 5% NaHCO<sub>3</sub> (aq) (3 x 5 mL). The aqueous solution was acidified with 3 M HCl, and extracted with diethyl ether (3 x 10 mL). The combined organic phases were dried with

anhydrous MgSO<sub>4</sub>. Removal of solvent by rotary evaporation yielded a solid residue (49 mg, 55%). mp 145-149; <sup>1</sup>H NMR (500 MHz, CD<sub>3</sub>OD) δ 8.10-8.07 (1H, m), 7.89-7.86 (1H, m), 7.81-7.78 (2H, m), 3.91 (2H, s); <sup>13</sup>C NMR (125 MHz, CD<sub>3</sub>OD) δ 172.15, 172.13, 149.3, 135.4, 134.8, 133.6, 131.5, 126.1, 45.1; ESI(-)MS (relative intensity): *m/z* 261 (54), 259 (100); MS/MS (CID 17%) of *m/z* 261: 214 (100).

### 2.3.3 Methylation of Ns derivatives

#### 2.3.3.1 *O*-Methylation

A solution of 50 mg mL<sup>-1</sup> of *N*-2-nitrobenzenesulfonyl-L-alanine (136 mg, 0.5 mmol) in DMF (2.75 mL) was added to 4 Å molecular sieves (2 g), previously activated at 600 °C for 12 h. The mixture was stirred at room temperature. After 5 min, CH<sub>3</sub>I (40 μL, 0.675 mmol) was added. After stirring for 24 h, the reaction mixture was centrifuged for 20 min. 5% aqueous Na<sub>2</sub>CO<sub>3</sub> (5 mL) was added to the supernatant, and the mixture was extracted with ethyl acetate (3 x 5 mL). The aqueous layer was acidified with 3 M HCl, and extracted with ethyl acetate (3 x 5 mL). The combined organic layers were washed with H<sub>2</sub>O, dried over anhydrous MgSO<sub>4</sub>, and concentrated to yield a solid residue (51 mg, 36%). <sup>1</sup>H NMR (300 MHz, CD<sub>3</sub>OD) δ 8.09-8.06 (1H, m), 7.87-7.78 (3H, m), 4.18 (1H, q, *J* = 7.3), 3.51 (3H, s), 1.39 (3H, d, *J* = 7.2); ESI(-)MS (relative intensity): *m/z* 287 (100), 273 (40); MS/MS (CID 23%) of *m/z* 287: 255 (100), 240 (8), 191 (62), 186 (12), 156 (8), 138 (6), 121 (6), 108 (4).

### 2.3.3.2 *N*-Methylation

Diazomethane was prepared from Diazald® (*N*-methyl-*N*-nitroso-*p*-toluenesulfonamide, 7.13 g, 30 mmol) according to Aldrich Technical Information Bulletin No. AL-113. An excess amount of freshly made diazomethane was added to an *N*s-amino acid (100 mg) dissolved in diethyl ether (25 mL) and methanol (2 mL). The reaction progress was monitored by TLC (4:1 DCM/hexanes). After all of the diazomethane was reacted (indicated by colour change from yellow to colourless, approximately 12 h), the product was concentrated by rotary evaporation. The residue was dissolved in dioxane (600  $\mu$ L), H<sub>2</sub>O (400  $\mu$ L), and H<sub>2</sub>SO<sub>4</sub> (25  $\mu$ L), and heated at 60 °C. After 24 h, diethyl ether was added and the mixture was extracted with 5% NaHCO<sub>3</sub> (aq) (3 x 5 mL). The aqueous layer was acidified with 3 M HCl and extracted with diethyl ether (3 x 5 mL). The combined organic phases were dried over anhydrous MgSO<sub>4</sub> and concentrated by rotary evaporation.

#### ***N*-2-Nitrobenzenesulfonyl[2,2-<sup>2</sup>H<sub>2</sub>]sarcosine (17, Ns[2,2-<sup>2</sup>H<sub>2</sub>]Sar)**

Ns[2,2-<sup>2</sup>H<sub>2</sub>]Gly yielded a white solid (57 mg, 55%). mp 138-140; <sup>1</sup>H NMR (500 MHz, CD<sub>3</sub>OD)  $\delta$  8.09-8.05 (1H, m), 7.80-7.73 (3H, m), 3.01 (3H, s); ESI(-)MS (relative intensity) 275 (100); MS/MS (CID 14%) of *m/z* 275: 227 (2), 211 (4), 156 (100).

#### ***N*-2-Nitrobenzenesulfonyl[1-<sup>13</sup>C]sarcosine (18, Ns[1-<sup>13</sup>C]Sar)**

Ns[1-<sup>13</sup>C]Gly yielded a white solid (32 mg, 43%). mp 137-139; <sup>1</sup>H NMR (500 MHz, CD<sub>3</sub>OD)  $\delta$  8.09-8.05 (1H, m), 7.82-7.73 (3H, m), 4.11 (2H, d, *J* = 5.1), 3.02 (3H, s); ESI(-)MS (relative intensity): *m/z* 274 (100); MS/MS (CID 15%) of *m/z* 274: *m/z* 226 (4), 210 (6), 198 (4), 186 (2), 156 (100), 141 (10).

***N*-2-Nitrobenzenesulfonyl[2-<sup>13</sup>C, <sup>15</sup>N]sarcosine (19, Ns[2-<sup>13</sup>C, <sup>15</sup>N]Sar)**

Ns[2-<sup>13</sup>C, <sup>15</sup>N]Gly yielded a white solid (30 mg, 28%). mp 144-146; <sup>1</sup>H NMR (500 MHz, CD<sub>3</sub>OD) δ 8.09-8.05 (1H, m), 7.82-7.73 (3H, m), 4.11 (2H, d, *J* = 141), 3.01 (3H, d, *J* = 2.9).

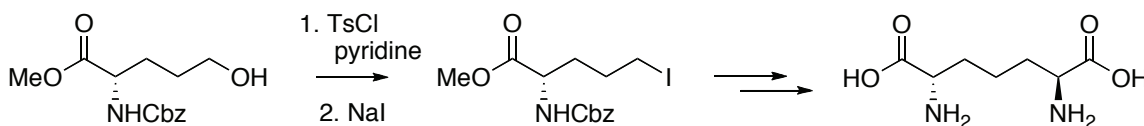
***N*-Methyl-*N*-2-nitrobenzenesulfonyl-β-alanine (29, NsNMeβAla)**

NsβAla yielded a white solid (99 mg, 95%). mp 93-95; <sup>1</sup>H NMR (500 MHz, CD<sub>3</sub>OD) δ 8.02-8.00 (1H, m), 7.84-7.76 (3H, m), 3.53 (2H, t, *J* = 7.2), 2.93 (3H, s), 2.61 (2H, t, *J* = 7.2); ESI(-)MS (relative intensity): *m/z* 287 (100), 215 (2); MS/MS (CID 17%) of *m/z* 287: 240 (100), 215 (25), 186 (12), 156 (6), 138 (28), 108 (2).

## CHAPTER 3 RESULTS AND DISCUSSION

### 3.1 Use of the Ns Protecting Group

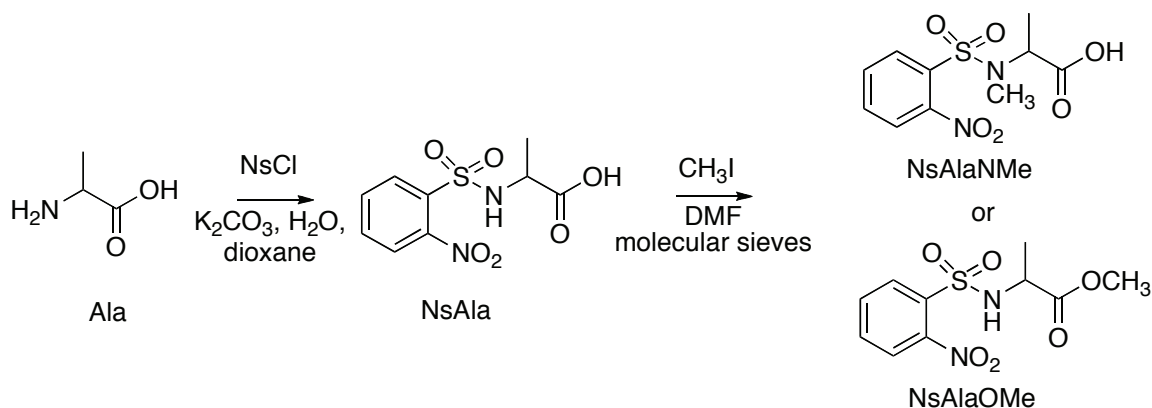
Initially, the goal of this thesis was to selectively synthesize individual stereoisomers of 2,6-diaminopimelic acid and some analogues from protected 5-hydroxynorvaline (Scheme 3.1). In earlier work by Yukun Zhou (MSc Thesis, Dalhousie University, 2002), the alkylation of a glycine Schiff base Ni (II) complex by an *N*-Cbz-protected iodide was attempted under several basic reaction conditions (e.g., NaOH/DMF, DBU/DMF, NaOMe/MeOH). The lack of success in these attempts may have been due to the acidic NH in the *N*-Cbz-protected iodide. To test this hypothesis and to explore the use of the Ns protecting group, the synthesis of an *N*-methyl analogue of 2,6-diaminopimelic acid was planned.



**Scheme 3.1.** Synthesis of (2*S*,6*S*)-diaminopimelic acid from protected 5-hydroxynorvaline.

In a trial experiment, the selective *N*-methylation of Ns-protected amino acids mediated by molecular sieves<sup>85</sup> reported by Monfregola and De Luca<sup>85</sup> was attempted using NsAla (Scheme 3.2). NsAla was prepared from the amino acid and NsCl under basic conditions according to a previously reported method.<sup>86</sup> A methylated product was

isolated in 36% yield. The  $^1\text{H}$  NMR spectrum of the reaction product showed a singlet resonance at  $\delta$  3.51, integrating to three hydrogen atoms. The chemical shift of this methyl resonance ( $\delta$  3.51) was consistent with the reported  $^1\text{H}$  NMR chemical shift ( $\delta$  3.81) assigned to an *N*-methyl group by Monfregola and De Luca.<sup>85</sup> However, this chemical shift assignment of the *N*-CH<sub>3</sub> peak was inconsistent with the  $\delta$  2.91 chemical shift reported for *N*-methyl-NsAla prepared by Biron and Kessler.<sup>87</sup> In this procedure, *N*-methylation was performed on NsAlaOMe using DBU and (CH<sub>3</sub>)<sub>2</sub>SO<sub>4</sub> in DMF, followed by S<sub>N</sub>2 dealkylation using LiI in ethyl acetate. The resonance observed for the sample prepared in this thesis ( $\delta$  3.51) is more consistent with an *O*-CH<sub>3</sub> group, and the molecular sieve mediated methylation therefore led to selective *O*-methylation of NsAla.



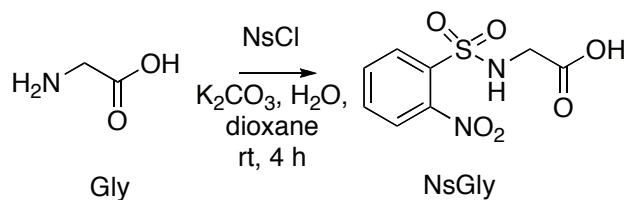
**Scheme 3.2.** *N*-Protection and methylation of alanine (Ala).

As part of the characterization process, ESI(-)MS was performed on both NsAla, and the methylation product, NsAlaOMe. Upon CID, deprotonated NsAla readily lost a neutral molecule or a radical of mass 47 u. As indicated in the introduction, carboxylate ions typically lose H<sub>2</sub>O (18 u), CO<sub>2</sub> (44 u), or formic acid (46 u) when subjected to CID. The loss of 47 u from the NsAla anion indicated a novel fragmentation process.

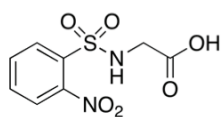
Determination of the structures of the neutral species and product ion, as well as the mechanism of their formation became the focus of this project.

### 3.2 Preparation of Ns Amino Acids

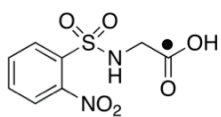
To correlate structure with fragmentation patterns, NsGly and a library of Ns amino acids were prepared according to the procedure reported by De Luca *et al.* (Scheme 3.3).<sup>86</sup> Almost all of the compounds were isolated after recrystallization as crystalline solids in 13-95% yield. Attempts were made to increase the yield by adding excess of reactant (2 equivalents excess of NsCl or 5 equivalents excess of amino acid), increasing the reaction time (6, 8, or 24 h) or heating the reaction at 60 °C, but none of these changes had a significant effect on the product yield. The 33 amino acid derivatives listed in Figure 3.1 were synthesized.



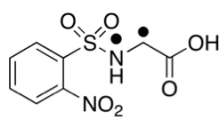
**Scheme 3.3.** Synthesis of Ns protected amino acids.



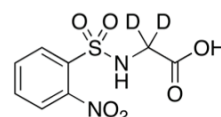
1 NsGly (44%)



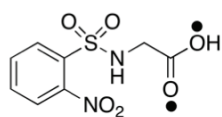
2 Ns[1-<sup>13</sup>C]Gly (43%)



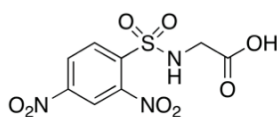
3 Ns[2-<sup>13</sup>C, <sup>15</sup>N]Gly (49%)



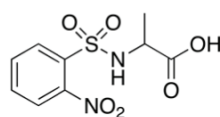
4 Ns[2,2-<sup>2</sup>H<sub>2</sub>]Gly (49%)



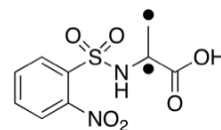
5 Ns[<sup>18</sup>O]Gly (55%)



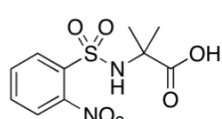
6 2,4-DNsGly (38%)



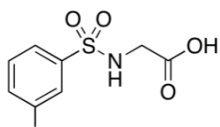
7 NsAla (43%)



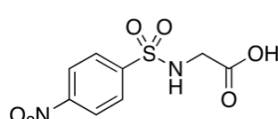
8 Ns[2,3-<sup>13</sup>C<sub>2</sub>]Ala (54%)



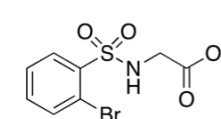
9 Ns2Aib (61%)



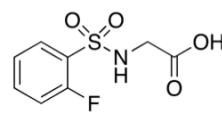
10 mNsGly (62%)



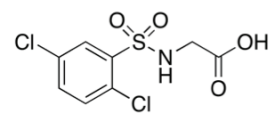
11 pNsGly (50%)



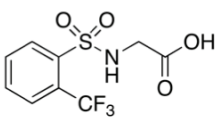
12 2BrBsGly (63%)



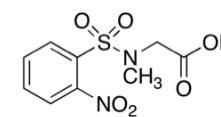
13 2FBsGly (36%)



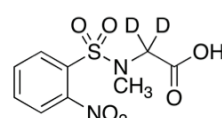
14 2,5-DCIBsGly (20%)



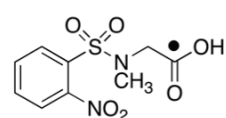
15 2CF<sub>3</sub>BsGly (23%)



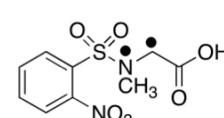
16 NsSar (32%)



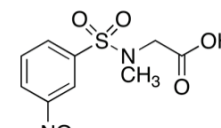
17 Ns[2,2-<sup>2</sup>H<sub>2</sub>]Sar (33%)



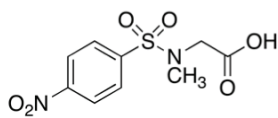
18 Ns[1-<sup>13</sup>C]Sar (43%)



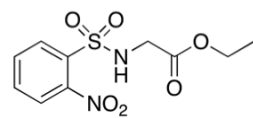
19 Ns[2-<sup>13</sup>C, <sup>15</sup>N]Sar (28%)



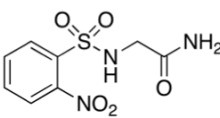
20 mNsSar (13%)



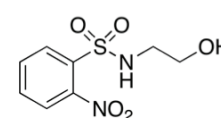
21 pNsSar (61%)



22 NsGlyOEt (73%)



23 NsGlyNH<sub>2</sub> (42%)



24 NsNHEtOH (37%)

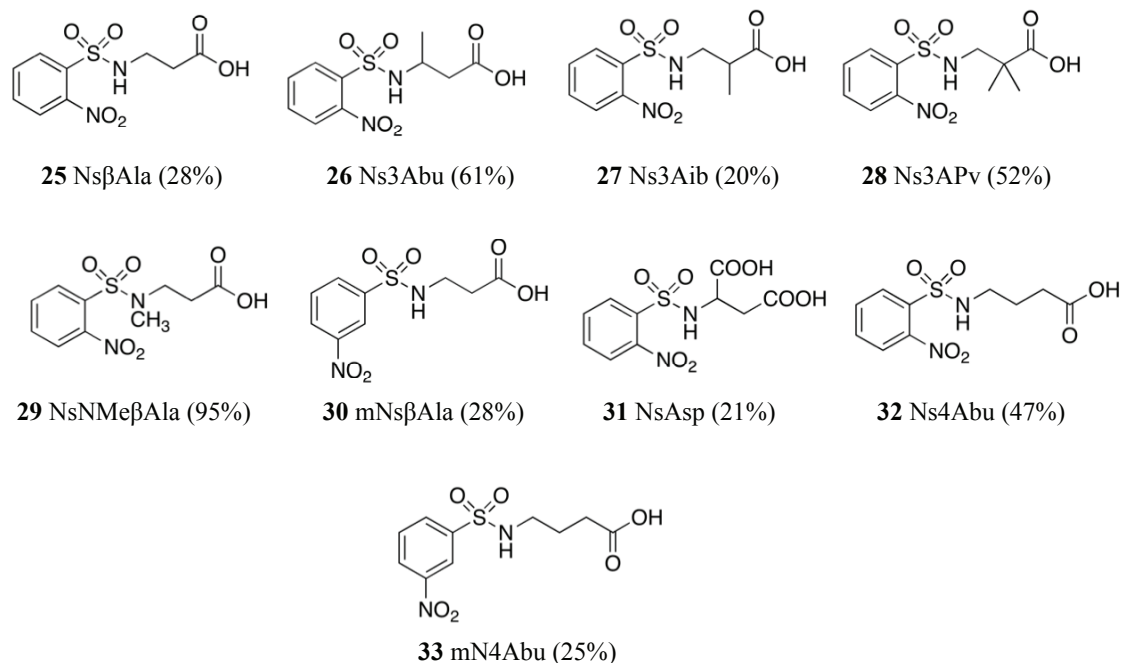
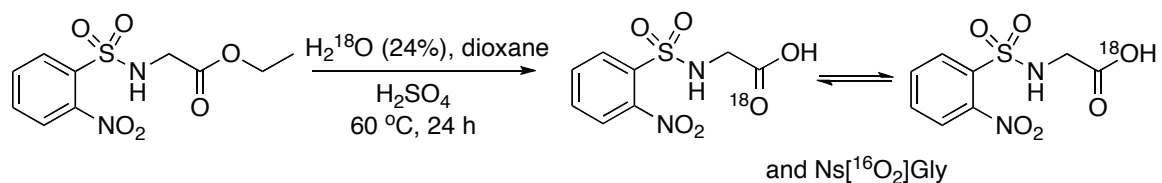


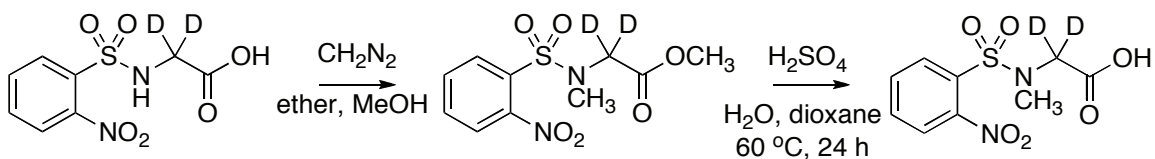
**Figure 3.1.** List of Ns amino acids prepared. The symbol ● denotes an isotopic label ( $^{13}\text{C}$ ,  $^{15}\text{N}$  or  $^{18}\text{O}$ ). The yield of the isolated derivative is given in parentheses.

Ns[ $^{18}\text{O}$ ]Gly was prepared by the acid-catalyzed hydrolysis of NsGlyOEt in a solution of dioxane,  $\text{H}_2^{18}\text{O}$  (24%) and  $\text{H}_2\text{SO}_4$  (Scheme 3.4). The hydrolysed product was isolated in 55% yield. The incorporation of  $^{18}\text{O}$  into the carboxylic acid group was indicated in the  $^{13}\text{C}$  NMR spectrum of the isolated product, by broadening of the carbonyl carbon resonance at  $\delta$  172. Typically, isotopic substitution with  $^{18}\text{O}$  causes an upfield shift of the NMR resonance of the directly attached carbon atom by 10-35 ppb for singly bonded atoms and 30-55 ppb for doubly bonded atoms.<sup>88</sup> The incorporation of  $^{18}\text{O}$  was confirmed using ESI(-)MS (see Section 3.3).



**Scheme 3.4.** Preparation of Ns[<sup>18</sup>O]Gly from NsGlyOEt.

*N,O*-Dimethyl Ns[2,2-<sup>2</sup>H<sub>2</sub>]Gly was synthesized by mixing diazomethane with the Ns amino acid. TLC performed on the reaction solution immediately after adding a small amount of diazomethane showed the formation of a spot with a similar R<sub>f</sub> value as NsGlyOEt, indicating that the methyl ester had been formed. An excess of diazomethane was added and the solution was allowed to react for approximately 24 h. At this point, all of the yellow colour had disappeared, indicating that diazomethane was no longer present in the solution. TLC indicated that the initial methyl ester product was no longer present, and only a spot with a higher R<sub>f</sub> value was observed. The structure of the *N,O*-dimethyl amino acid was confirmed by <sup>1</sup>H NMR and this product was used without purification in the next step. (<sup>1</sup>H NMR (300 MHz, CDCl<sub>3</sub>) δ 8.09-8.04 (1H, m), 7.75-7.62 (3H, m), 3.67 (3H, s), 3.04 (3H, s)). The dimethylated Ns[2,2-<sup>2</sup>H<sub>2</sub>]Gly was hydrolysed in a solution of dioxane, H<sub>2</sub>O and H<sub>2</sub>SO<sub>4</sub> at 60 °C to give Ns[2,2-<sup>2</sup>H<sub>2</sub>]Sar. This procedure was repeated using Ns[1-<sup>13</sup>C]Gly, Ns[2-<sup>13</sup>C,<sup>15</sup>N]Gly and NsβAla to give the corresponding *N*-methyl amino acids. The reactions for Ns[2,2-<sup>2</sup>H<sub>2</sub>]Gly are shown in Scheme 3.5.



**Scheme 3.5.** Methylation of Ns[2,2-<sup>2</sup>H<sub>2</sub>]Gly to give Ns[2,2-<sup>2</sup>H<sub>2</sub>]Sar.

### 3.3 Ionization of Ns Amino Acids

In an ion trap mass spectrometer, the full-scan ESI(-) mass spectra showed intense peaks corresponding to deprotonated Ns amino acids (Table 3.1) and minor peaks that were later assigned as fragment ions by CID experiments. The abundance of the minor ions was increased by application of a sufficient in-source fragmentation voltage. The lack of other peaks in the mass spectra indicates that the Ns derivatives were prepared with low levels of acidic contaminants.

The ESI(-) mass spectrum of NsGly (Figure 3.2) showed an intense  $[M - H]^-$  ion at  $m/z$  259 and minor ions at  $m/z$  212, 186 and 184. Due to the presence of <sup>13</sup>C and <sup>34</sup>S isotopes at natural abundance, peaks were observed for the  $[M + 1 - H]^-$  and  $[M + 2 - H]^-$  ions at  $m/z$  260 and  $m/z$  261 in relative intensities of approximately 10% and 4%, respectively. In the ESI(-) mass spectrum of Ns[<sup>18</sup>O]Gly (Figure 3.3), the relative intensity of the  $[M + 2 - H]^-$  peak was much greater (about 52%); this confirmed the incorporation of <sup>18</sup>O. The low intensity of the  $[M + 4 - H]^-$  peak at  $m/z$  263 demonstrated that only one <sup>18</sup>O atom was incorporated. The level of <sup>18</sup>O incorporation (about 31%) was consistent with the H<sub>2</sub><sup>18</sup>O content in the hydrolysis reaction mixture.

**Table 3.1.** Product ions from CID of deprotonated Ns- $\alpha$ -amino acids.

No.	Compound	[M – H] <sup>-</sup> ( <i>m/z</i> ) <b>a</b>	Selected Product Anions ( <i>m/z</i> )							
			<b>b</b>	<b>c</b>	<b>d</b>	<b>e</b>	<b>f</b>	<b>g</b>	<b>h</b>	<b>I</b>
<b>1</b>	NsGly	259	212	184	157	141	138	93	72	76
<b>1'</b>	Ns[ <sup>34</sup> S]Gly	261	214	186	159	143	138			78
<b>2</b>	Ns[1- <sup>13</sup> C]Gly	260	213	184	157	141	138		73	76
<b>3</b>	Ns[2- <sup>13</sup> C, <sup>15</sup> N]Gly	261	214	186	157	141	138		74	78
<b>4</b>	Ns[2,2- <sup>2</sup> H <sub>2</sub> ]Gly	261	214	186	158	142	138		74	78
<b>5</b>	Ns[ <sup>18</sup> O]Gly	261	214	186 184	159 157	141 143	138		72 74	76
<b>6</b>	2,4-DNsGly	304	257	229	202		138			
<b>7</b>	NsAla	273	226	198	157	141	138		86	90
<b>8</b>	Ns[2,3- <sup>13</sup> C <sub>2</sub> ]Ala	275	228	200	157	141	138		88	92
<b>9</b>	Ns2Aib	287	240	212			138			
<b>12</b>	2BrBsGly	292	212	184						
<b>13</b>	2FBsGly	232	212	184	157	141			72	72
<b>14</b>	2,5-DCIBsGly	282	246	218	191					

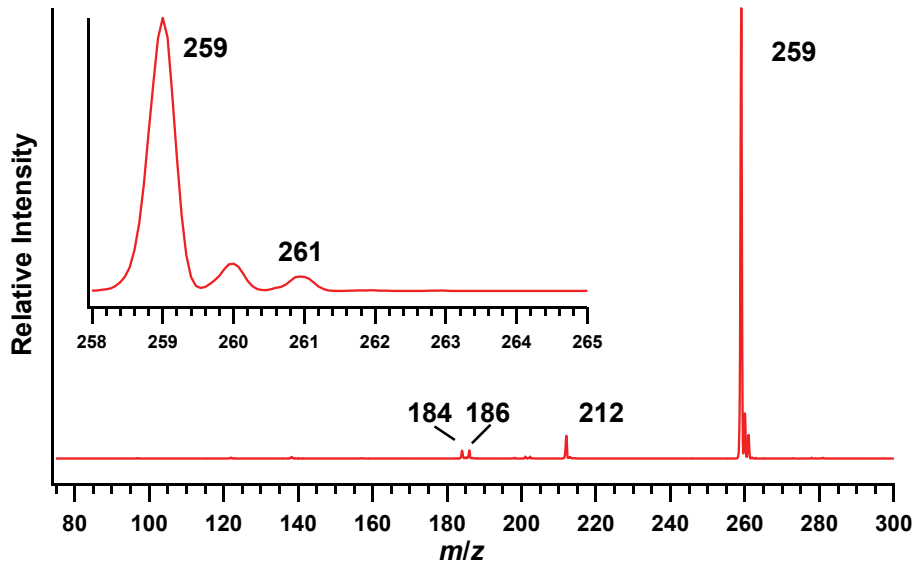


**Figure 3.2.** The ESI(-) mass spectrum of NsGly.

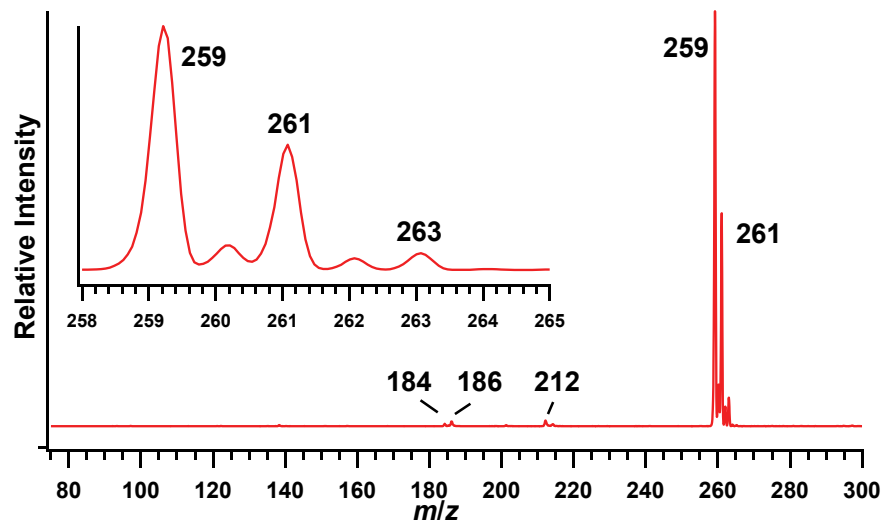


**Figure 3.3.** The ESI(-) mass spectrum of Ns[ $^{18}\text{O}$ ]Gly.

### 3.4 CID of Deprotonated NsGly: Sequential Neutral Losses

Upon CID, the  $[M - H]^-$  ion of NsGly (**1a**) fragmented to an abundant ion at  $m/z$  212 and a series of minor ions (**1b-1f**, **1i**) at  $m/z$  184, 156, 141, and 138 and 76 (Figure 3.4.A and Table 3.1). Ions at  $m/z$  212, 184 and 157 were formed with increased abundance by in-source fragmentation. CID of the ions generated in source showed a stepwise fragmentation pattern (Figure 3.4.B, C and D), indicating precursor-product ion relationships of  $m/z$  259  $\rightarrow$  212  $\rightarrow$  184  $\rightarrow$  157  $\rightarrow$  93 and  $m/z$  259  $\rightarrow$  212  $\rightarrow$  141 and 72. The minor ion at  $m/z$  138 (Figure 3.4.A) was not observed upon CID of the in-source fragment ions and was most likely formed from the  $[M - H]^-$  ion by another pathway.

The composition of the product ions was explored by conducting CID on the  $[M + 2 - H]^-$  ion in the isotope cluster of ion **1a**. Because of the approximately 4% natural abundance of  $^{34}\text{S}$ , most of the  $[M + 2 - H]^-$  ions contain  $^{34}\text{S}$  and product ions retaining sulfur will show increased mass.<sup>89</sup> As shown by the data in Table 3.1 and Figure 3.5, the product ions **1b**, **1c** and **1e** retained sulfur, whereas no sulfur was present in **1f** and **1h**.

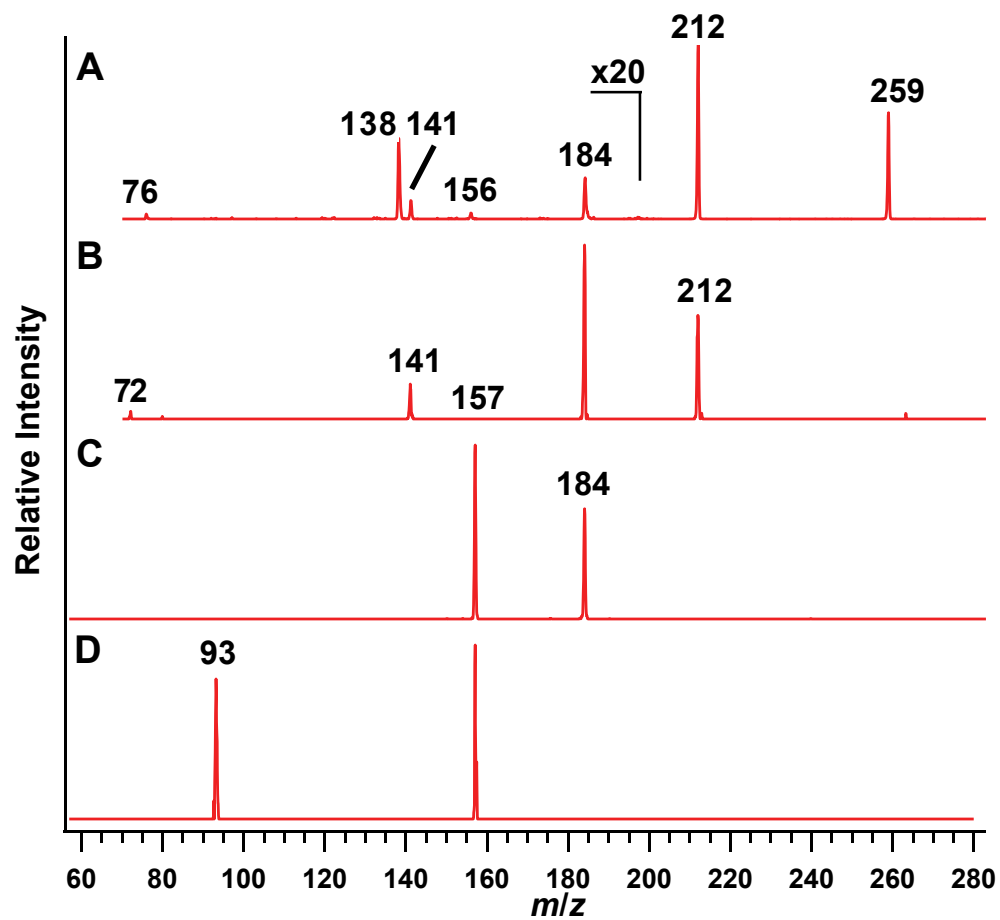


**Figure 3.4.** Product ion mass spectra obtained by CID of **A:** deprotonated NsGly (CID 17%); **B:**  $m/z$  212 ion formed in source (CID 18%); **C:**  $m/z$  184 ion formed in source (CID 22%); **D:**  $m/z$  157 ion formed in source (CID 26%). Unless indicated otherwise, the mass spectra presented in the figures were collected on the ion trap mass spectrometer.

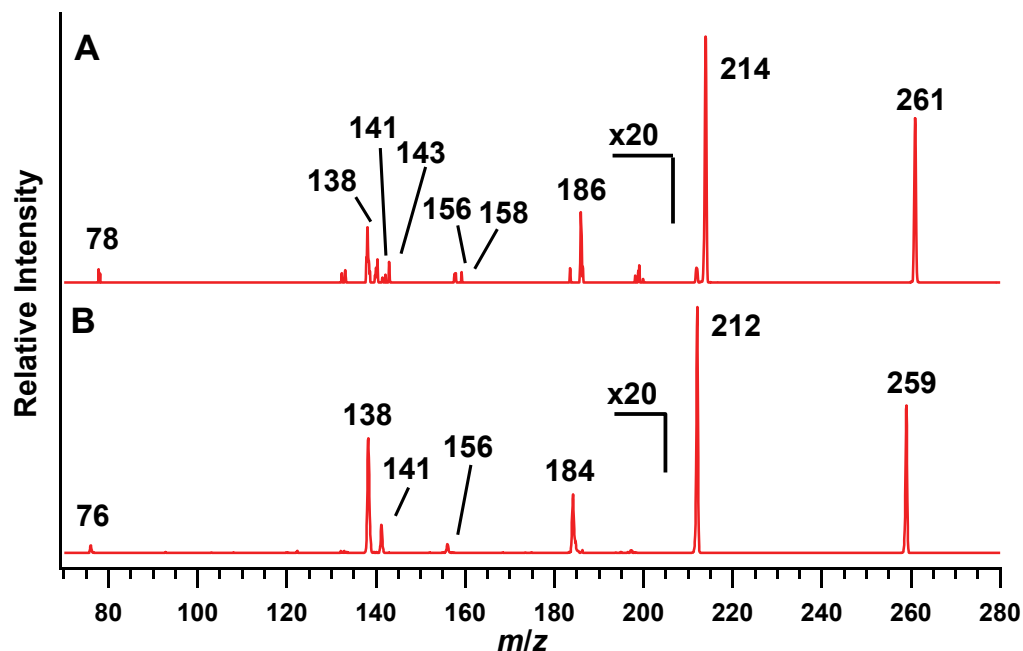


**Figure 3.5.** Product ion mass spectra obtained by CID of **A**: deprotonated Ns[<sup>34</sup>S]Gly (CID 18%); **B**: deprotonated NsGly (CID 18%).

In the initial fragmentation reaction (i.e.  $m/z$  259  $\rightarrow$  212, Figure 3.4A), the odd mass differences between the precursor and product ions indicated the loss of a neutral molecule containing one nitrogen atom. In the mass spectra collected for the series of NsGly derivatives prepared from isotopically labeled glycines (structures shown in Figure 3.1), all isotopic labels were retained in the  $m/z$  212 ion **1b** (Table 3.1, Figures 3.6, 3.7 and 3.8). Deuterium was introduced into an exchangeable position by dissolving NsGly in CH<sub>3</sub>O<sup>2</sup>H, forming NsN<sup>2</sup>HCH<sub>2</sub>CO<sub>2</sub> or NsN<sup>-</sup>CH<sub>2</sub>CO<sub>2</sub><sup>2</sup>H upon ESI, but the isotopic label was not retained in **1b**, the product of the initial fragmentation reaction. The neutral molecule formed in this initial fragmentation reaction, therefore, is likely formed from the nitro group and the exchangeable proton.

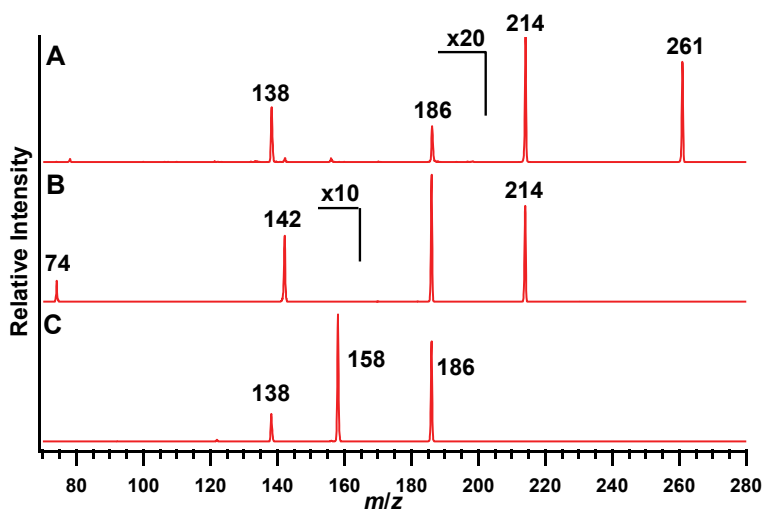


**Figure 3.6.** Product ion mass spectra obtained by CID of **A:** deprotonated Ns[2,2-<sup>2</sup>H<sub>2</sub>]Gly (CID 17%); **B:** *m/z* 214 ion formed in source (CID 18%); **C:** *m/z* 186 ion formed in source (CID 22%).

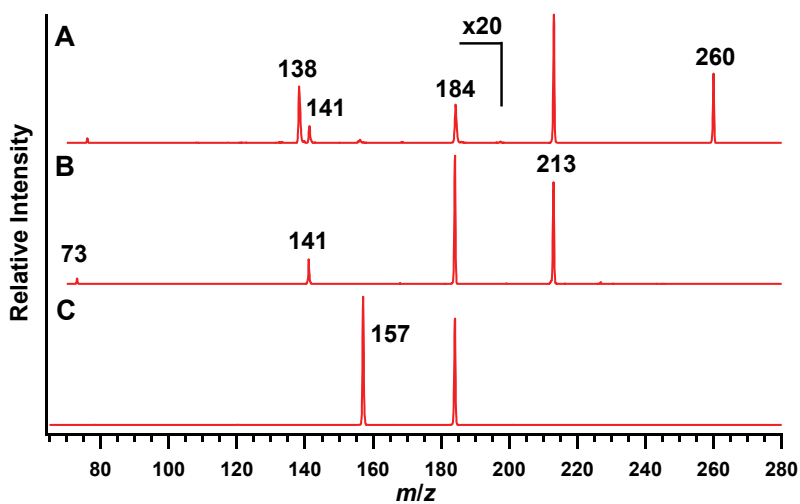


**Figure 3.7.** Product ion mass spectra obtained by CID of **A:** deprotonated Ns[1-<sup>13</sup>C]Gly (CID 18%); **B:** *m/z* 213 ion formed in source (CID 18%); **C:** *m/z* 184 ion formed in source (CID 22%).

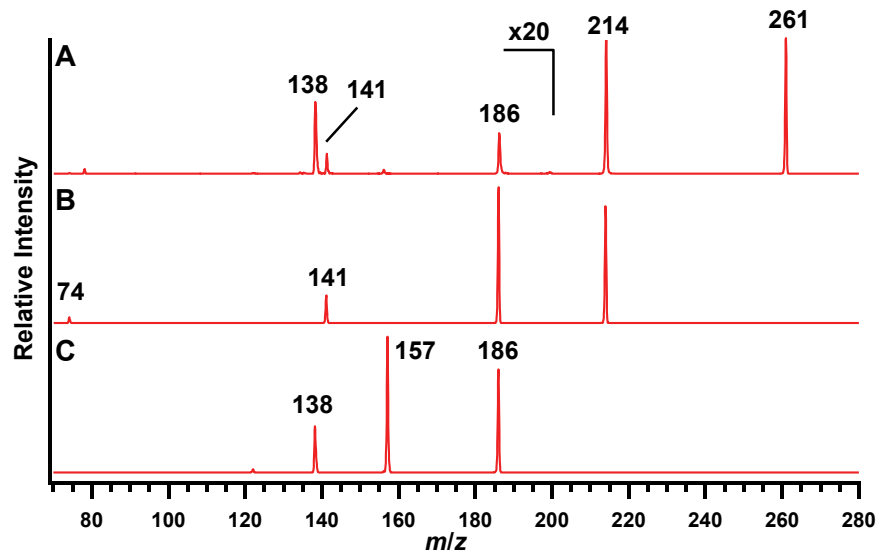
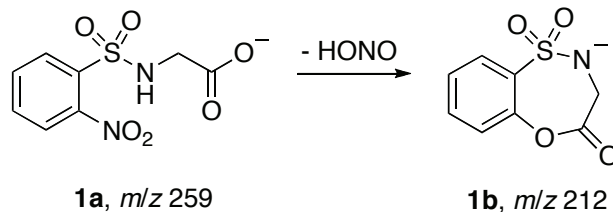


**Figure 3.8.** Product ion mass spectra obtained by CID of **A:** deprotonated Ns[2-<sup>13</sup>C, <sup>15</sup>N]Gly (CID 17%); **B:** *m/z* 214 ion formed in source (CID 18%); **C:** *m/z* 186 ion formed in source (CID 22%).

### 3.4.1 *Ortho* Cyclization Pathway

The mass spectral evidence collected for NsGly is consistent with a fragmentation pathway showing successive losses of HONO, CO, HCN and SO<sub>2</sub>. Previously, consecutive losses of HCN and SO<sub>2</sub> were observed from the heterocyclic ring in deprotonated bicyclic thiazide diuretic drugs (Scheme 1.17).<sup>50</sup> The similar losses observed during the fragmentation of the NsGly anion suggest the formation of an analogous bicyclic sulfonamide ion (**1b**, Scheme 3.6). This cyclization is consistent with the loss of the aromatic nitro group as HONO after nucleophilic attack on the ring by the ionized carboxyl group and donation of the sulfonamide proton to the nitro group. A similar *ortho* cyclization was previously observed by Eichinger and colleagues<sup>41</sup> when a substituent at the *ortho* position of the aromatic ring was a good leaving group.



**Scheme 3.6.** Proposed *ortho* cyclization of deprotonated NsGly to form HONO and a sulfonamide ion at  $m/z$  212.

In-source fragmentation of the  $[M - H]^-$  ion of NsGly **1a** gave the  $m/z$  212 ion (**1b**), which, upon CID, fragmented to an major ion at  $m/z$  184 (**1c**) and two minor ions at  $m/z$  141 and  $m/z$  72 (Figure 3.4B). The even mass difference between **1b** and **1c** indicated that the loss corresponded to a neutral molecule not containing nitrogen. The mass spectra of Ns[2,2- $^2\text{H}_2$ ]Gly (Figure 3.6) and Ns[2- $^{13}\text{C}_2$ ,  $^{15}\text{N}$ ]Gly (Figure 3.8) showed retention of all isotopic labels in the  $m/z$  184 ion, but the mass spectrum of Ns[1- $^{13}\text{C}$ ]Gly (Figure 3.7) showed an odd mass difference between ions **1b** and **1c**, demonstrating the loss of the isotopic label. The  $m/z$  214 ion generated in source from Ns[ $^{18}\text{O}$ ]Gly lost one half of its isotopic label upon CID (Figure 3.9). Therefore, the neutral molecule lost from the  $m/z$  212  $\rightarrow$  184 transition is most likely CO, formed from the carbonyl carbon and oxygen of the amino acid.

In the selected Ns[ $^{18}\text{O}$ ]Gly anion at  $m/z$  261, each ion contains one atom of  $^{18}\text{O}$ , but  $^{18}\text{O}$  is distributed over the two equivalent oxygen atoms in the carboxyl group. After *ortho* cyclization, however, the oxygen atoms are no longer equivalent. One is bonded to the aromatic ring and the other is in the carbonyl group. Because only one  $^{18}\text{O}$  was present in the  $m/z$  214 ion, an equal mixture of  $^{16}\text{O}$  and  $^{18}\text{O}$  are found at each

nonequivalent position. Thus the formation of pairs of product ions separated by 2 u demonstrates that only one of the original carboxyl group oxygen atoms is retained in the product ions (Figure 3.9).

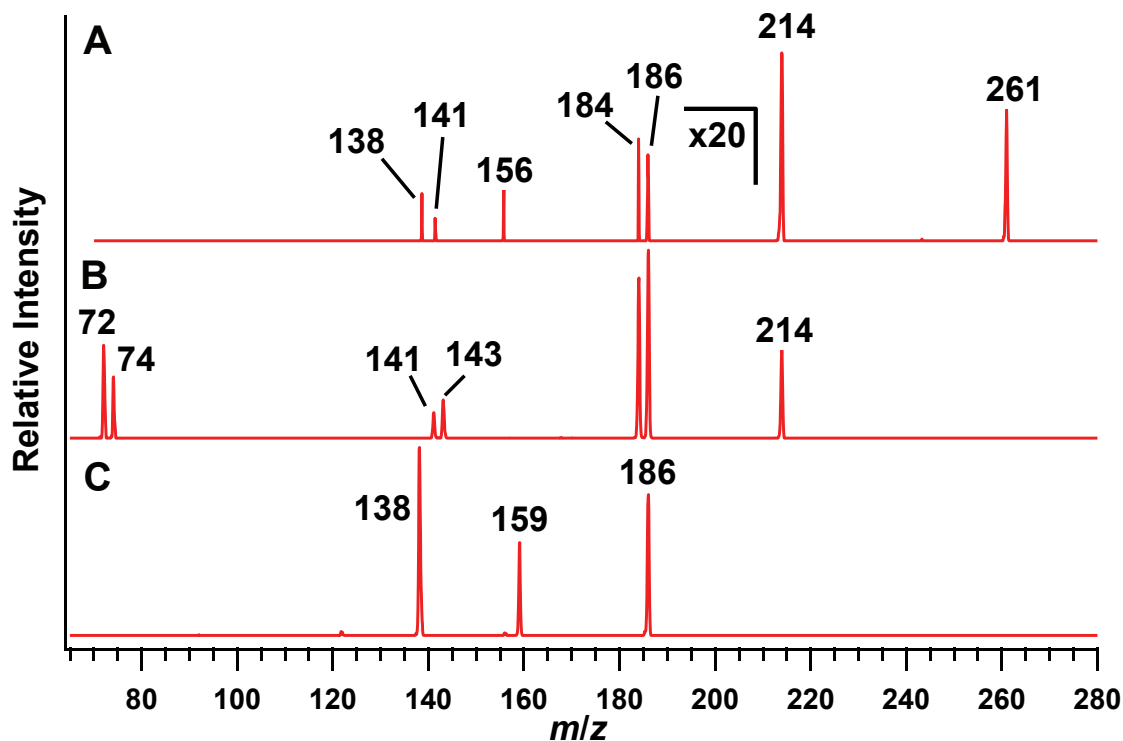


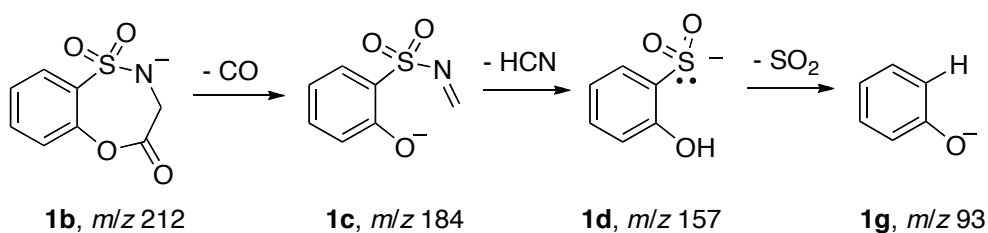
**Figure 3.9.** Product ion mass spectra of ions obtained by CID of **A:** deprotonated Ns[<sup>18</sup>O]Gly (CID 17%); **B:** *m/z* 215 ion formed in source (CID 19%); **C:** *m/z* 186 ion formed in source (CID 20%).

CID of the in-source *m/z* 184 ion (**1c**) derived from NsGly gave only a product ion at *m/z* 157 (**1d**) (Figure 3.4C), indicating that the ions at *m/z* 141 and 72 (Figure 3.4B) were not derived from **1c**. The product ion **1d** formed by fragmentation of Ns[2-<sup>13</sup>C,<sup>15</sup>N]Gly (Figure 3.8) had no isotopic labels but one deuterium atom from Ns[2,2-

$^2\text{H}_2\text{]Gly}$  (Figure 3.6) was retained. The neutral molecule lost in this fragmentation therefore must be HCN, derived from H-C2-N of the amino acid. The last step in this fragmentation pathway is consistent with the neutral loss of  $\text{SO}_2$  (64 u) from the  $m/z$  157 ion to give an ion at  $m/z$  93.

The observed sequential losses of CO, HCN and  $\text{SO}_2$  are consistent with the proposed bicyclic structure of the  $m/z$  212 ion **1b** (Scheme 3.7). Ring opening of **1b** is accompanied by formation of CO and a phenoxide ion (**1c**). Abstraction of a proton from C $\alpha$  in the glycine subunit by the phenoxide oxygen generates HCN and a phenoxide ion (**1d**). Loss of  $\text{SO}_2$  occurs from the sulfinate ion **1d** and proton transfer gives the phenoxide ion **1g**. The loss of  $\text{SO}_2$  from sulfinate ions has also been observed by Garcia and colleagues<sup>50</sup> and Zhang.<sup>45</sup>

The ortho cyclization pathway proposed in Scheme 3.6 and Scheme 3.7 is consistent with the results collected for isotopically labeled NsGly and literature precedents for the fragmentations of analogous ions.

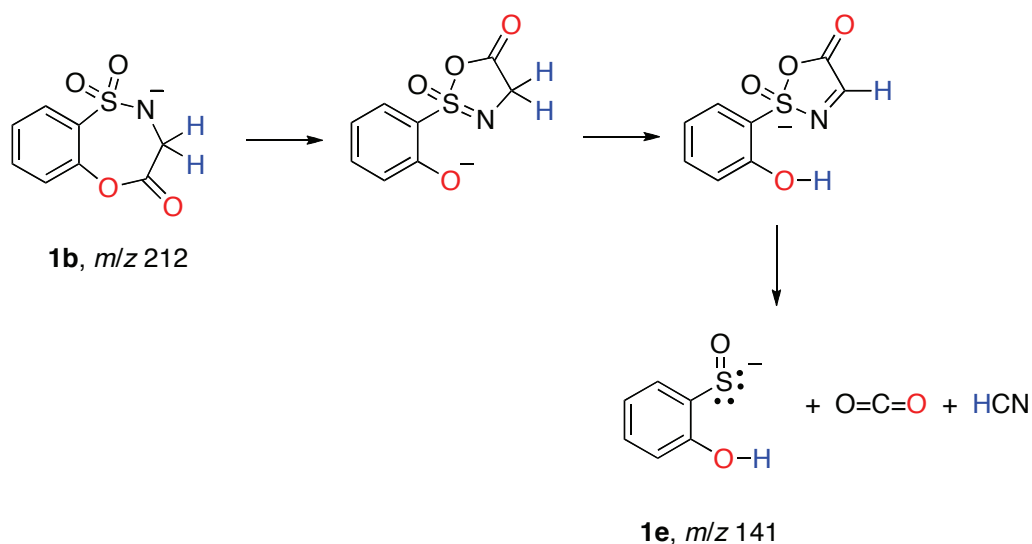


**Scheme 3.7.** Suggested structures for the fragmentation pathway from  $m/z$  212.

### 3.4.2 *Ortho* Cyclization Pathway 2

Product ions at  $m/z$  141 (**1e**) and 72 (**1h**) were also formed upon CID of the  $m/z$  212 ion **1b** generated in source (Figure 3.4B). These ions were not derived from the other product ion at  $m/z$  184, indicating a second fragmentation pathway of the  $m/z$  212 ion **1b**. The  $m/z$  141 anion retained  $^{34}\text{S}$  from the  $[\text{M} + 2 - \text{H}]^-$  anion and one-half of the isotopic label from  $\text{Ns}[2,2\text{-}^2\text{H}_2]\text{Gly}$  and  $\text{Ns}[^{18}\text{O}]\text{Gly}$ , whereas the anion at  $m/z$  72 retained one-half of the label from  $\text{Ns}[^{18}\text{O}]\text{Gly}$  and all labels present in  $\text{Ns}[1\text{-}^{13}\text{C}]\text{Gly}$ ,  $\text{Ns}[2\text{-}^{13}\text{C},^{15}\text{N}]\text{Gly}$  and  $\text{Ns}[2,2\text{-}^2\text{H}_2]\text{Gly}$  (Table 3.1).

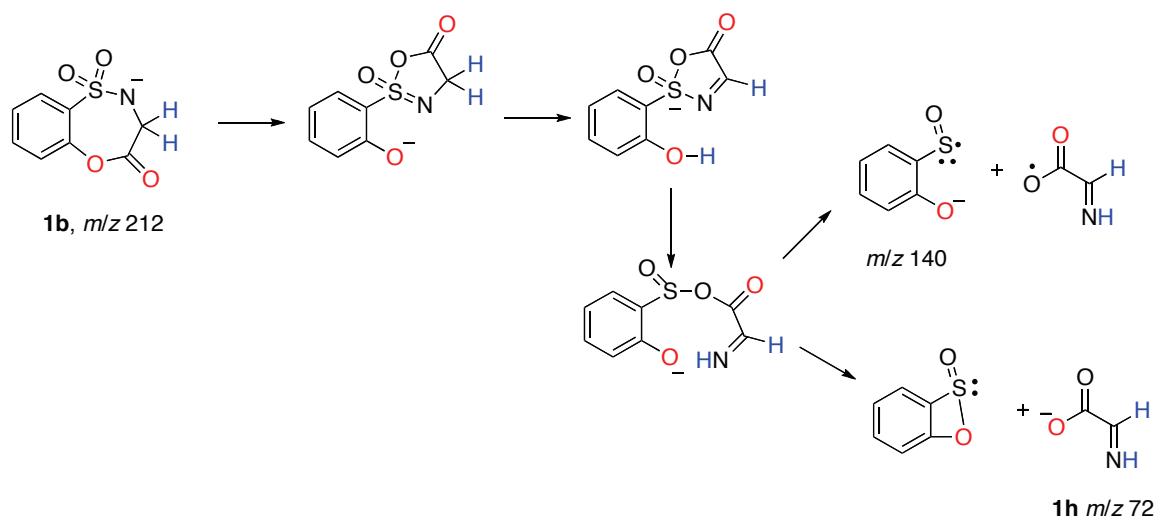
Based on the retention of sulfur and the aromatic ring, a likely molecular formula for the  $m/z$  141 ion is  $\text{C}_6\text{H}_5\text{SO}_2$ . If one of the two oxygen atoms is derived from the carboxyl group of glycine, as shown by  $^{18}\text{O}$  labeling, then an oxygen originally bonded to sulfur must be lost. A rearrangement and subsequent fragmentation consistent with these results is presented in Scheme 3.8. In the first step, the transfer of the carbonyl group to an oxygen on sulfur creates a stable phenoxide ion which then abstracts an  $\alpha$ -proton from the amino acid subunit. This step is consistent with the appearance of one deuterium in the  $m/z$  142 ion derived from  $\text{Ns}[2,2\text{-}^2\text{H}_2]\text{Gly}$ . The loss of  $\text{CO}_2$  and  $\text{HCN}$  forms the  $m/z$  141 ion as a 2-hydroxybenzenesulfenate ion (**1e**).



**Scheme 3.8.** Proposed structures for the fragmentation of  $m/z$  212 to give  $m/z$  141.  $^{18}\text{O}$  labels are shown in red,  $^2\text{H}$  labels are shown in blue.

A similar rearrangement is proposed (Scheme 3.9) to account for the formation of the  $m/z$  72 ion. A key step in this proposed sequence is the transfer of a proton from the oxygen to nitrogen and cleavage of the S-N bond. The ion at  $m/z$  72 would then be formed by heterolytic cleavage of the S-O bond. The rearrangement in the first step is consistent with the retention of  $^{18}\text{O}$  from one position in the  $m/z$  212 ion, and the proton transfer step is consistent with the retention of both labels from  $\text{Ns}[2,2\text{-}^2\text{H}_2]\text{Gly}$  in the  $m/z$  72 ion.

Alternatively, homolytic cleavage would yield an ion at  $m/z$  140. While this ion was not observed in the mass spectra collected on the ion trap mass spectrometer, it was observed when the in-source  $m/z$  212 ion was subjected to CID in the triple quadrupole mass spectrometer (Figure 3.11).



**Scheme 3.9.** Proposed structures for the fragmentation of  $m/z$  212 to give  $m/z$  140 and 72.

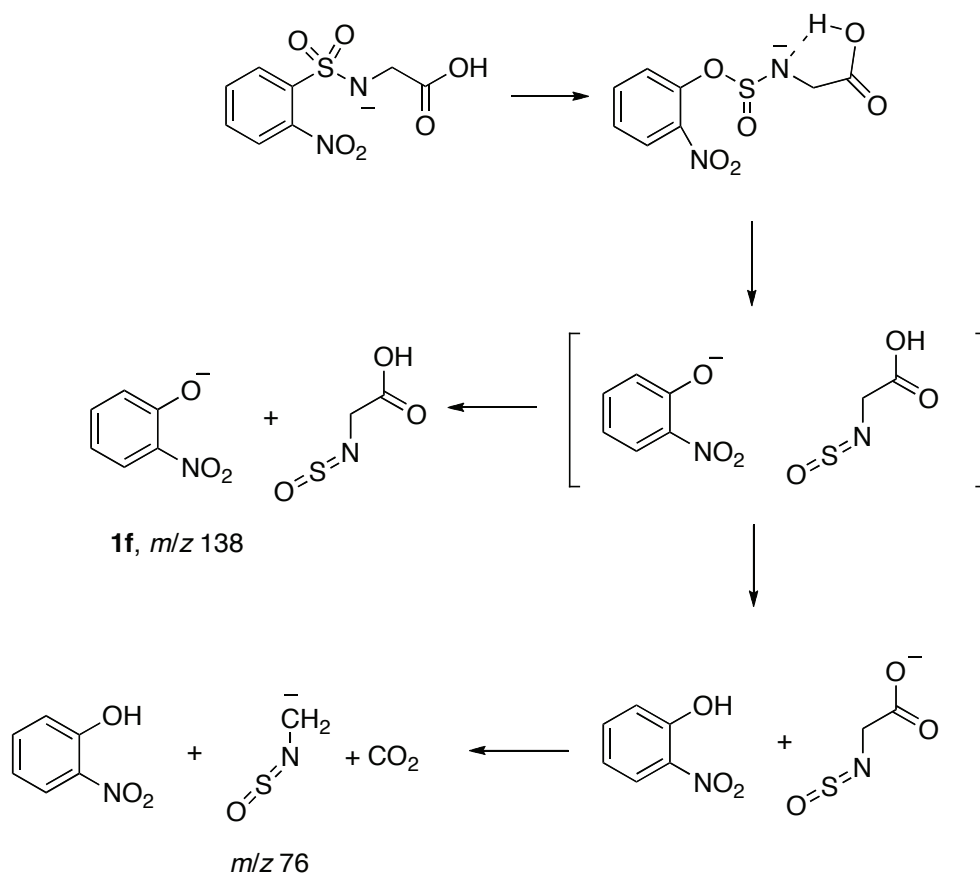
$^{18}\text{O}$  labels are indicated in red, and  $^2\text{H}$  labels are indicated in blue.

### 3.4.3 Sulfonamide Rearrangement Pathway

Another minor ion formed upon CID of the  $[\text{M} - \text{H}]^-$  ion of NsGly was observed at  $m/z$  138 (**1f**) (Figure 3.4A). Since this ion was not observed upon CID of the in-source fragment ions, it most likely formed directly from the  $[\text{M} - \text{H}]^-$  ion. **1f** did not retain sulfur (Figure 3.5). The Smiles rearrangement has been shown to occur in the gas-phase through an intramolecular nucleophilic attack on the aromatic ring, resulting in the displacement of a leaving group from the same carbon (See Section 1.2.2.2).<sup>36</sup> The solution phase reaction is aided by an electron-withdrawing group on the aromatic ring, such as  $\text{NO}_2$ . Evidence for the Smiles rearrangement would be provided in the CID spectrum of deprotonated  $\text{Ns}[^{18}\text{O}]\text{Gly}$ . The  $^{18}\text{O}$  label, however, was lost in  $m/z$  138, indicating that a Smiles rearrangement did not occur prior to fragmentation.

Rearrangement of the NsGly anion ionized at the sulfonamide group followed by S-O bond cleavage is proposed as a route to the  $m/z$  138 ion (Scheme 3.10). After bond cleavage, the transient ion-neutral complex may dissociate to the  $m/z$  138 ion or undergo proton transfer to generate a carboxylate ion. Decarboxylation yields an ion at  $m/z$  76, which was detected as a very minor ion upon CID of deprotonated NsGly in the ion trap mass spectrometer (Figure 3.4A). The  $m/z$  76 ion, however, has greater prominence in the analogous spectrum collected on the triple quadrupole mass spectrometer discussed in detail in a later section of this thesis.

In the triple quadrupole mass spectrometer, no label from deprotonated Ns[1- $^{13}\text{C}$ ]Gly, Ns[2- $^{13}\text{C}$ ,  $^{15}\text{N}$ ]Gly and Ns[ $^{18}\text{O}$ ]Gly appeared in the  $m/z$  138 product ion. Sulfur and labels from Ns[2- $^{13}\text{C}$ ,  $^{15}\text{N}$ ]Gly and Ns[2,2- $^2\text{H}_2$ ]Gly were retained in the  $m/z$  76 ion, demonstrating the formation of the  $m/z$  76 and 138 ions from different parts of the NsGly anion. These labeling results are consistent with the fragmentation pathway proposed in Scheme 3.10.



**Scheme 3.10.** Suggested structures for the fragmentation of  $m/z$  259 to form  $m/z$  138 and 76 initiated by sulfonamide rearrangement.

A dual bond cleavage pathway introduced in the next section also leads to a product ion at  $m/z$  138. However, this  $m/z$  138 ion is formed by fragmentation of the ion at  $m/z$  186 as a second step in the dual bond cleavage pathway. While the  $m/z$  186 ion is present in the CID mass spectrum of deprotonated NsGly collected on the triple quadrupole mass spectrometer (Figure 3.11), it is not observed in the equivalent spectrum collected on the ion trap mass spectrometer (Figure 3.4A). This suggests that the  $m/z$  138 ion is formed by the sulfonamide rearrangement pathway in the ion trap mass spectrometer, whereas both sulfonamide rearrangement and dual bond cleavage are

possible when more energetic conditions are provided by the triple quadrupole mass spectrometer.

### 3.5 Effect of Structural Variations on Fragmentation Processes

#### 3.5.1 Position of the Nitro Substituent

Upon ESI(-)MS/MS, Ns amino acids having a *meta*- or *para*- nitro group did not undergo *ortho* cyclization and fragmented by a different process. CID of deprotonated mNsGly and pNsGly gave major product ions at  $m/z$  186 (Figure 3.10). CID of deprotonated mNsGly also gave a product ion at  $m/z$  215, corresponding to decarboxylation. CID of the  $m/z$  186 ions from mNsGly and pNsGly gave product ion peaks (Figure 3.10, inset) resulting from the loss of SO and SO<sub>2</sub>, respectively. Loss of SO<sub>2</sub> from aryl sulfinate ions has been documented by Zhang.<sup>45</sup> Thus the MS/MS results indicate that sulfinate ions are generated by CID of the [M – H]<sup>–</sup> ions of mNsGly and pNsGly. Consequently, a neutral molecule is formed from the amino acid subunit.

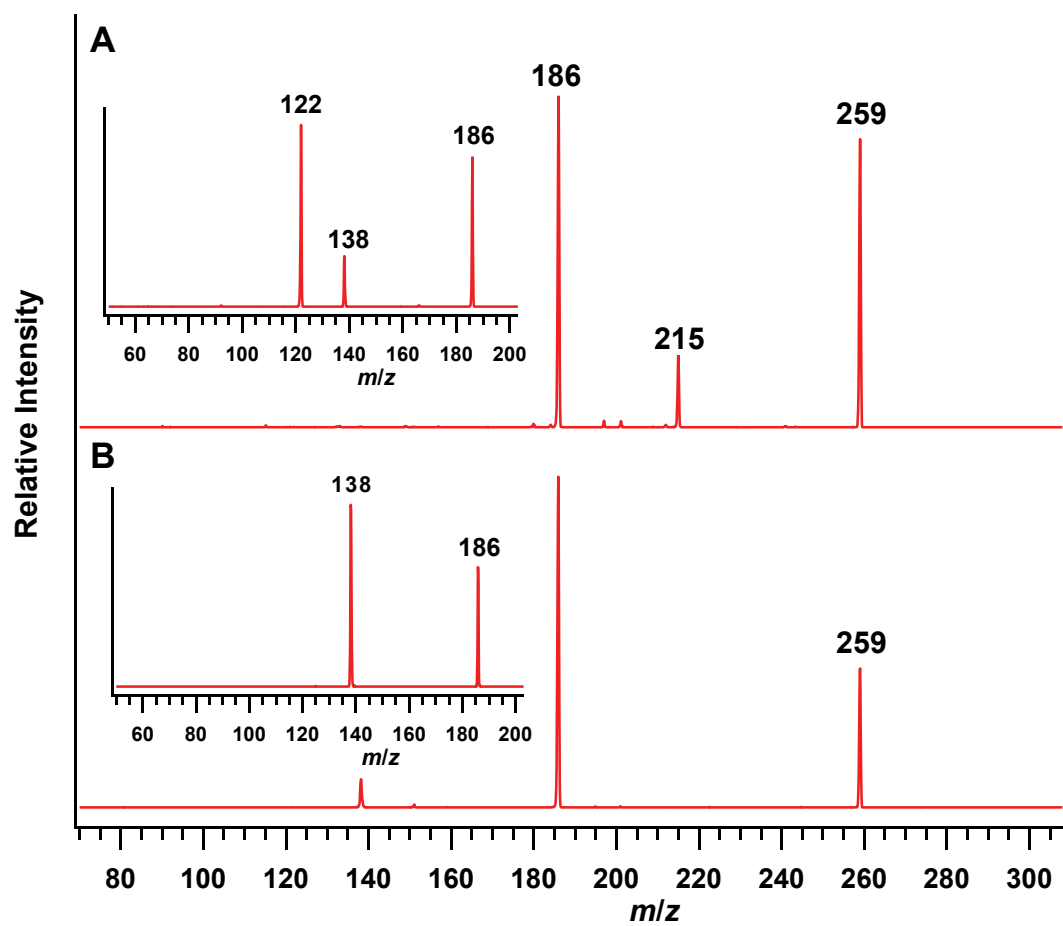
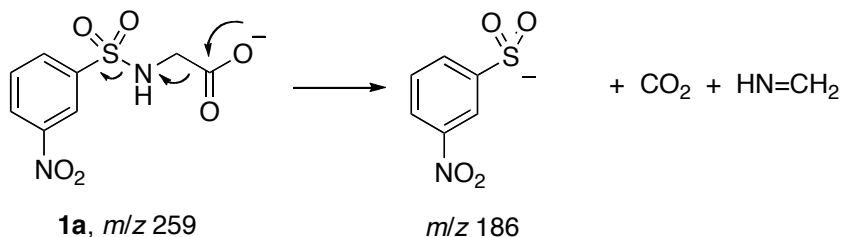


**Figure 3.10.** Product ion mass spectra obtained by CID of **A:** deprotonated mNsGly (CID 23%); **B:** deprotonated pNsGly (CID 22%). CID mass spectra of the  $m/z$  186 (CID 24%) and  $m/z$  186 (CID 18%) ions generated in source are shown as insets.

### 3.5.1.1 Dual Bond Cleavage Pathway

The fragmentation of mNsGly and pNsGly likely corresponded to a combined neutral loss of CO<sub>2</sub> and HN=CH<sub>2</sub>, resulting from the cleavage of two single bonds (Scheme 3.11).



**Scheme 3.11.** Dual bond cleavage of the  $m/z$  259 ion leading to a sulfinate product ion at  $m/z$  186, through the loss of CO<sub>2</sub> and HNCH<sub>2</sub>.

In the MS/MS spectra of NsGly obtained from the QqQ, product ions from both the *ortho* cyclization (i.e.,  $m/z$  212 and 184) and dual bond cleavage pathways (i.e.,  $m/z$  186) were observed (Figure 3.11). The QqQ uses argon as the collision gas instead of the helium atoms of the ion trap, so higher energy collisions occur and some of the ions have sufficient energy to fragment by a higher energy process, as well as by the lower energy pathway seen in the ion trap mass spectrometer. The greater abundance of the ions in the *ortho* cyclization pathway also indicates that the energy barrier for cyclization is lower than that for dual bond cleavage.

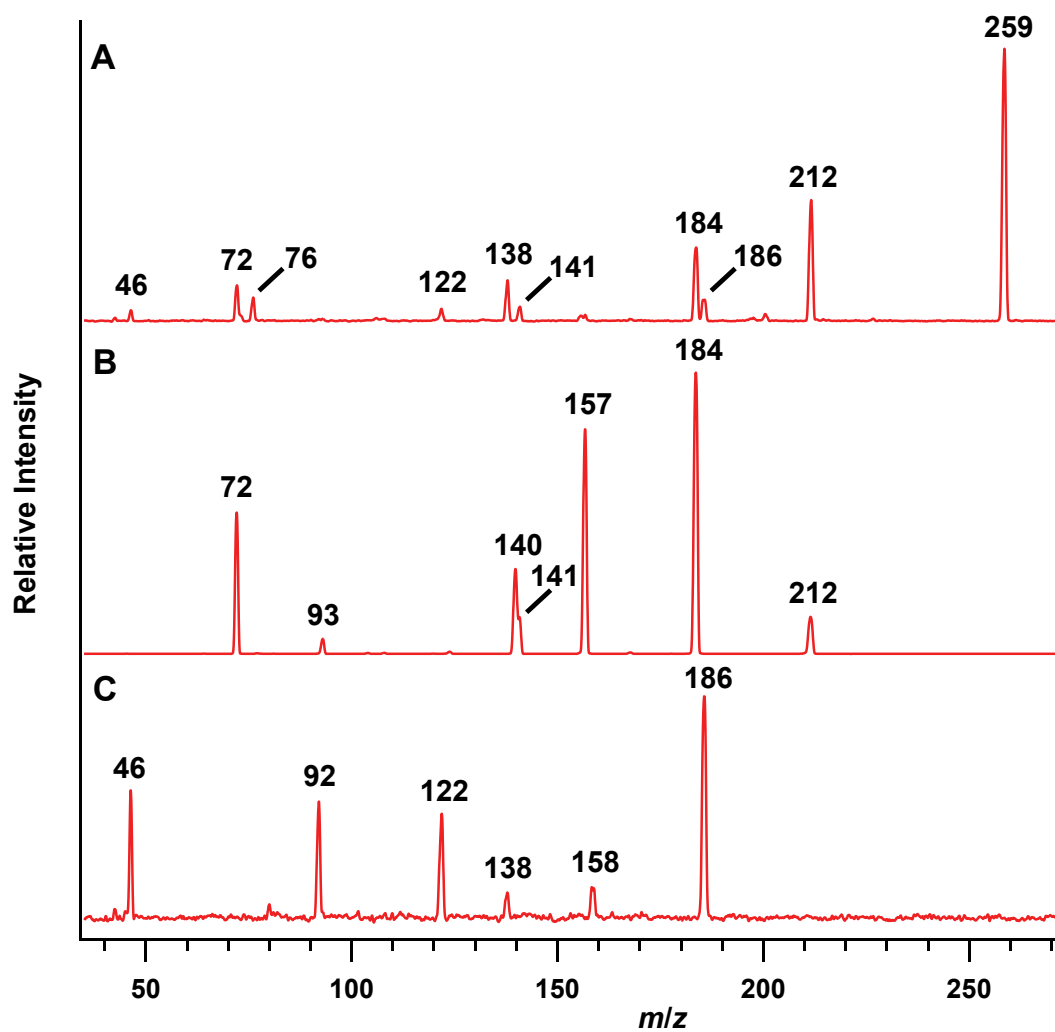


**Figure 3.11.** Triple quadrupole CID mass spectra of **A:** deprotonated NsGly (20 V cone; 10 eV); **B:** the  $m/z$  212 ion formed in source (30 V cone; 15 eV); **C:** the  $m/z$  186 ion formed in source (30 V cone; 15 eV).

### 3.5.2 Variations of the *Ortho* Substituent

To determine whether *ortho* cyclization could occur when the nitro group was replaced by other substituents, 2FBsGly, 2,5-DClBsGly, 2BrBsGly and 2CF<sub>3</sub>BsGly were synthesized and investigated by ESI(-)MS/MS.

In the CID mass spectra of the *ortho* halogen derivatives (Figure 3.12A and Figure 3.13A), a predominant product ion at  $m/z$  212 was formed by loss of HF and HBr from deprotonated 2FBsGly and 2BrBsGly, respectively. Similarly, loss of HCl from deprotonated 2,5-DClBsGly gave the analogous product ion at  $m/z$  246 (Figure 3.14A). Sequential neutral losses of CO and HCN were obtained upon CID of the ions generated in source (Figures 3.12BC, 3.13B, and 3.14BC) confirming the structural identities of the intermediate ions in the *ortho* cyclization pathway (Scheme 3.7) of the 2FBsGly, 2,5-DClBsGly and 2BrBsGly anions.

The loss of HCl upon CID of deprotonated 2,5-DClBsGly was confirmed by performing CID on each ion in the isotope cluster (Figure 3.15). The ions at  $m/z$  282 and 286 contained only one chlorine isotope and only loss of H<sup>35</sup>Cl or H<sup>37</sup>Cl was observed (Figure 3.15B and D). The ion at  $m/z$  284, however, contained both isotopes and losses of H<sup>35</sup>Cl and H<sup>37</sup>Cl were observed. The correlation of the neutral losses with the isotopic composition demonstrates that the neutral molecule formed contains chlorine.

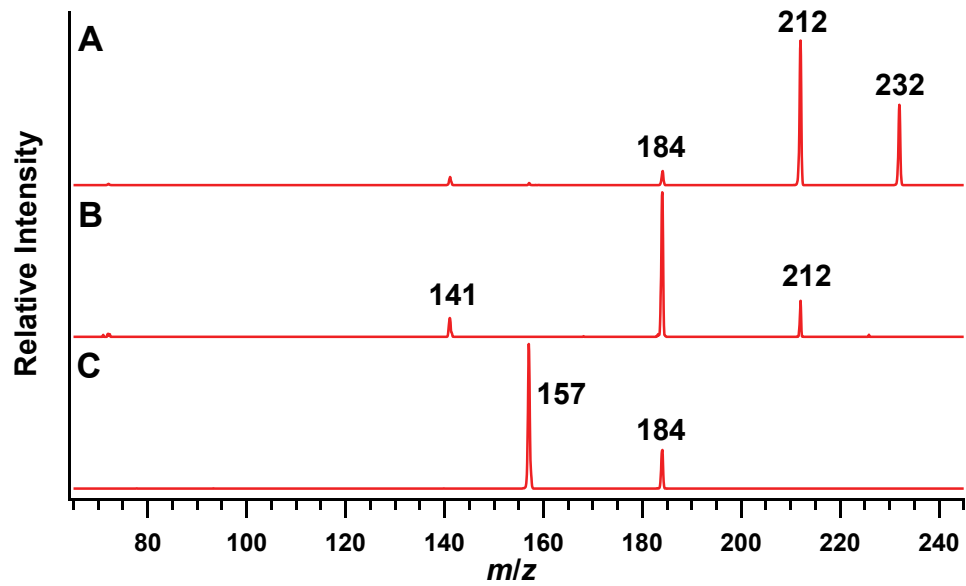


**Figure 3.12.** Product ion mass spectra obtained by CID of **A:** deprotonated 2FBsGly (CID 18%); **B:**  $m/z$  212 ion generated in source (CID 18%); **C:**  $m/z$  184 ion generated in source (CID 22%).

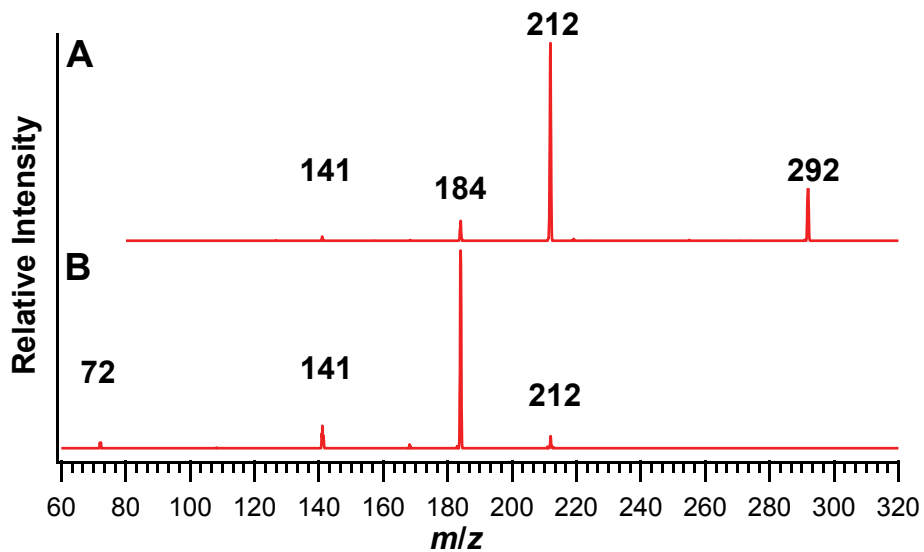


**Figure 3.13.** Product ion mass spectra obtained by CID of **A:** deprotonated 2BrBsGly (CID 18%); **B:**  $m/z$  212 ion formed in source (CID 20%).

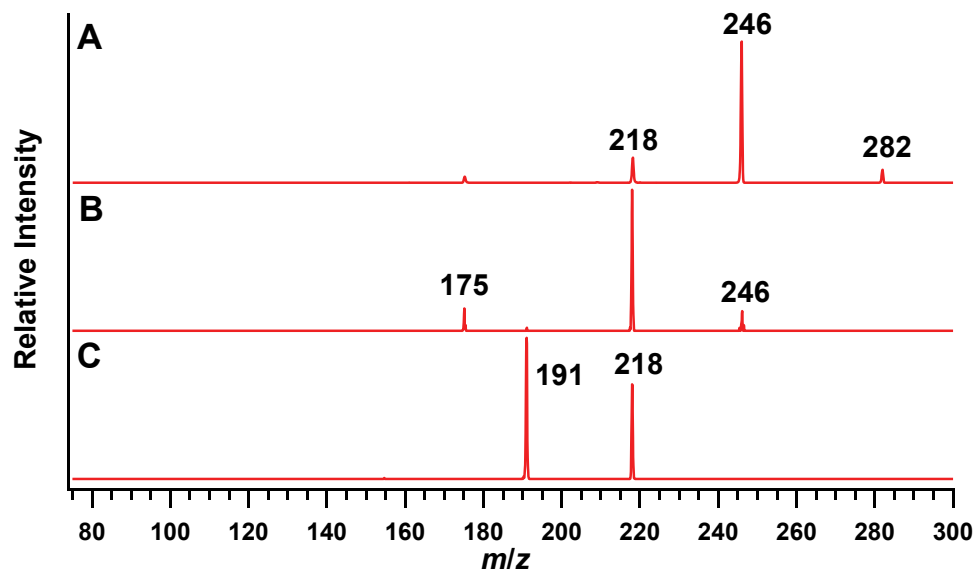


**Figure 3.14.** Product ion mass spectra obtained by CID of **A:** deprotonated 2,5-DCIBsGly (CID 20%); **B:**  $m/z$  246 ion formed in source (CID 20%); **C:**  $m/z$  218 ion formed in source (CID 20%).

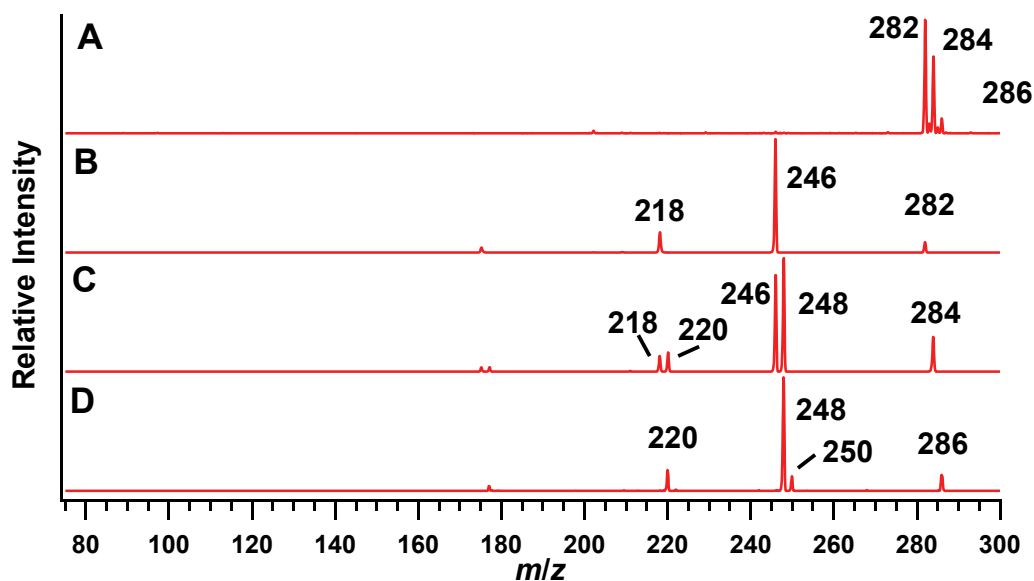


**Figure 3.15.** Mass spectra of deprotonated 2,5-DCIBsGly. **A:** ESI(-)MS of 2,5-DCIBsGly; **B:** CID spectrum of  $[M - H]^-$  (CID 20%); **C:** CID spectrum of  $[M + 2 - H]^-$  (CID 20%); **D:** CID spectrum of  $[M + 4 - H]^-$  (CID 20%).

Loss of the *ortho* substituent, however, was not observed when deprotonated 2CF<sub>3</sub>BsGly (*m/z* 282) was subjected to CID (Figure 3.16). Instead, a predominant product ion at *m/z* 209 was observed. The neutral loss in this fragmentation reaction was consistent with the dual bond cleavage pathway (Scheme 3.11) and the losses of SO and SO<sub>2</sub> observed upon CID of the *m/z* 209 ion formed in source are consistent with the formation of the expected sulfinate ion by dual bond cleavage. In this instance, *ortho* cyclization requires the cleavage of a C-C bond and the formation of F<sub>3</sub>C<sup>-</sup> as a leaving group. As indicated by gas-phase acidities (Table 3.2), the trifluoromethyl anion is less stable in the gas phase than halide ions and the nitrite ion, and would be a poorer leaving group.

Hydrogen bonding between the halogen or nitro substituent and the sulfonamide hydrogen atom could assist the formation of the neutral hydrogen halide and HONO, with the sulfonamide hydrogen becoming part of the neutral molecule. When CF<sub>3</sub> is the substituent, hydrogen bonding to fluorine is possible, but the formation of a C-H bond is required to form CHF<sub>3</sub>. In other words, CHF<sub>3</sub> must be formed by distinct bond breaking and bond forming steps, while bond breaking and bond forming can occur at the same time when the *ortho* substituent is a halogen or a nitro group and the substituent does not have to leave as a distinct anion.

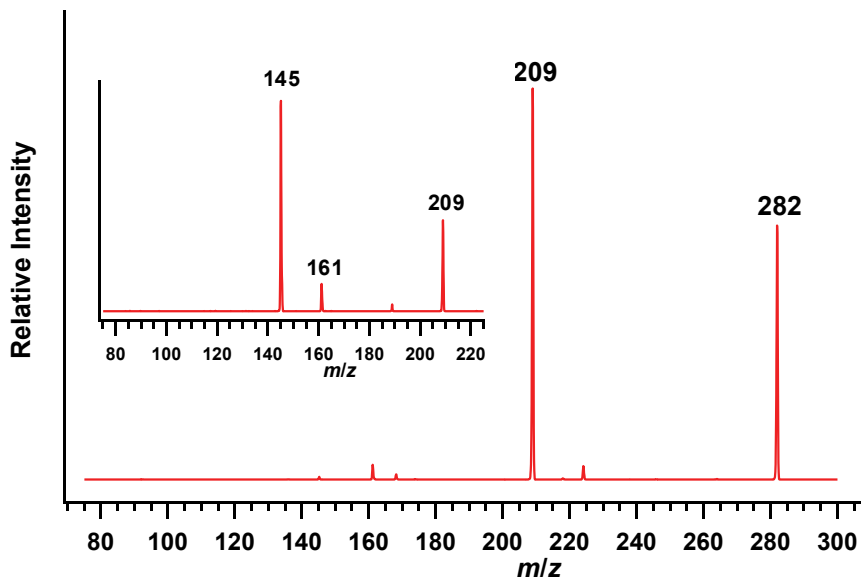


**Figure 3.16.** Product ion mass spectrum obtained by CID of deprotonated 2CF<sub>3</sub>BsGly (CID 22%). CID mass spectrum of *m/z* 209 (CID 22%) shown in inset.

**Table 3.2.** Experimental gas phase acidities.

Acid	GPA ( $\Delta_r G^\circ$ , kJ mol <sup>-1</sup> ) <sup>90</sup>
HBr	1331
HCl	1373
HF	1530
HONO	1396
CHF <sub>3</sub>	1547

### 3.5.3 Electron Density of the Aryl Ring

The electron density of the aryl ring was decreased by the addition of a second nitro group. The loss of HONO from deprotonated 2,4-DNsGly (Figure 3.17A) occurred at a slightly lower collision energy than that needed to observe loss of HONO from deprotonated NsGly (Figure 3.4A). With a third electron withdrawing group on the aryl ring, intramolecular nucleophilic attack by the carboxylate ion became more favourable in accord with the lower collision energy needed for HONO loss. The product ion formed by HONO loss in source underwent successive losses of CO, HCN and SO<sub>2</sub> upon CID (Figure 3.17B, C and D), consistent with the expected *ortho* cyclization. The [M – H]<sup>–</sup> ion of 2,4-DNsGly also underwent a sulfonamide rearrangement leading to the formation of the *m/z* 183 ion (Figure 3.17A). The analogous sulfonamide rearrangement is described for NsGly in Section 3.4.3. The *m/z* 183 ion then loses NO to give the ion at *m/z* 153 (Figure 3.17E).

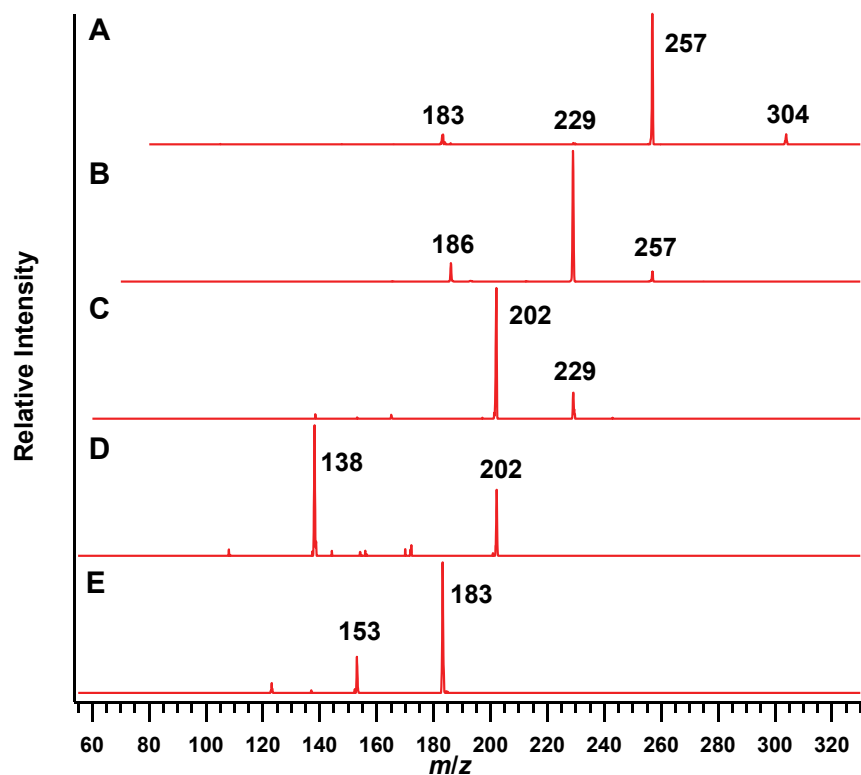


**Figure 3.17.** Product ion mass spectra obtained by CID of **A:** deprotonated 2,4-DNsGly (CID 15%); **B:**  $m/z$  257 ion generated in source (CID 17%); **C:**  $m/z$  229 ion generated in source (CID 22%); **D:**  $m/z$  202 ion generated in source (CID 30%); **E:**  $m/z$  183 ion generated in source (CID 30%).

### 3.5.4 Substituent at $C\alpha$ of the Amino Acid Subunit

Methyl groups were positioned at  $C\alpha$  of the amino acid subunit by preparing Ns derivatives of alanine and 2-aminoisobutyric acid. Prominent product ions at  $m/z$  226 and 240 were observed in the CID mass spectra of deprotonated NsAla (Figure 3.18) and Ns2Aib (Figure 3.19), respectively. As observed for the NsGly anion, the formation of

these product ions indicated the loss of HONO and *ortho* cyclization. CID of these ions formed in source (Figure 3.18B and Figure 3.19B) resulted in loss of CO. A subsequent loss of CH<sub>3</sub>CN was observed in the pathway of the NsAla ion (Figure 3.18C), but the analogous proton transfer was not possible in the Ns2Aib ion. When the series of CID experiments were repeated on the Ns[2,3-<sup>13</sup>C<sub>2</sub>]Ala anion (Figure 3.20), the isotopic labels were retained upon loss of HONO and CO, but lost as <sup>13</sup>CH<sub>3</sub><sup>13</sup>CN in the third step of the *ortho* cyclization pathway of NsAla fragmentation.

Product ions at *m/z* 141 and 86 were formed by CID of the *m/z* 226 ion generated in source from deprotonated NsAla (Figure 3.18B). The isotopic labels from the Ns[2,3-<sup>13</sup>C<sub>2</sub>]Ala ion were retained in the ion at lower *m/z* (Figure 3.20B). Overall, the formation of these ions is consistent with the *ortho* cyclization 2 pathway (Scheme 3.8 and Scheme 3.9).

A minor ion at *m/z* 138 was formed by CID of the NsAla and Ns2Aib anions (Figure 3.18A and Figure 3.19). In the absence of ions at *m/z* 186 from the dual bond cleavage pathway (Scheme 3.11), the formation of the *m/z* 138 ion is most consistent with the sulfonamide rearrangement pathway (Scheme 3.10).

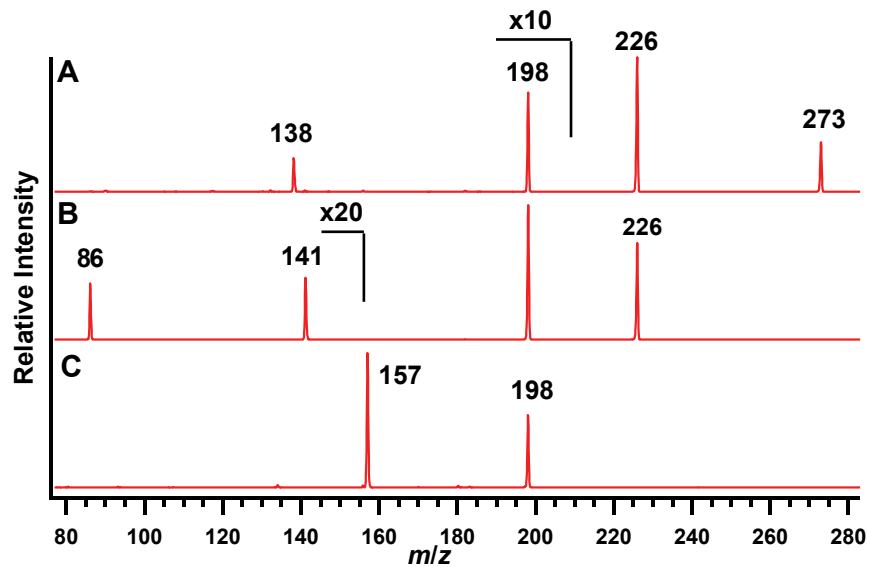


**Figure 3.18.** Product ion mass spectra obtained by CID of **A:** deprotonated NsAla (CID 18%); **B:**  $m/z$  226 ion formed in source (CID 18%); **C:**  $m/z$  198 ion formed in source (CID 27%).

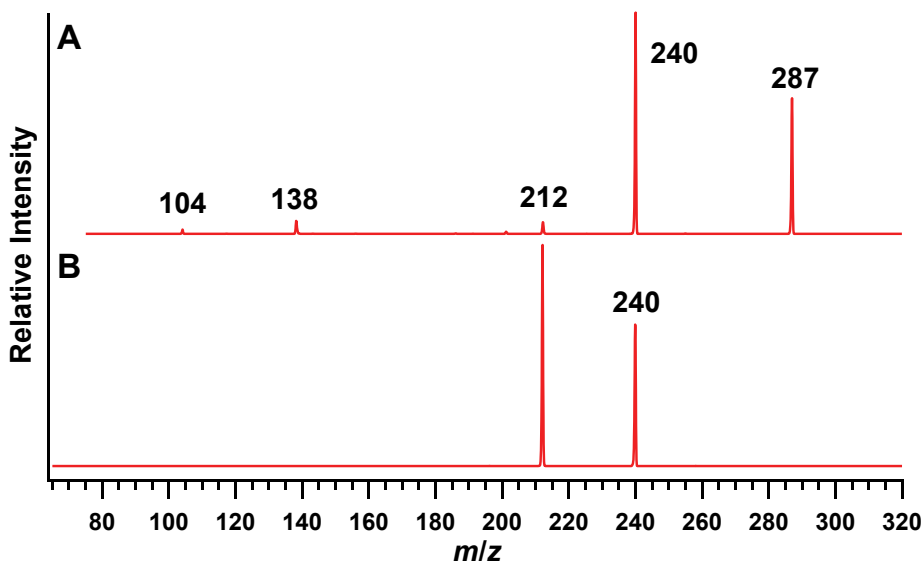


**Figure 3.19.** Product ion mass spectra obtained by CID of **A:** deprotonated Ns2Aib (CID 18%); **B:**  $m/z$  240 ion formed in source (CID 18%).

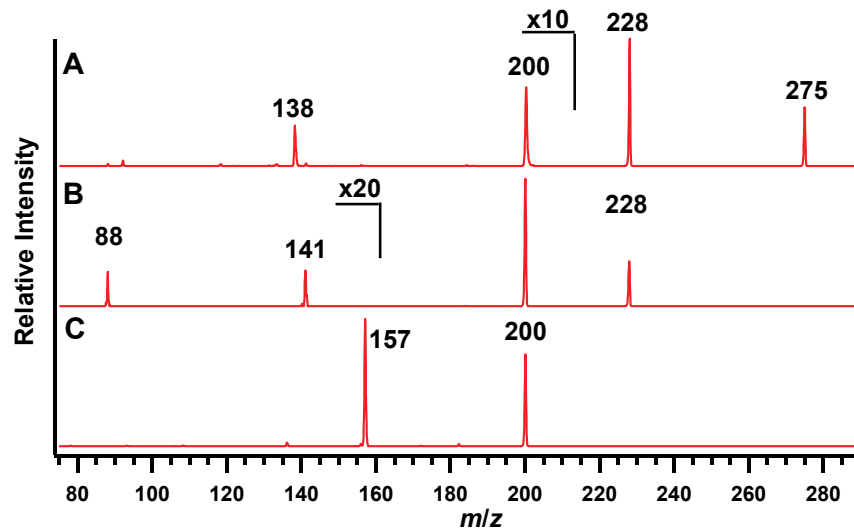


**Figure 3.20.** Product ion mass spectra obtained by CID of **A:** deprotonated Ns[2,3- $^{13}\text{C}_2$ ]Ala (CID 18%); **B:**  $m/z$  228 ion formed in source (CID 18%); **C:**  $m/z$  200 ion formed in source (CID 26%).

### 3.5.5 Ionization Site

The model compounds benzenesulfonamide and glycine have similar gas-phase acidities (1394 and 1400  $\text{kJ mol}^{-1}$ , respectively).<sup>90</sup> Thus ionization of NsGly would be expected at either the sulfonamide or carboxyl group. The transfer of a proton from one group to the other, however, would occur via a favourable 5-membered cyclic transition state and both anions would be expected in the gas phase.

The fragmentation pathways proposed for deprotonated NsGly start from either the carboxylate ion (Scheme 3.6 and 3.11) or the sulfonamide ion (Scheme 3.10). To correlate ionization site with the fragmentation pathway, a series of Ns derivatives in which ionization would occur at only one site or predominantly one site were investigated.

Upon CID of NsGlyNH<sub>2</sub>, the [M – H]<sup>–</sup> ion at *m/z* 258 fragmented to form an abundant product ion at *m/z* 194 (Figure 3.21). This neutral loss of 64 corresponds to the formation of SO<sub>2</sub>. CID of the *m/z* 194 ion produced a major ion at *m/z* 133 with minor ions at *m/z* 121 and 137. However, this mass spectrum had a very low intensity, 1000x lower than the mass spectrum of the isolated *m/z* 194 ion, suggesting that the major product ion formed in this fragmentation had *m/z* < 50 and was not detected by the ion trap mass spectrometer. For NsGlyNH<sub>2</sub>, ionization is expected predominantly at the sulfonamide (the gas phase acidity of the acetamide group is 1485 kJ mol<sup>–1</sup>).<sup>90</sup> Loss of SO<sub>2</sub> as the predominant fragmentation process has been seen in sulfonamide anions.<sup>46,49</sup>

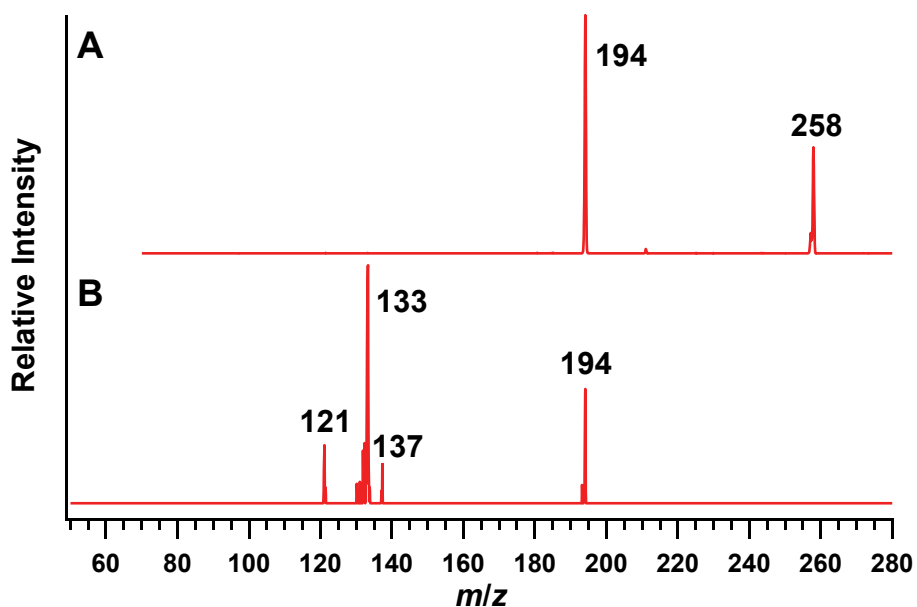


**Figure 3.21.** Product ion mass spectra obtained by CID of **A:** deprotonated NsGlyNH<sub>2</sub> (CID 17%); **B:** *m/z* 194 ion formed in source (CID 30%).

Ionization of NsNHEtOH (EtOH GPA 1555 kJ mol<sup>–1</sup>)<sup>90</sup> was also expected predominantly at the sulfonamide. Upon CID of the [M – H]<sup>–</sup> ion of NsNHEtOH, a major

product ion at  $m/z$  198 was observed with minor ions at  $m/z$  181 and 138 (Figure 3.22). Formation of the  $m/z$  198 ion was accompanied by a neutral loss of 47 u, indicating that loss of HONO was still the predominant fragmentation process. The *ortho* cyclization may be due to a lower energy barrier for proton transfer than NsGlyNH<sub>2</sub>. The alkoxide anion is also a good nucleophile, and has been shown to be involved in *ortho* cyclization in the gas phase (Section 1.4.2).<sup>41</sup>

CID of the  $m/z$  198 ion formed in source generated a major product ion at  $m/z$  141 through a loss of 57 u, consistent with the formation of HCN and CH<sub>2</sub>O. Although similar to the formation of **1e** observed in the fragmentation of NsGly (Section 3.4.2), this fragmentation process required higher collision energy and the intermediary of a higher energy phenoxide ion.

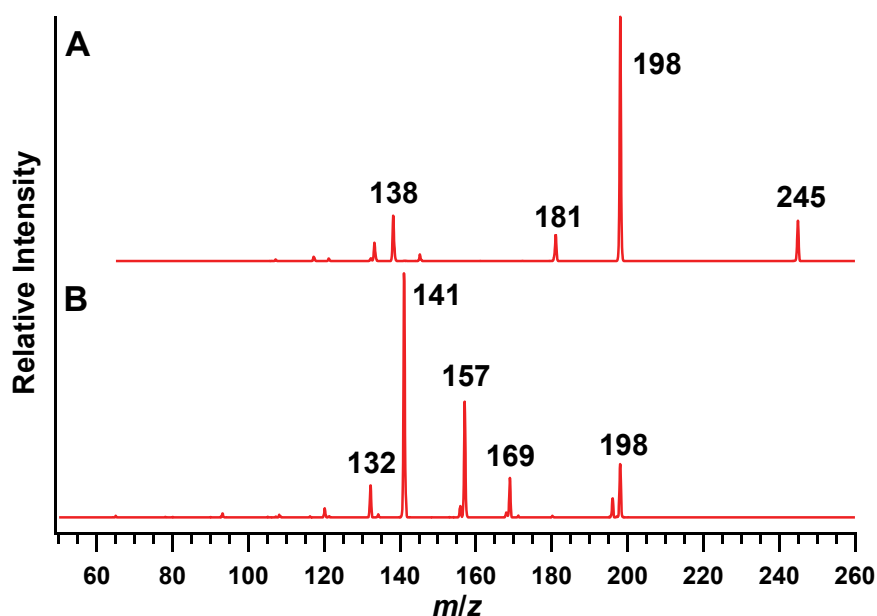


**Figure 3.22.** Product ion mass spectra obtained by CID of **A:** deprotonated NsNHtOH (CID 18%); **B:**  $m/z$  198 ion formed in source (CID 28%).

The mass spectrum of NsGlyOEt was collected to investigate the effect of blocking ionization on the carboxyl group by esterification. Upon CID, the  $[M - H]^-$  ion at  $m/z$  287 formed product ions at  $m/z$  270, 241, 240, 186, 156, 138 and 93 (Figure 3.23). A neutral loss of 46 u, giving the  $m/z$  241 ion, corresponds to a loss of  $\text{CH}_3\text{CH}_2\text{OH}$  (Scheme 3.12). The  $m/z$  240 ion is formed through a neutral loss of 47 u, which could correspond to a loss of HONO (Scheme 3.12). The most abundant product ion at  $m/z$  186 is likely due to *N*-alkylation followed by dual bond cleavage (Scheme 3.13) similar to the fragmentation of NsGly described in Section 3.5.1.1. Further fragmentation of the  $m/z$  186 ion could have formed the ion at  $m/z$  138, through a loss of SO, but the  $m/z$  138 ion was more likely formed through the sulfonamide rearrangement pathway described in Section 3.4.3. However, other ions were not formed in source, and so further experiments are required in order to correlate structures with the product ions.

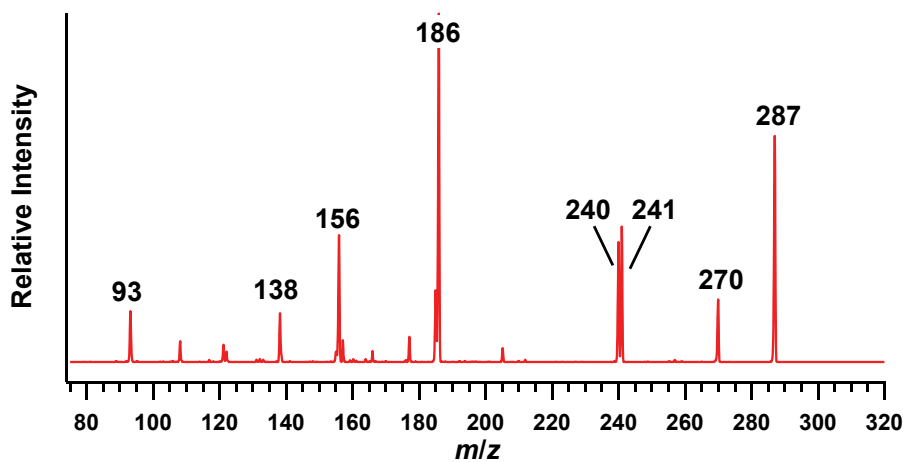
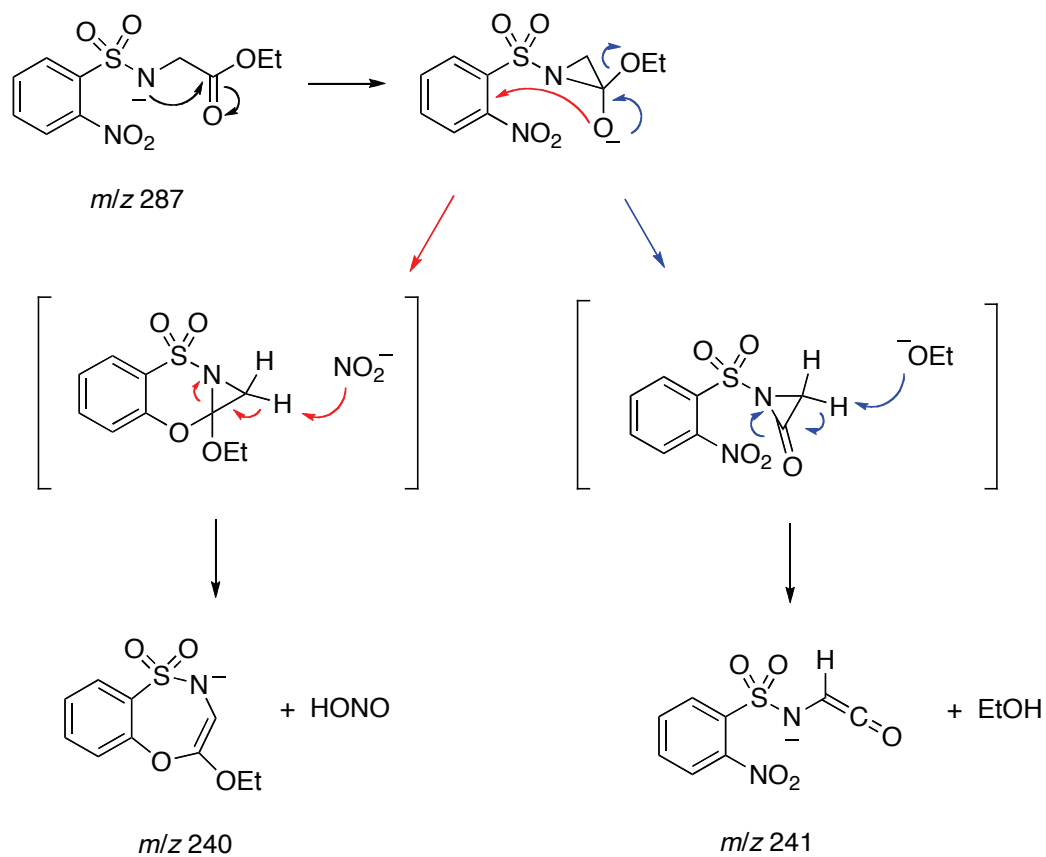
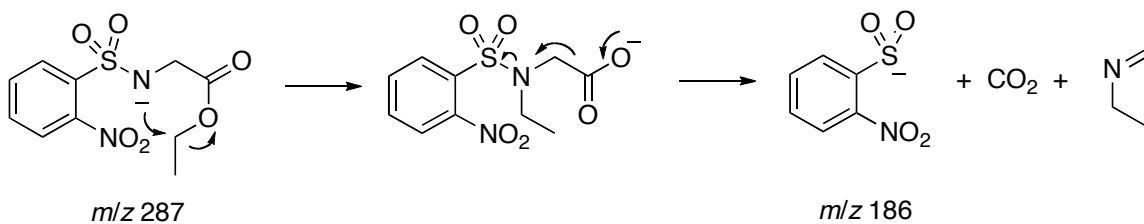


**Figure 3.23.** Product ion mass spectrum obtained by CID of deprotonated NsGlyOEt (CID 22%).



**Scheme 3.12.** Losses of HONO and EtOH from deprotonated NsGlyOEt.



**Scheme 3.13.** *N*-Alkylation and dual bond cleavage of deprotonated NsGlyOEt.

Since it was proposed that the neutral loss of 47 u observed in NsGly derivatives involved the loss of the nitro group and the sulfonamide proton, the mass spectra of NsSar were collected to determine if the absence of the sulfonamide proton affected the loss of HONO and *ortho* cyclization. Upon CID, the  $[M - H]^-$  ion of NsSar fragmented to form a major ion at  $m/z$  156 (**16b**) and minor ions at  $m/z$  226, 209, 141 and 138 (Figure 3.24A). Isotopic labels were retained in the  $m/z$  227 and 210 ions formed from CID of Ns[1- $^{13}\text{C}$ ]Sar (Figure 3.25B).

A neutral loss of 47 from the  $[M - H]^-$  ion of NsSar gave the ion at  $m/z$  226. This product ion was not formed in source and MS/MS experiments could not be performed, but it is possible that this ion is formed by an *ortho* cyclization and the loss of HONO. A neutral loss of  $\text{SO}_2$  from **16a** likely formed the  $m/z$  209 ion. The lowest energy fragmentation process seen upon CID of NsSar was the formation of the  $m/z$  156 ion (Figure 3.24A). CID of Ns[1- $^{13}\text{C}$ ]Sar and Ns[2,2- $^2\text{H}_2$ ]Sar also formed  $m/z$  156 as a major product ion, indicating that the isotopic labels were lost in this fragmentation (Figure 3.25). Upon CID, the ion at  $m/z$  156 fragmented to form only an ion at  $m/z$  108, through a neutral loss of 48 u, SO. This indicates that the sulfur was still present in the  $m/z$  156 ion and a structure for this ion is proposed in Scheme 3.14.

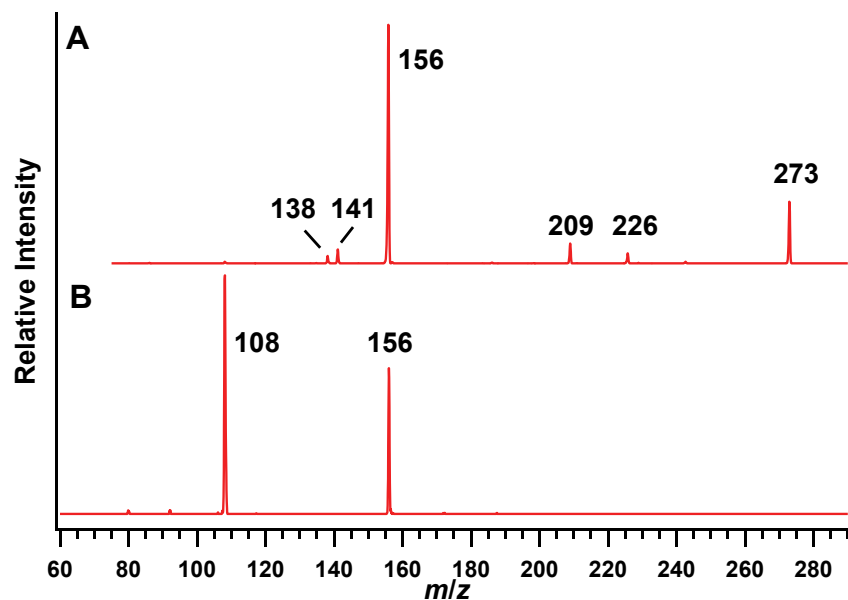


**Figure 3.24.** Product ion mass spectra obtained by CID of **A:** deprotonated NsSar (CID 17%); **B:**  $m/z$  156 ion formed in source (CID 19%).

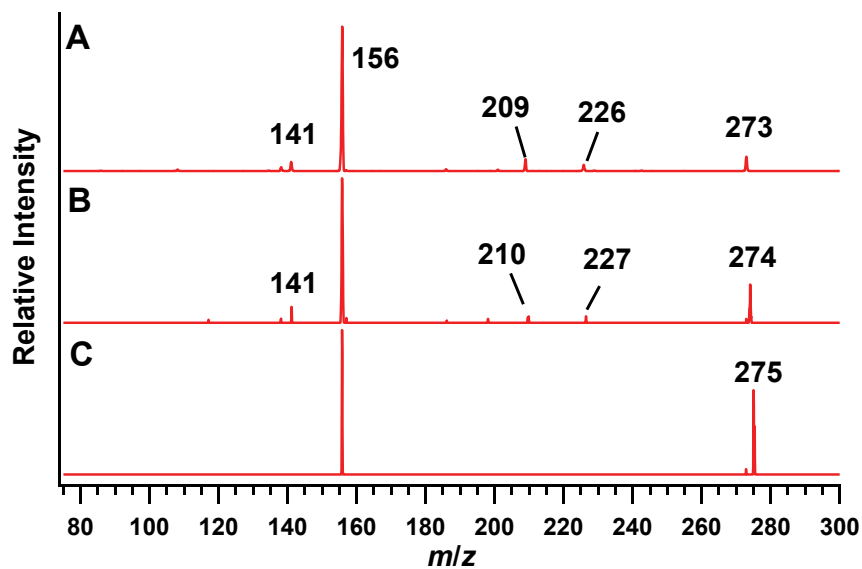
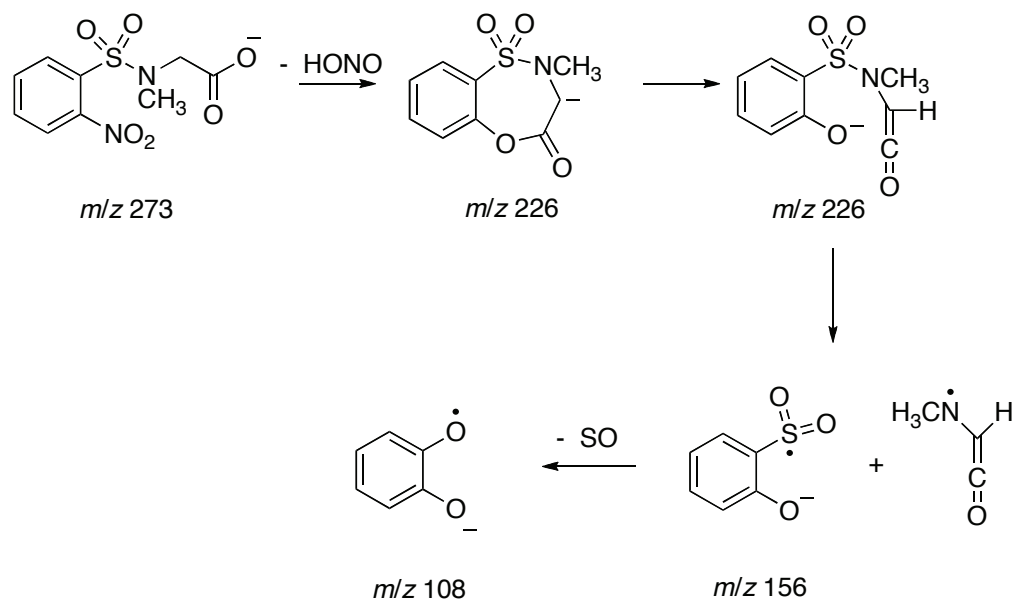


**Figure 3.25.** Product ion mass spectra obtained by CID of **A:** deprotonated NsSar (CID 17%); **B:** deprotonated Ns[1- $^{13}\text{C}$ ]Sar (CID 15%); **C:** deprotonated Ns[2,2- $^2\text{H}_2$ ]Sar (CID 14%).



**Scheme 3.14.** Fragmentation process of deprotonated NsSar to give ions at  $m/z$  226, 156 and 108.

Upon CID, deprotonated mNsSar and pNsSar gave major product ions at  $m/z$  186 (Figures 3.26 and 3.27) consistent with the dual bond cleavage fragmentation process proposed for mNsGly and pNsGly (Section 3.5.1.1). For the sarcosine derivatives, ionization only occurs at the carboxyl group, the ionization state proposed for the dual bond cleavage pathway (Scheme 3.11). Upon CID, the  $m/z$  186 ion formed in source formed product ions at  $m/z$  138 and 122 by a loss of SO and SO<sub>2</sub>, respectively, and indicating that a sulfinate ion was formed by the dual bond cleavage pathway.

In the CID mass spectra of both the mNsGly (Figure 3.10A) and mNsSar (Figure 3.26A) anions, loss of CO<sub>2</sub> was also evident. Corresponding decarboxylated ions were not formed from pNsGly (Figure 3.10B), pNsSar (Figure 3.27), NsGly (Figure 3.4) or NsSar (Figure 3.24) suggesting that the heterolytic bond cleavage associated with

decarboxylation of the mNsGly and mNsSar ions generates a stabilized product ion rather than the expected C $\alpha$  anion (Scheme 3.15). When the nitro group is *meta* to the sulfonamide group, addition of the C $\alpha$  anion to the aromatic ring provides a delocalized anion that is stabilized by both electron withdrawing substituents. In the pNs derivatives, the position of the nitro group would make it less effective at stabilizing charge on the bicyclic anion. The nucleophilic addition to the ring is reversible. CID of the decarboxylated mNsSar ion generated in source (Figure 3.26B) gave loss of CH<sub>3</sub>NCH<sub>2</sub> as the predominant fragmentation reaction, completing the dual bond cleavage fragmentation.

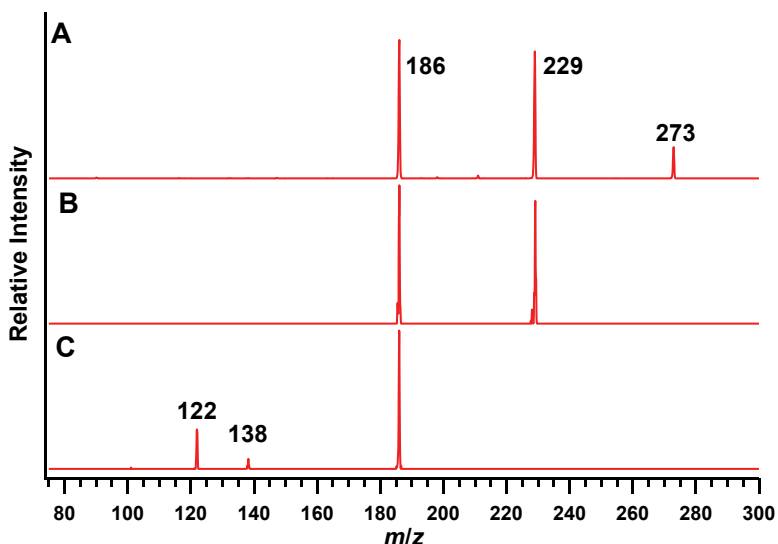


**Figure 3.26.** Product ion mass spectra obtained by CID of **A:** deprotonated mNsSar (CID 20%); **B:** *m/z* 229 ion formed in source (CID 18%); **C:** *m/z* 186 ion formed in source (CID 24%).

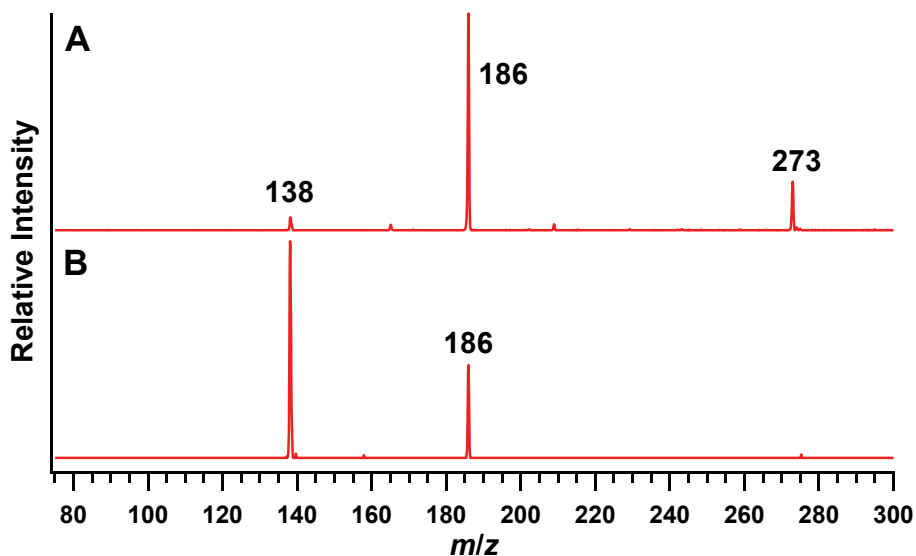
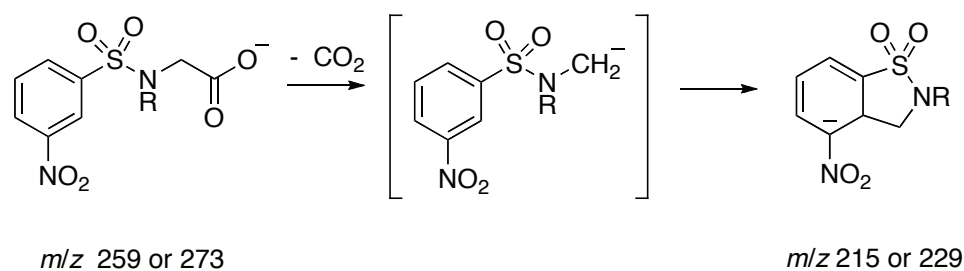


**Figure 3.27.** Product ion mass spectra obtained by CID of **A**: deprotonated pNsSar (CID 18%); **B**: *m/z* 186 ion formed in source (CID 18%).



**Scheme 3.15.** Decarboxylation of mNsGly (R = H) or mNsSar (R = CH<sub>3</sub>).

### 3.5.6 Fragmentation Pathways of Homologous Ns Amino Acids

The Ns derivatives of  $\beta$ -alanine and 4-aminobutanoic acid were prepared to investigate the possible formation of larger rings by loss of HONO and *ortho* cyclization. The ESI(-) mass spectrum of Ns $\beta$ Ala showed the formation of an abundant [M - H]<sup>-</sup> ion at *m/z* 273 (**25a**). Upon CID (Figure 3.28A), **25a** fragmented to major ions at *m/z* 226

(**25b**) and 201 (**25c**), and minor ions at  $m/z$  184, 182, and 138. CID of the  $[M + 2 - H]^-$  ion of Ns $\beta$ Ala indicated that the ions at  $m/z$  226, 201, 184, and 182 contained sulfur.

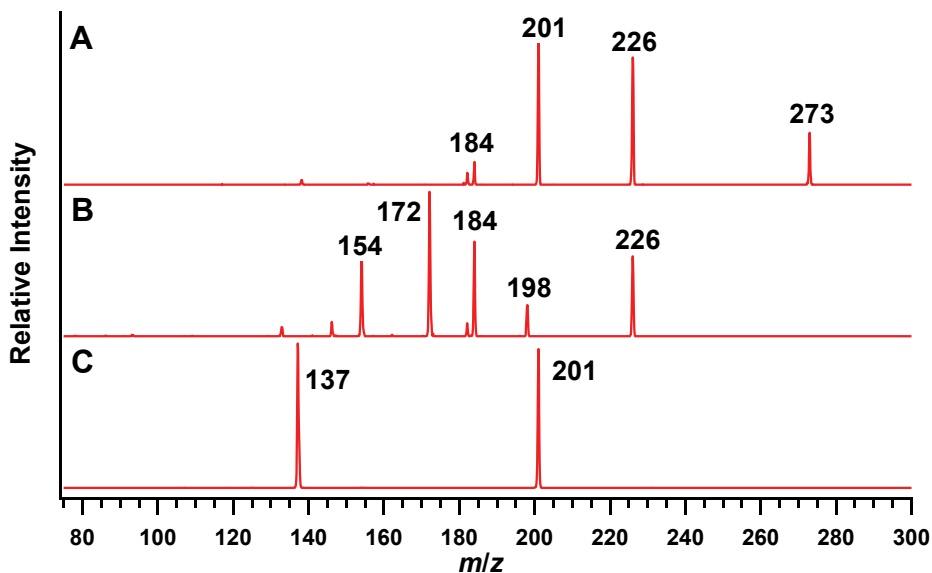
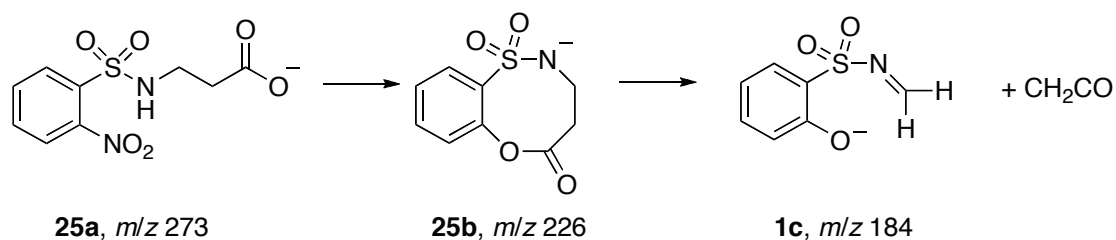


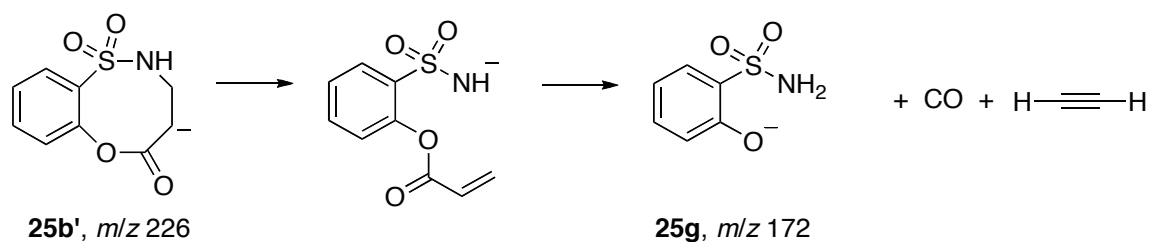
**Figure 3.28.** Product ion mass spectra obtained by CID of **A:** deprotonated Ns $\beta$ Ala (CID 22%); **B:**  $m/z$  226 ion formed in source (CID 29%); **C:**  $m/z$  201 ion formed in source (CID 20%).

One of the major fragmentation processes ( $m/z$  273  $\rightarrow$  226) showed a neutral loss of 47 u, indicating formation of HONO and *ortho* cyclization to form the eight-membered ring in the bicyclic product ion, **25b** (Scheme 3.16). The structure of **25b** is analogous to that of **1b** formed by fragmentation of NsGly, involving an *ortho* cyclization and loss of the nitro group and amide proton (Scheme 3.6).



**Scheme 3.16.** Proposed structures for the fragmentation of deprotonated NsβAla to form an ion at *m/z* 226, followed by fragmentation to form at ion at *m/z* 184.

Fragmentation of **25b** generated in source gave major product ions at *m/z* 198, 184, 172, and 154 (Figure 3.28B). Loss of ketene (CH<sub>2</sub>=C=O, 42 u) from **25b** would account for the formation of the *m/z* 184 product ion with the same structure as **1c** formed from NsGly (Scheme 3.16). However, the *m/z* 184 ion was not formed by in-source fragmentation and its structure could not be probed by CID. The most abundant product ion formed from CID of **25b** was *m/z* 172 (**25g**), which corresponded to a neutral loss of 54. This fragmentation process could occur if the *m/z* 226 ion rearranges in source to an enolate ion **25b'**, which could fragment to give CO and ethyne as neutral losses (Scheme 3.17). The ion at *m/z* 198 (**25d**) is accompanied by a neutral loss of 28, which may correspond to CO, one of the neutral losses observed in the lowest energy fragmentation pathway of NsGly. Since these product ions were not formed in source and MS/MS experiments were not possible, establishing a fragmentation pathway will require isotopic labeling or other mass spectrometric experiments.

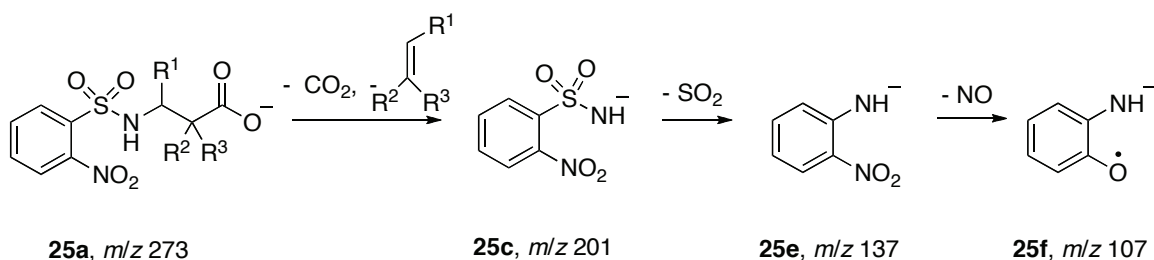


**Scheme 3.17.** Proposed structure for the fragmentation of in-source *m/z* 226 to form an ion at *m/z* 172.

ESI(-)MS/MS was also performed on Ns3Abu, Ns3Aib and Ns3Apv. These structural analogues of Ns $\beta$ Ala also showed a neutral loss of 47 u (HONO) giving product ions at *m/z* 240 (Ns3Abu, Figure 3.29, and Ns3Aib, Figure 3.30) and *m/z* 254 (Ns3Apv, Figure 3.31). Subsequent loss of ketene as a second step in the fragmentation pathway of the Ns3Abu anion was indicated by a minor ion at *m/z* 198 that retained the methyl group in Ns3Abu. Similarly, minor ions at *m/z* 184 indicated losses of methyl ketene and dimethyl ketene as second steps in the fragmentation pathways of Ns3Aib and Ns3Apv anions, respectively. The observed losses of ketene, methyl- and dimethyl ketene are consistent with the proposed cleavage of the C $\alpha$ -C $\beta$  bond in the  $\beta$ -alanine subunit of these Ns derivatives of  $\beta$ -amino acids.

The second major product ion (*m/z* 201, **25c**) formed by CID of the in-source [M – H]<sup>–</sup> ion of Ns $\beta$ Ala (Figure 3.28A) was accompanied by the formation of a neutral molecule of mass 72 u. The even mass indicated that the molecule did not contain nitrogen. CID of **25c** formed in source gave only a product ion at *m/z* 137 (**25e**, Figure 3.28C). This neutral loss of 64 u is consistent with the formation of SO<sub>2</sub> from a sulfonamide ion (**25c**). An abundant product ion at *m/z* 201 was also formed by CID of

deprotonated Ns3Abu (Figure 3.29A), Ns3Aib (Figure 3.30A) and Ns3Apv (Figure 3.31). CID of the  $m/z$  201 and 137 ions generated in source led to losses of  $\text{SO}_2$  and  $\text{NO}$ , respectively. CID of  $m/z$  203 formed in source from the  $[\text{M} + 2 - \text{H}]^-$  ion of Ns3APv (Figure 3.31C) also gave only  $m/z$  137 as a product ion, confirming the loss of sulfur in this fragmentation process. Thus, the formation of **25c** was independent of the structure of the  $\beta$ -amino acid subunit, an outcome consistent with the proposed dual bond cleavage process (Scheme 3.18). A dual bond cleavage pathway, analogous to that proposed as a higher energy fragmentation pathway of NsGly (Section 3.5.1.1), was proposed for the conversion of  $\beta$ -amino acid subunit into  $\text{CO}_2$  and an olefin.



**Scheme 3.18.** Fragmentation of deprotonated Ns $\beta$ Ala ( $\text{R}^1 = \text{R}^2 = \text{R}^3 = \text{H}$ ), Ns3Abu ( $\text{R}^1 = \text{CH}_3$ ,  $\text{R}^2 = \text{R}^3 = \text{H}$ ), Ns3Aib ( $\text{R}^1 = \text{R}^2 = \text{H}$ ,  $\text{R}^3 = \text{CH}_3$ ), and Ns3Apv ( $\text{R}^1 = \text{H}$ ,  $\text{R}^2 = \text{R}^3 = \text{CH}_3$ ) to form  $m/z$  201, and its subsequent fragmentation to  $m/z$  137 and 107.

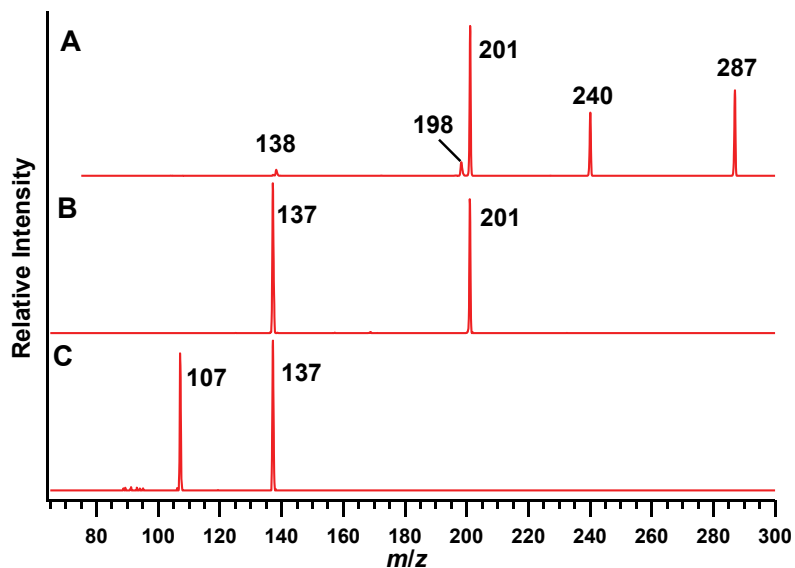


**Figure 3.29.** Product ion mass spectra obtained by CID of **A:** deprotonated Ns3Abu (CID 22%); **B:**  $m/z$  201 ion formed in source (CID 21%); **C:**  $m/z$  137 ion formed in source (CID 31%).

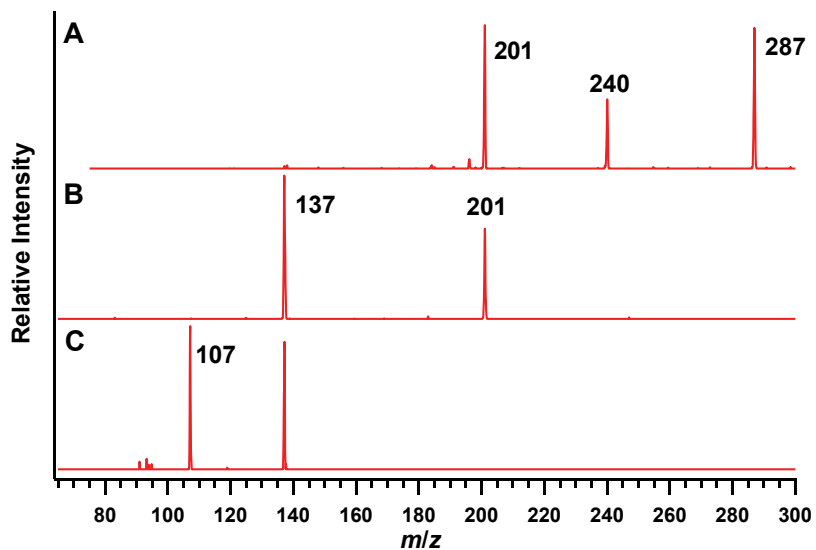


**Figure 3.30.** Product ion mass spectra obtained by CID of **A:** deprotonated Ns3Aib (CID 22%); **B:**  $m/z$  201 formed in source (CID 21%); **C:**  $m/z$  137 formed in source (CID 31%).

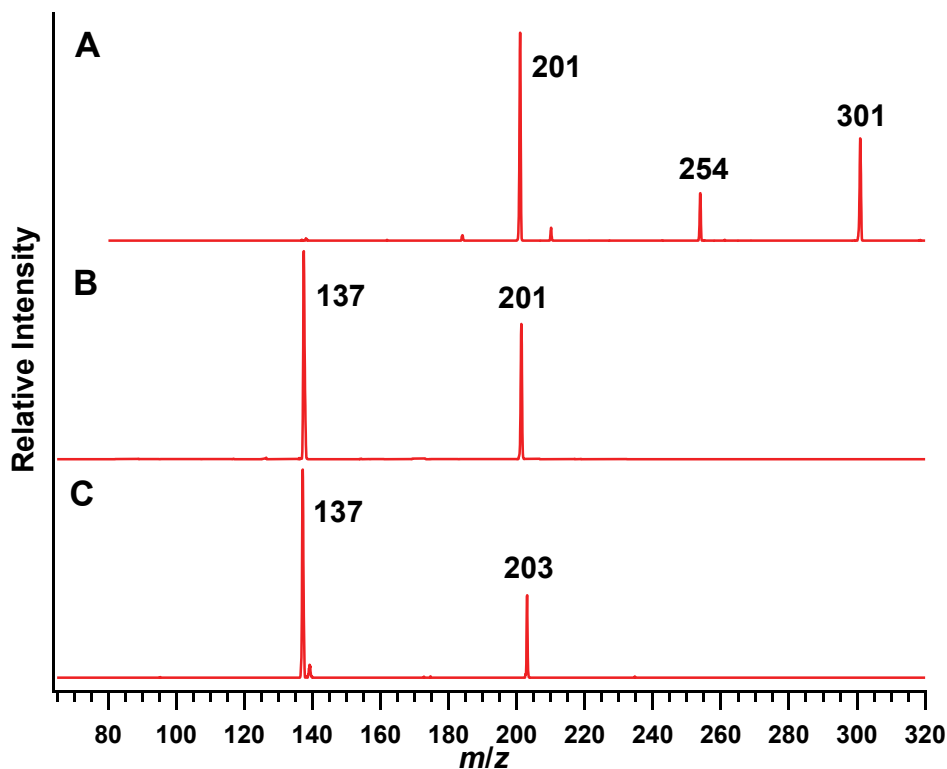


**Figure 3.31.** Product ion mass spectra obtained by CID of **A:** deprotonated Ns3APv (CID 22%); **B:**  $m/z$  201 ion formed in source (CID 20%); **C:**  $m/z$  203 ion formed in source (CID 21%).

The minor ion at  $m/z$  138 (Figure 3.28A) was not observed upon CID of the in-source fragment ions. Like **1f** observed as a fragment ion of the NsGly ion, it was most likely formed directly from the  $[M - H]^-$  ion of Ns $\beta$ Ala.

Upon CID, the  $[M - H]^-$  ion of NsNMe $\beta$ Ala formed a major product ion at  $m/z$  240 and minor product ions at  $m/z$  215, 186, 156 and 138 (Figure 3.32). The  $m/z$  240 ion (**29b**) was formed by a loss of 47 u, which corresponded to *ortho* cyclization and loss of HONO. The high abundance of this ion indicates the ability of deprotonated NsNMe $\beta$ Ala

(**29a**) to form an enolate ion (**29b**) upon cyclization (Scheme 3.19). The ion at  $m/z$  215 could be formed through dual bond cleavage and the loss of  $\text{CO}_2$  and ethene, with a structure analogous to **25c** formed from  $\text{Ns}\beta\text{Ala}$ . Other product ions were not formed in source, however, and further experiments are required in order to confirm their structures.

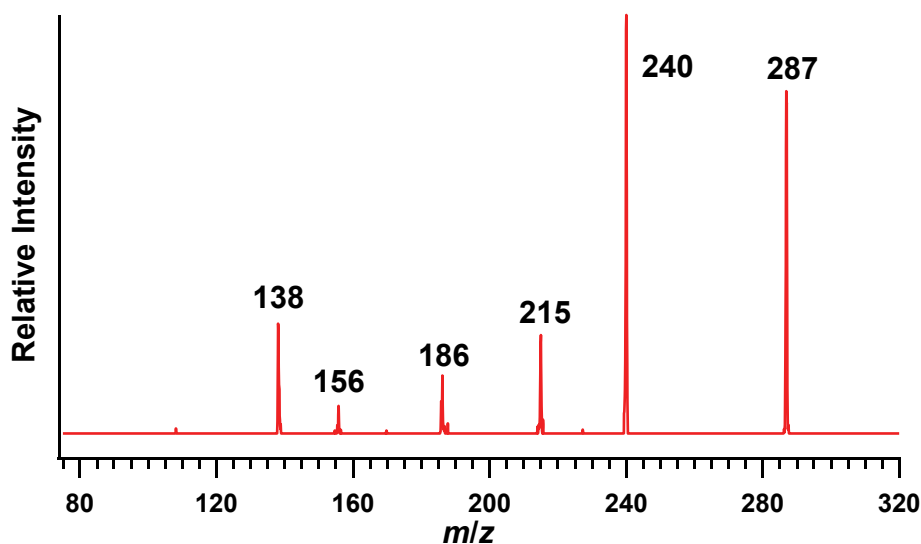
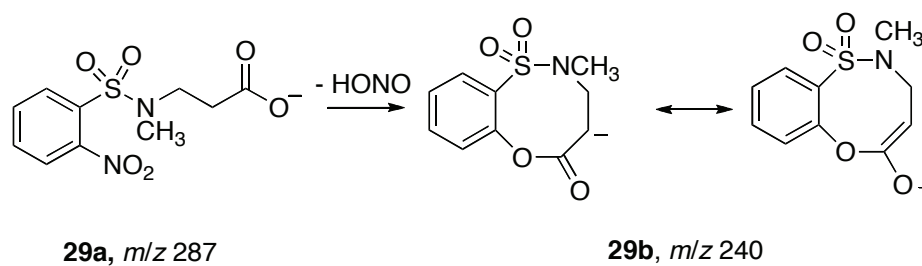


**Figure 3.32.** Product ion mass spectrum obtained by CID of  $\text{NsNMe}\beta\text{Ala}$  (CID 17%).



**Scheme 3.19.** Fragmentation of the  $[\text{M} - \text{H}]^-$  ion of  $\text{NsNMe}\beta\text{Ala}$  (**29a**) to form **29b** through the loss of  $\text{HONO}$ .

The minor ion at  $m/z$  138 noted in the CID mass spectrum of deprotonated Ns $\beta$ Ala (Figure 3.28) was also formed by CID of the Ns3Abu (Figure 3.29A), Ns3Aib (Figure 3.30A), Ns3Apv (Figure 3.31A) and NsNMe $\beta$ Ala (Figure 3.32A) anions. Thus, structural changes in the  $\beta$ -amino acid subunit did not alter the structure of the  $m/z$  138 anion. The formation of the  $m/z$  138 ion from the deprotonated  $\beta$ -amino acid derivatives can be accounted for by the pathway proposed for the formation of the  $m/z$  138 ion from the NsGly anion (Scheme 3.10).

Ns4Abu was also examined by ESI(-)MS/MS to determine if a bicyclic structure with a 9-membered ring would form through *ortho* cyclization. CID of the  $[M - H]^-$  ion of Ns4Abu at  $m/z$  287 gave two major product ions at  $m/z$  240, corresponding to a loss of HONO, and  $m/z$  201 (**25c**) (Figure 3.33A). The neutral loss of 47 u forming the  $m/z$  240 ion indicates that an *ortho* cyclization forming a 9-membered ring occurs, but it is a less favourable process than the formation of the  $m/z$  201 ion. The more favourable formation of the  $m/z$  201 ion was likely accompanied by the formation of a 5-membered lactone as the neutral product (Scheme 3.20). The formation of these products is consistent with the nucleophilic attack by the carboxylate group at C4 of the amino acid subunit and displacement of the sulfonamide ion. While nucleophilic displacement is a possible route to the  $m/z$  201 ion from deprotonated Ns $\beta$ Ala, the neutral product would be a higher energy 4-membered lactone and the dual bond cleavage pathway (Scheme 3.18) is likely more favourable.

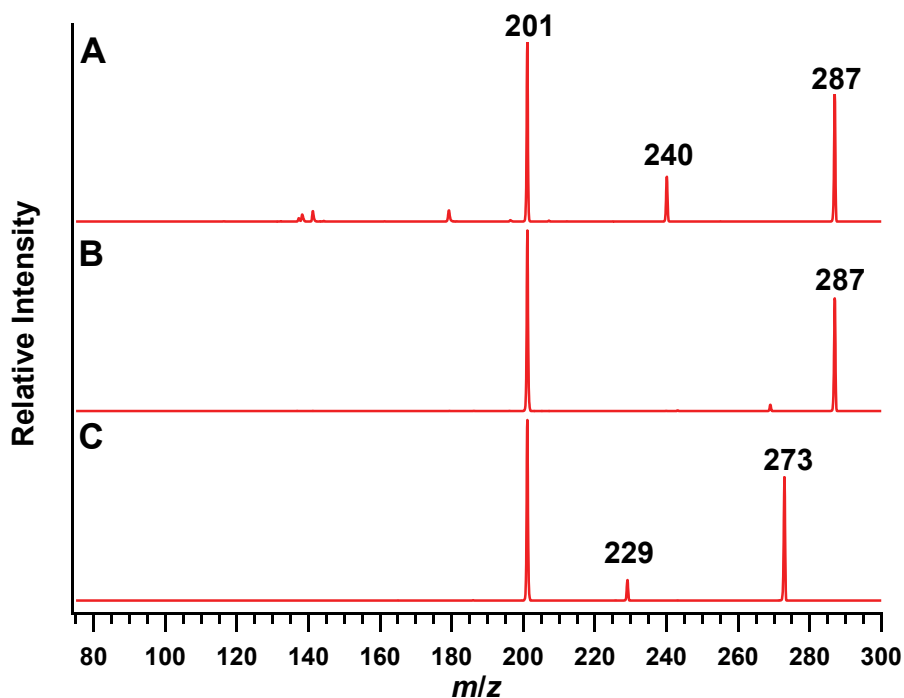
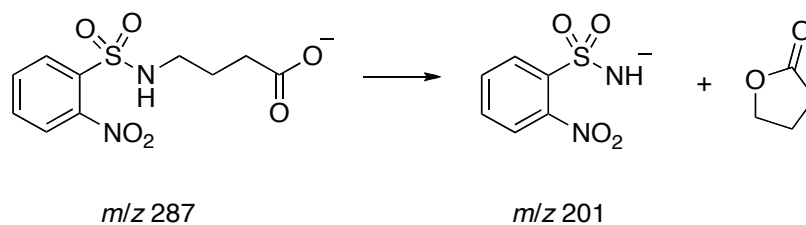


**Figure 3.33.** Product ion mass spectra obtained by CID of **A:** deprotonated Ns4Abu (CID 22%); **B:** deprotonated mNs4Abu (CID 22%); **C:** deprotonated mNs $\beta$ Ala (CID 22%).



**Scheme 3.20.** Fragmentation of the Ns4Abu anion to form the  $m/z$  201 ion and a neutral 5-membered lactone.

Upon CID, the  $[M - H]^-$  ion of mNs4Abu (Figure 3.33B) formed only a product ion at  $m/z$  201, which was also likely accompanied by the formation of a 5-membered lactone. CID of the  $[M - H]^-$  ion of mNs $\beta$ Ala (Figure 3.33C) also formed the  $m/z$  201 ion

as the most abundant product ion. Since the formation of a 4-membered lactone is less favourable, this fragmentation likely occurred through a dual bond cleavage forming CO<sub>2</sub> and ethene. A neutral loss of 44 u, CO<sub>2</sub>, giving a product ion at  $m/z$  229 was also present in the CID spectrum of mNsβAla (Figure 3.33C), which may occur through a mechanism similar to the decarboxylation seen by CID of mNsGly (Section 3.5.1).

Although *ortho* cyclization occurs when the carboxyl and sulfonamide groups are separated by a longer chain length, as seen in NsβAla and Ns4Abu, these results show that *meta* cyclization with a loss of HONO is not a favourable fragmentation process. The attack of the nucleophile at the carbon atom bonded to the nitro group places a negative charge on three of the aromatic ring carbons, but not the carbon bonded to the sulfonamide group. The latter likely makes a strong contribution to charge stabilization in the *ortho*-cyclized structure, lowering the energy of the transition state, making *ortho* cyclization more favourable.

In contrast with CID of the [M – H]<sup>–</sup> ion of NsGly, which showed only one abundant product ion corresponding to a loss of 47 u (Figure 3.4), CID of the [M – H]<sup>–</sup> ion of NsβAla (Figure 3.28) shows two abundant fragmentation processes in the ion trap mass spectrometer, indicating that these two pathways have similar energy barriers for fragmentation. The mechanism of fragmentation to form the  $m/z$  201 ion from deprotonated NsβAla is likely a dual bond cleavage, similar to the fragmentation of deprotonated NsGly forming the  $m/z$  186 ion, through the loss of CO<sub>2</sub> and ethene. Formation of the same  $m/z$  201 ion from Ns4Abu and mNs4Abu likely occurs through a nucleophilic displacement mechanism by formation of a 5-membered lactone.

### 3.5.7 Potential Competing Fragmentation Pathways

As a dicarboxylic acid, aspartic acid incorporates the structure of both an  $\alpha$ - and a  $\beta$ -amino acid. Thus, the fragmentation pathways characterized for the NsGly (and NsAla) and Ns $\beta$ Ala anions earlier in this thesis are potential fragmentations of deprotonated NsAsp.

Upon CID, deprotonated NsAsp formed a major product ion at  $m/z$  186 (Figure 3.34A), which is likely due to a dual bond cleavage similar to the fragmentation process seen in NsGly (Scheme 3.11). CID of the in-source  $m/z$  186 ion led to the loss of SO and the formation of  $m/z$  138. The  $m/z$  138 ion fragmented further to form  $m/z$  108 with a loss of NO. The  $m/z$  186 ion also lost SO<sub>2</sub> as a neutral product to form a minor ion at  $m/z$  122, which fragmented further to form an ion at  $m/z$  92 through a loss of NO. These fragmentations are consistent with the formation of the  $m/z$  186 ion by the dual bond cleavage process described for the NsGly anion earlier in this thesis (Section 3.5.1.1). Hydrogen bonding between the sulfonamide hydrogen and the ionized  $\alpha$ -carboxyl group in the NsAsp ion aligns the S-N, N-C $\alpha$  and C $\alpha$ -CO<sub>2</sub><sup>-</sup> bonds in approximately an anti conformation (Figure 3.35). The anti conformation results in good orbital overlap for  $\pi$ -bond formation, which facilitates the dual bond cleavage.

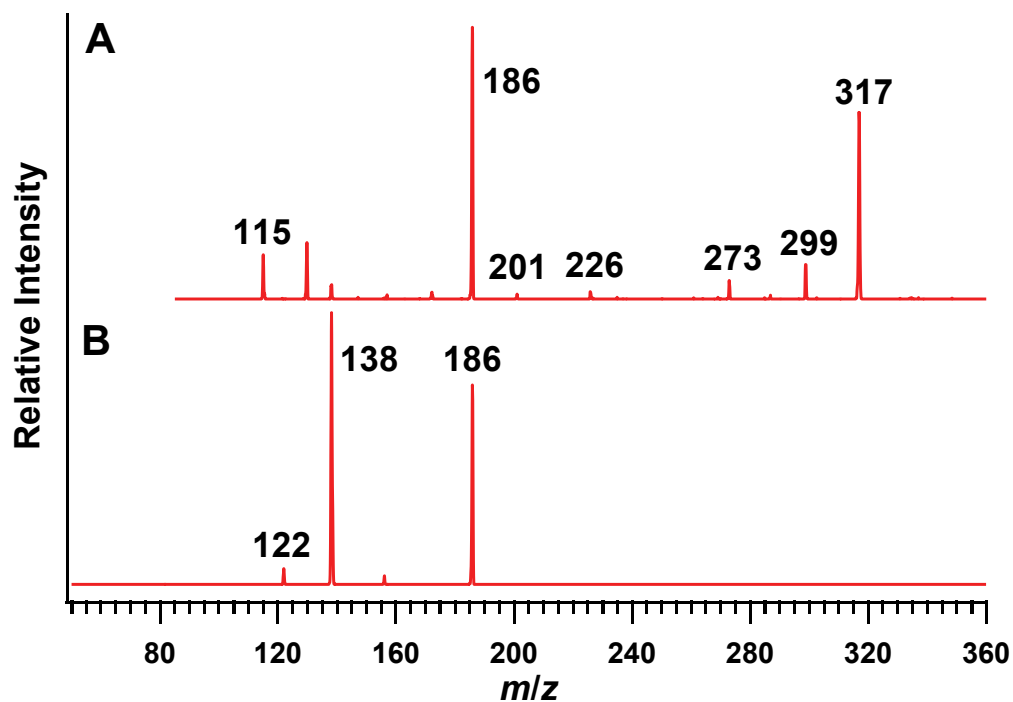


**Figure 3.34.** Product ion mass spectra obtained by CID of **A:** deprotonated NsAsp (CID 20%); **B:**  $m/z$  186 ion generated in source (CID 17%).

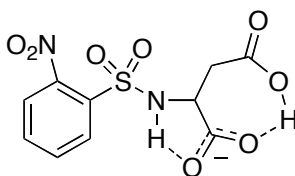
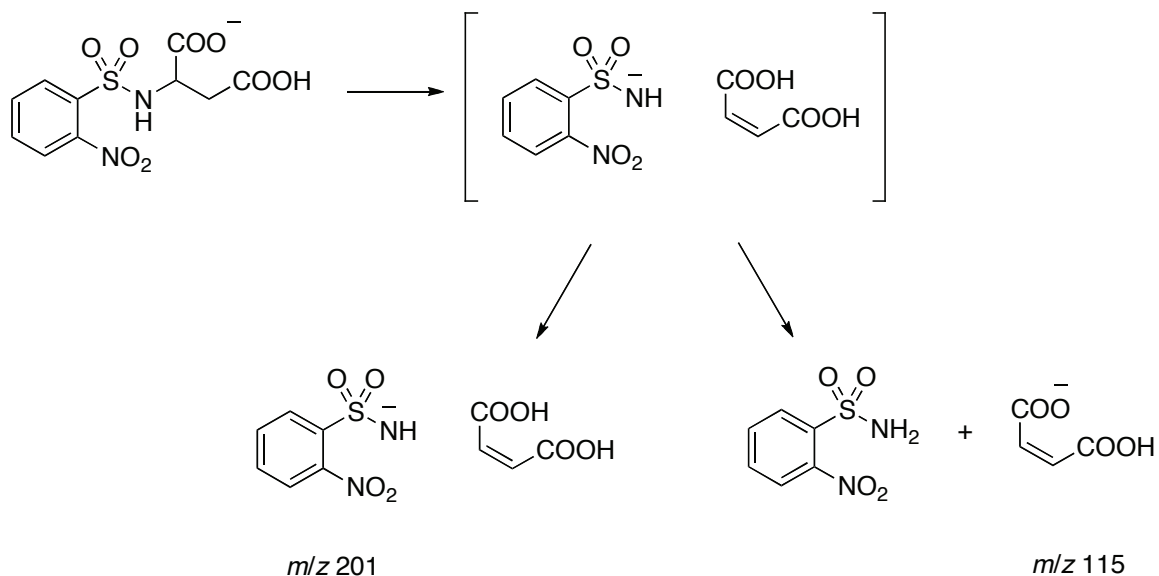


**Figure 3.35.** Hydrogen bond formation in deprotonated NsAsp.

Loss of H<sub>2</sub>O and CO<sub>2</sub> were observed to form the ions at  $m/z$  299 and 273, respectively. These losses are consistent with the fragmentation behavior of the monoanion of a dicarboxylic acid.<sup>16</sup> The  $m/z$  273 ion can behave as NsβAla, and undergo *ortho* cyclization to form the  $m/z$  226 ion, or undergo dual bond cleavage to form the  $m/z$

201 ion. The ion at  $m/z$  115 formed as the complementary ion of the  $m/z$  201 ion (Scheme 3.21).<sup>6,28</sup> Complementary ions result from competing fragmentation reactions, and form two ions for which the sum of the  $m/z$  values is one less than the  $m/z$  of the  $[M - H]^-$  ion.



**Scheme 3.21.** Competing fragmentation processes of deprotonated NsAsp forming complementary ions at  $m/z$  201 and 115.

While several of the fragmentation processes described earlier in this thesis were possible for the NsAsp ion, only one was observed as a major process (Figure 3.34A). This dual bond cleavage pathway was not observed for the anions of NsGly and NsAla in the ion trap mass spectrometer, suggesting that fragmentation reactions are influenced by functional group interactions in the precursor ion. In deprotonated NsAsp, the nucleophilicity of the ionized  $\alpha$ -carboxyl group could be reduced by hydrogen bonding to the nonionized side-chain carboxyl group (Figure 3.35). Therefore, in addition to defining feasible fragmentation pathways through structural variations, potential functional group

interactions in ions of more complicated structure must be considered as part of the process of predicting fragmentation pathways. Further refinement of this analysis requires investigation of other Ns derivatives having complex structures.

## CHAPTER 4 CONCLUSIONS

A library of Ns amino acid derivatives, including isotopic labels and systematic structural variations, was prepared and characterized by melting points, NMR and ESI(-)MS. Conditions developed for the selective hydrolysis of an ester in the presence of a sulfonamide were applied to the synthesis of Ns[<sup>18</sup>O]Gly and isotopically labeled derivatives of NsSar and NsNMeβAla.

ESI(-) mass spectra obtained for the synthesized compounds on an ion trap mass spectrometer showed intense peaks corresponding to the deprotonated Ns amino acids. CID experiments on these  $[M - H]^-$  ions established precursor-product ion relationships in fragmentation pathways. Four major fragmentation pathways were established for Ns- $\alpha$ - and  $\beta$ -amino acids. These fragmentation processes were supported by evidence from isotopically labeled derivatives and structural analogues. A novel *ortho* cyclization characterized for the Ns- $\alpha$ -amino acid anions was accompanied by a loss of the aromatic substituent at the *ortho* position and the sulfonamide proton. *Ortho* cyclization was observed when the aromatic substituent was a good leaving group. The mass spectra of NsNHEtOH also showed that a good nucleophile other than a carboxyl group can also result in *ortho* cyclization. In the mass spectra of NsGlyNH<sub>2</sub>, where ionization is expected primarily at the sulfonamide group, the loss of SO<sub>2</sub> was the lowest energy process and *ortho* cyclization was not observed.

The ion formed after *ortho* cyclization could undergo two different fragmentation processes. The first pathway observed involved successive losses of CO, HCN, and SO<sub>2</sub>. The second pathway involved a more complicated rearrangement, which resulted in the

loss of one oxygen atom originally bonded to sulfur, and ions at  $m/z$  141, 140, and 72. A sulfonamide rearrangement pathway was also observed for the deprotonated Ns amino acids, forming an ion at  $m/z$  138, and was observed in almost all derivatives prepared, indicating that this process was independent of the different structural features of the Ns derivatives.

A dual bond cleavage pathway was observed for mNsGly and pNsGly. The resulting product ion at  $m/z$  186 was accompanied by a loss of  $\text{CO}_2$  and  $\text{HNCH}_2$ . The dual bond cleavage process was observed in CID spectra of NsGly collected on a triple quadrupole mass spectrometer. A similar dual bond cleavage process forming a product ion at  $m/z$  201 was observed for Ns $\beta$ Ala and its structural analogues.

The structural variations indicated that *ortho* cyclization and dual bond cleavage were observed when Ns- $\alpha$ -amino acids were ionized at the carboxyl group. The CID mass spectra of NsGlyOEt, where ionization could only occur at the sulfonamide, was more complicated, and showed many product ions.

*Ortho* cyclization was also observed when the amino acid chain length was longer, although the mass spectra of Ns $\beta$ Ala and Ns4Abu also showed a second fragmentation that presumably required a similar input of energy.

NsAsp, a dicarboxylic acid, has structural subunits analogous to NsGly and Ns $\beta$ Ala. While the four major processes described in this thesis could potentially occur, only one major fragmentation process was observed upon CID, indicating that functional group interactions may influence the direction of fragmentation.

Future work on this project requires the collection of further evidence in support of the fragmentation pathways proposed in this thesis. Theoretical computations could be

used to predict the energetics for each reaction and establish the feasibility of the proposed pathways. Further mass spectrometric experiments on isotopically labeled derivatives of Ns $\beta$ Ala would provide valuable evidence on the fragmentation processes observed for the  $\beta$ -amino acids. Similar experiments should also be performed for NsNH<sub>2</sub>EtOH, NsGlyOEt, and NsSar. Also, CID mass spectra should also be collected on the triple quadrupole mass spectrometer for several compounds. The higher energies provided by collisions with argon in the QqQ could provide more information about the relative energies of the fragmentation pathways of the Ns derivatives. The ion trap mass spectrometer was limited by its mass range, and cannot detect ions with  $m/z < 50$ . Looking at the low mass range with the triple quadrupole mass spectrometer could also provide more evidence, particularly for NsGlyNH<sub>2</sub>, which likely formed product ions  $< m/z 50$  that could not be detected by the ion trap mass spectrometer.

## REFERENCES

- (1) Thevis, M.; Schänzer, W. *Mass Spectrom. Rev.* **2007**, *26*, 79–107.
- (2) Geyer, H.; Parr, M. K.; Koehler, K.; Mareck, U.; Schänzer, W.; Thevis, M. *J. Mass Spectrom.* **2008**, *43*, 892–902.
- (3) Thevis, M.; Schänzer, W. *Anal. Bioanal. Chem.* **2007**, *388*, 1351–1358.
- (4) Levsen, K.; Schiebel, H.-M.; Terlouw, J. K.; Jobst, K. J.; Elend, M.; Preiß, A.; Thiele, H.; Ingendoh, A. *J. Mass Spectrom.* **2007**, *42*, 1024–1044.
- (5) US Department of Commerce, N. NIST Standard Reference Database 1A  
<http://www.nist.gov/srd/nist1a.cfm> (accessed Mar 7, 2013).
- (6) Niessen, W. M. A. *Mass Spectrom. Rev.* **2012**, *31*, 626–665.
- (7) Kinter, M.; Sherman, N. E. *Protein Sequencing and Identification Using Tandem Mass Spectrometry*; 1st ed.; Wiley-Interscience, 2000.
- (8) Hoffmann, E. de; Stroobant, V. *Mass Spectrometry: Principles and Applications*; John Wiley & Sons, 2007.
- (9) Bowie, J. H. *Mass Spectrom. Rev.* **1990**, *9*, 349–379.
- (10) Mayer, P. M.; Poon, C. *Mass Spectrom. Rev.* **2009**, *28*, 608–639.
- (11) Solomons, T. W. G.; Fryhle, C. *Organic Chemistry*; 9th ed.; Wiley, 2007.
- (12) Remko, M.; Von der Lieth, C.-W. *Bioorg. Med. Chem.* **2004**, *12*, 5395–5403.
- (13) Bandu, M. L.; Watkins, K. R.; Bretthauer, M. L.; Moore, C. A.; Desaire, H. *Anal. Chem.* **2004**, *76*, 1746–1753.
- (14) Graul, S. T.; Squires, R. R. *J. Am. Chem. Soc.* **1990**, *112*, 2506–2516.
- (15) Squires, R. R. *Acc. Chem. Res.* **1992**, *25*, 461–467.
- (16) Grossert, J. S.; Fancy, P. D.; White, R. L. *Can. J. Chem.* **2005**, *83*, 1878–1890.

- (17) Leenheer, J. A.; Rostad, C. E.; Gates, P. M.; Furlong, E. T.; Ferrer, I. *Anal. Chem.* **2001**, *73*, 1461–1471.
- (18) Kosjek, T.; Žigon, D.; Kralj, B.; Heath, E. *J. Chromatogr. A* **2008**, *1215*, 57–63.
- (19) Marchese, S.; Gentili, A.; Perret, D.; Ascenzo, G. D.; Pastori, F. *Rapid Commun. Mass Spectrom.* **2003**, *17*, 879–886.
- (20) Ferrer, I.; Thurman, E. M. *Anal. Chem.* **2005**, *77*, 3394–3400.
- (21) Rabbolini, S.; Verardo, E.; Da Col, M.; Gioacchini, A. M.; Traldi, P. *Rapid Commun. Mass Spectrom.* **1998**, *12*, 1820–1826.
- (22) McLafferty, F. W. *Anal. Chem.* **1959**, *31*, 82–87.
- (23) Raftery, M. J.; Bowie, J. H. *Int. J. Mass Spectrom. Ion Processes* **1988**, *85*, 167–186.
- (24) Stringer, M. B.; Bowie, J. H.; Holmes, J. L. *J. Am. Chem. Soc.* **1986**, *108*, 3888–3893.
- (25) Stringer, M. B.; Bowie, J. H.; Eichinger, P. C. H.; Currie, G. J. *J. Chem. Soc., Perkin Trans. 2* **1987**, 385–390.
- (26) Zollinger, M.; Seibl, J. *Org. Mass Spectrom.* **1985**, *20*, 649–661.
- (27) Grossert, J. S.; Cook, M. C.; White, R. L. *Rapid Commun. Mass Spectrom.* **2006**, *20*, 1511–1516.
- (28) Greene, L. E.; Grossert, J. S.; White, R. L. *J. Mass Spectrom.* **2013**, *48*, 312–320.
- (29) Sanger, F. *Biochem. J.* **1945**, *39*, 507–515.
- (30) Porter, R.; Sanger, F. *Biochem. J.* **1948**, *42*, 287–294.
- (31) George, M.; Ramesh, V.; Srinivas, R.; Giblin, D.; Gross, M. L. *Int. J. Mass Spectrom.* **2011**, *306*, 232–240.

- (32) Schröder, D.; Buděšínský, M.; Roithová, J. *J. Am. Chem. Soc.* **2012**, *134*, 15897–15905.
- (33) Steill, J. D.; Oomens, J. *J. Am. Chem. Soc.* **2009**, *131*, 13570–13571.
- (34) Tian, Z.; Kass, S. R. *J. Am. Chem. Soc.* **2008**, *130*, 10842–10843.
- (35) Bowers, M. T.; Kemper, P. R.; Von Helden, G.; Van Koppen, P. A. M. *Science* **1993**, *260*, 1446–1451.
- (36) Truce, W. E.; Kreider, E. M.; Brand, W. W. In *Organic Reactions*; Bittman, R.; Dauben, W. C.; Fried, J.; House, H. O.; Kende, A. S.; Marshall, J. A.; McKusick, B. C.; Meinwald, J., Eds.; John Wiley & Sons, Inc.; Vol. 18, pp. 99–216.
- (37) Zhou, Y.; Pan, Y.; Cao, X.; Wu, J.; Jiang, K. *J. Am. Soc. Mass Spectrom.* **2007**, *18*, 1813–1820.
- (38) Wang, T.; Nibbering, N. M. M.; Bowie, J. H. *Org. Biomol. Chem.* **2010**, *8*, 4080–4084.
- (39) Wang, F. *Rapid Commun. Mass Spectrom.* **2006**, *20*, 1820–1821.
- (40) Eichinger, P.; Bowie, J.; Hayes, R. *J. Am. Chem. Soc.* **1989**, *111*, 4224–4227.
- (41) Eichinger, P.; Bowie, J. *Org. Mass Spectrom.* **1992**, *27*, 995–999.
- (42) Kim, W. K.; Ryu, W. S.; Han, I.-S.; Kim, C. K.; Lee, I. *J. Phys. Org. Chem.* **1998**, *11*, 115–124.
- (43) Binkley, R.; Flechtner, T.; Tevesz, M.; Winnik, W.; Zhong, B. *Org. Mass Spectrom.* **1993**, *28*, 769–772.
- (44) Smith, J. D.; OHair, R. A. J.; Williams, T. D. *Phosphorus Sulfur Silicon Relat. Elem.* **1996**, *119*, 49–59.
- (45) Zhang, X. *J. Mol. Struct.* **2012**, *1028*, 1–6.
- (46) Xiang, Z. *Comp. Theor. Chem.* **2012**, *991*, 74–81.

- (47) Sun, M.; Dai, W.; Liu, D. Q. *J. Mass Spectrom.* **2008**, *43*, 383–393.
- (48) Richter, D.; Dünnbier, U.; Massmann, G.; Pekdeger, A. *J. Chromatogr. A* **2007**, *1157*, 115–121.
- (49) Hu, N.; Liu, P.; Jiang, K.; Zhou, Y.; Pan, Y. *Rapid Commun. Mass Spectrom.* **2008**, *22*, 2715–2722.
- (50) Garcia, P.; Popot, M. A.; Fournier, F.; Bonnaire, Y.; Tabet, J. C. *J. Mass Spectrom.* **2002**, *37*, 940–953.
- (51) Woo, H.; Kim, J. W.; Han, K. M.; Lee, J. H.; Hwang, I. S.; Lee, J. H.; Kim, J.; Kweon, S. J.; Cho, S.; Chae, K. R.; Han, S. Y.; Kim, J. *Food Addit. Contam.* **2013**, *30*, 209–217.
- (52) Sarmah, A. K.; Meyer, M. T.; Boxall, A. B. A. *Chemosphere* **2006**, *65*, 725–759.
- (53) Baran, W.; Adamek, E.; Ziemiańska, J.; Sobczak, A. *J. Hazard. Mater.* **2011**, *196*, 1–15.
- (54) M. Casewell; C. Friis; E. Marco; P. McMullin; I. Phillips *J. Antimicrob. Chemother.* **2003**, *52*, 159.
- (55) Renew, J. E.; Huang, C.-H. *J. Chromatogr. A* **2004**, *1042*, 113–121.
- (56) Díaz-Cruz, M. S.; García-Galán, M. J.; Barceló, D. *J. Chromatogr. A* **2008**, *1193*, 50–59.
- (57) Isidori, M.; Lavorgna, M.; Nardelli, A.; Pascarella, L.; Parrella, A. *Sci. Total Environ.* **2005**, *346*, 87–98.
- (58) Le-Minh, N.; Khan, S. J.; Drewes, J. E.; Stuetz, R. M. *Water Res.* **2010**, *44*, 4295–4323.
- (59) Jury, K. L.; Khan, S. J.; Vancov, T.; Stuetz, R. M.; Ashbolt, N. J. *Crit. Rev. Env. Sci. Technol.* **2011**, *41*, 243–270.

- (60) Lindsey, M. E.; Meyer, M.; Thurman, E. M. *Anal. Chem.* **2001**, *73*, 4640–4646.
- (61) Hartig, C.; Storm, T.; Jekel, M. *J. Chromatogr. A* **1999**, *854*, 163–173.
- (62) Hirsch, R.; Ternes, T. A.; Haberer, K.; Mehlich, A.; Ballwanz, F.; Kratz, K.-L. *J. Chromatogr. A* **1998**, *815*, 213–223.
- (63) Toshiyuki Kan; Tohru Fukuyama *Chem. Commun.* **2004**, *0*, 353–359.
- (64) Biron, E.; Chatterjee, J.; Kessler, H. *J. Pep. Sci.* **2006**, *12*, 213–219.
- (65) Kelley, B. T.; Joullié, M. M. *Org. Lett.* **2010**, *12*, 4244–4247.
- (66) Wels, B.; Kruijtzter, J. a. W.; Liskamp, R. M. J. *Org. Lett.* **2002**, *4*, 2173–2176.
- (67) Deruiter, J.; Brubaker, A. N.; Garner, M. A.; Barksdale, J. M.; Mayfield, C. A. *J. Pharm. Sci.* **1987**, *76*, 149–152.
- (68) Mitsunobu, O.; Yamada, M. *Bull. Chem. Soc. Jpn.* **1967**, *40*, 2380–2382.
- (69) Swamy, K. C. K.; Kumar, N. N. B.; Balaraman, E.; Kumar, K. V. P. P. *Chem. Rev.* **2009**, *109*, 2551–2651.
- (70) Mitsunobu, O. *Synthesis* **1981**, *1981*, 1–28.
- (71) Fukuyama, T.; Jow, C.; Cheung, M. *Tetrahedron Lett.* **1995**, *36*, 6373–6374.
- (72) Fukuyama, T.; Cheung, M.; Jow, C. K.; Hidai, Y.; Kan, T. *Tetrahedron Lett.* **1997**, *38*, 5831–5834.
- (73) Guisado, C.; Waterhouse, J. E.; Price, W. S.; Jorgensen, M. R.; Miller, A. D. *Org. Biomol. Chem.* **2005**, *3*, 1049–1057.
- (74) Hidai, Y.; Kan, T.; Fukuyama, T. *Tetrahedron Lett.* **1999**, *40*, 4711–4714.
- (75) Nihei, K.; Kato, M. J.; Yamane, T.; Palma, M. S.; Konno, K. *Bioorg. Med. Chem. Lett.* **2002**, *12*, 299–302.
- (76) Zapf, C. W.; Del Valle, J. R.; Goodman, M. *Bioorg. Med. Chem. Lett.* **2005**, *15*, 4033–4036.

- (77) Falkiewicz, B.; Kołodziejczyk, A. S.; Liberek, B.; Wiśniewski, K. *Tetrahedron* **2001**, *57*, 7909–7917.
- (78) Reichwein, J. F.; Liskamp, R. M. J. *Tetrahedron Lett.* **1998**, *39*, 1243–1246.
- (79) Gillespie, T. A.; Winger, B. E. *Mass Spectrom. Rev.* **2011**, *30*, 479–490.
- (80) Cocker, W. *J. Chem. Soc.* **1943**, 373–378.
- (81) Baganz, H.; Peißker, H.; Beier, G. *Arch. Pharm.* **1957**, *290*, 609–615.
- (82) Petersen, S. G.; Rajska, S. R. *J. Org. Chem.* **2005**, *70*, 5833–5839.
- (83) Feldman, I. *Zh. Obshch. Khim.* **1962**, *32*, 1043–1046.
- (84) Singh, S. P.; Michaelides, A.; Merrill, A. R.; Schwan, A. L. *J. Org. Chem.* **2011**, *76*, 6825–6831.
- (85) Monfregola, L.; De Luca, S. *Amino Acids* **2010**, *41*, 981–990.
- (86) De Luca, S.; Moglie, R. D.; De Capua, A.; Morelli, G. *Tetrahedron Lett.* **2005**, *46*, 6637–6640.
- (87) Biron, E.; Kessler, H. *J. Org. Chem.* **2005**, *70*, 5183–5189.
- (88) Vederas, J. C. *Nat. Prod. Rep.* **1987**, *4*, 277–337.
- (89) Dehoffman, E.; Auriel, M. *Org. Mass Spectrom.* **1989**, *24*, 748–758.
- (90) Linstrom, P. J.; Mallard, W. G.; Eds. NIST Chemistry WebBook, NIST Standard Reference Database Number 69. <http://webbook.nist.gov/chemistry/#SpData> (accessed Jul 9, 2013).
- (91) Ventura, R.; Segura, J. *J. Chromatogr. B.* **1996**, *687*, 127–144.